Can batch reverse osmosis make desalination more affordable and sustainable?

by

Quantum J. Wei

S.B., Massachusetts Institute of Technology - 2015
S.M., Massachusetts Institute of Technology - 2017

Submitted to the Department of Mechanical Engineering
in partial fulfillment of the requirements for the degree of

Doctor of Philosophy in Mechanical Engineering

at the

MASSACHUSETTS INSTITUTE OF TECHNOLOGY

June 2021

Author .....
Department of Mechanical Engineering
May 7, 2021

Certified by .....
John H. Lienhard
Abdul Latif Jameel Professor of Water
Thesis Supervisor

Accepted by .....
Nicolas Hadjiconstantinou
Chairman, Committee on Graduate Students

Can batch reverse osmosis make desalination more affordable and sustainable?

by

Quantum J. Wei

Submitted to the Department of Mechanical Engineering
on May 7, 2021, in partial fulfillment of the
requirements for the degree of
Doctor of Philosophy in Mechanical Engineering

Abstract

Reverse osmosis (RO) desalination can help to ensure secure water resources, but the process remains costly. From 2007-2017, global desalination capacity nearly doubled, from 47 to 92 million m^3 /day, with RO accounting for two thirds of installed capacity. Despite this growth, the total volume of treated water accounts for less than half a percent of global freshwater consumption. To be part of a sustainable water supply, RO must be made cheaper. RO energy consumption can never fall below the thermodynamic least work of separation, which is 1 kWh/m^3 for 50% recovery of seawater. Practically speaking, RO energy consumption will not reach the thermodynamic limit but may be further reduced through improvements in system design.

Batch RO is the most energy-efficient RO process. It saves energy because the feed pressure varies over time with the osmotic pressure. In this thesis we further develop the batch RO technology to identify its benefits and limitations. We demonstrated the first batch RO system using a flexible bladder and validated theoretical models of energy consumption and water production. Next, we investigated practical losses associated with batch operation. This work shows that current batch RO designs are not attractive due to the combined inefficiencies of salt retention and water loss. Incomplete flushing of brine from cycle-to-cycle leads to an elevated feed salinity relative to the feed intake, boosting energy consumption by about $\sim$10%. De-pressurization during the reset phases of the batch RO cycle leads to water loss via osmosis. This water loss is significant ($\sim$10%) under seawater conditions. We introduce an improved batch RO design which rapidly flushes the system to reduce downtime and water loss. Unfortunately, there does not appear to be a practical way to avoid the salt retention penalty. Batch RO has more economic value in increasing plant productivity, rather than reducing energy consumption. We conclude that batch RO is a promising technology and identify future directions for research and commercialization.

Thesis Supervisor: John H. Lienhard
Title: Abdul Latif Jameel Professor of Water

For mama, who knows me better than I know myself.

And baba, who taught me how to treat people.

OUR WORLD IS FUNGIBLE
YOU ARE CHANGING THE WORLD
ARE YOU BUILDING A BETTER WORLD?
ARE YOU RIDING A WAVE?

- WIFI ATTEMPT ✓
- CLEAR OUT TABLES
- CLEAR SHELVES
- TAG UP EVERYTHING!

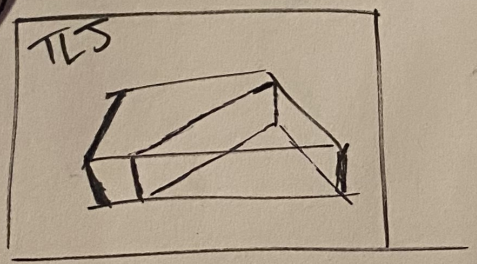

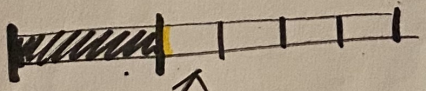

TRACK PROGRESS

EYEBALL
SPACETIME MEASUREMENT

PEOINESE

RACHEL & MINTO
PLANT INSPIRED
FASHION SHOW!

Thanks

It is not practical to account for everyone who contributed to this thesis. Here are some highlights.

Professor Lienhard, for giving me space and pushing me further.

My thesis committee, for reading and advising.

Supporters of this work, financial and otherwise.

Mentors, including/especially the ones I didn't realize were mentors at the time.

I wanted another slide of my friends, but it's a real pain to collect the photos.

Teammates, from whom I learn.

Xinhong, for introducing me to art.

Emily, for pulling me outside the lines.

Carly, for pointing out the obvious.

The Institute, where I learned how the (physical) world works.

AB2, for getting me through.

All the places I've lived and played.

Late-night conversations.

(Science) fiction.

Everyone who said no.

To all the strong women in my life.

Lucky. Ollie. Marco. Chewy. Loki.

My friend families. You know who you are.

Quark and Quasar, who branched out.

My parents, for thinking differently.

This doctoral thesis has been examined by a Committee of the Department of Mechanical Engineering as follows:

Professor John H. Lienhard .....
Thesis Supervisor
Abdul Latif Jameel Professor of Water

Professor Amos Winter .....
Member, Thesis Committee
Associate Professor of Mechanical Engineering

Professor Allan Myerson .....
Member, Thesis Committee
Professor of the Practice, Chemical Engineering

Professor Emily W. Tow .....
Member, Thesis Committee
Assistant Professor of Mechanical Engineering
Olin College of Engineering

Contents

List of Figures

List of Tables

When it fails to rain, we can desalinate.

1

Motivation

By 2050 it is estimated that six billion people will face clean water scarcity due to growing demand (population and economic growth) and an increasingly unreliable supply (climate change) [1]. This number may even be an underestimate [2]. Essentially all of our freshwater comes from the hydrological cycle (rain) [3]. This accounts for 1% of the water on Earth. There is more freshwater (2%) in glaciers and ice caps, but that is inaccessible to us. The oceans contain the remainder of Earth's (salty) water. Water desalination allows us to tap into the oceans and expand our supply of freshwater. Desalination alone will not – and should not – solve our water problems. However, it is a powerful tool which we should use when it makes sense.

As such, it is vitally important to find cheaper and more sustainable methods of water recovery. Although reverse osmosis (RO) desalination was relatively expensive when it was first introduced in the 1970s, its energy consumption has reduced dramatically as a result of improvements in membrane permeability, pump efficiency, and energy recovery [4]. However, the energy consumption of RO plants is still significant, leading researchers to explore different system configurations in an effort to reduce costs. Batch RO is the most energy-efficient configuration, but its practical limitations have not yet been fully explored. This thesis details our work in demonstrating and developing this technology.

1.1 Energy consumption in reverse osmosis processes

In the conventional RO process (continuous RO), a pressurized and saline feed stream flows through the RO system continuously (Fig. 1-1A). The RO membrane separates the feed into two streams: pure permeate and concentrated brine, which constantly flow out of the system. The feed passes only once through the system (which may have multiple stages), and the permeate is recovered at the desired rate.

In the batch RO process (Fig. 1-1B), the feed/retentate stream is recirculated through the system multiple times until the desired amount of permeate is recovered. In this time-variant process, the feed pressure can vary over time as the average system concentration increases.

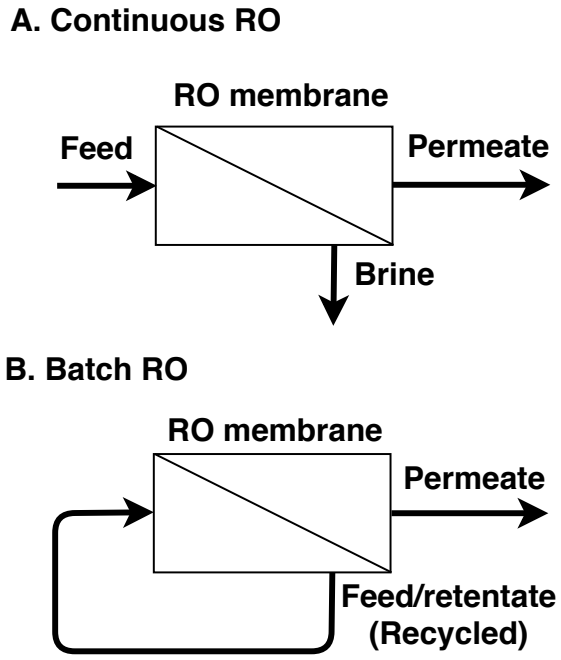

Figure 1-1: (A) In continuous RO (a steady-state process), the feed passes only once through the system and the desired amount of permeate is recovered. (B) In batch RO (a time-variant process), the retentate recirculates through the system multiple times before the desired amount of permeate is recovered. Following permeate production, the system is reset by flushing of the brine and introduction of new feed (not pictured here).

Several authors [5, 6, 7] frame batch RO as the ideal desalination process where feed pressure precisely matches the osmotic pressure. The specific energy consump-

tion of this ideal batch RO process, $SEC_{\text{batch,ideal}}$, is equivalent to the least work of separation (normalized by product volume) for a given feed osmotic pressure π_f and recovery ratio RR [5]:

$$SEC_{\text{batch,ideal}} = \frac{W_{\text{least}}}{V_p} = \frac{\pi_f}{RR} \ln \left[\frac{1}{1 - RR} \right] \tag{1.1}$$

where W_{least} is the least work of separation for the specified desalination process and V_p is the volume of permeate obtained from the process. The equation above assumes a linear relationship between osmotic pressure and concentration, a uniform concentration throughout the system, and zero losses associated with mass transfer resistance, mixing, friction, or component inefficiency. Actual batch RO systems will consume more energy than this as a result of practical realities such as spatial variations in concentration and a finite net driving pressure [5].

Energy consumption in cross-flow RO processes is nicely illustrated by a pressure-recovery diagram, as introduced by Liu et al. [5]. In this simplified model, the total area under the feed pressure curve corresponds to the energy consumed during each process, because instantaneous recovery ratio is proportional to the permeate volume. The batch RO process requires much less energy than continuous RO at the same recovery, as shown in Figure 1-2.

In a continuous RO system, the system osmotic pressure profile is steady in time and all variations occur in space. The applied feed pressure must overcome the brine osmotic pressure, which is larger than the feed osmotic pressure. A continuous RO system is **unbalanced**: the permeate flux at the front of the system is multiple times greater than at the back of the system. A more balanced system could produce the same amount of fresh water using less energy, such as in multi-stage RO systems [8, 9]. However, no process can consume less energy than the thermodynamic least work of separation, represented by the area under the osmotic pressure curve.

The batch RO process achieves the lowest practical energy consumption by varying feed pressure over time. The high-pressure pump can apply a low pressure at the beginning of the batch RO process and gradually increase the pressure in accordance

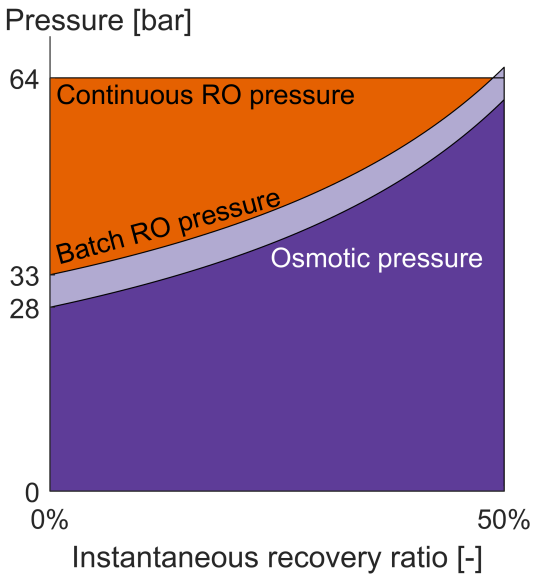

Figure 1-2: Pressure-recovery diagram for continuous and batch RO at 50% recovery. The batch RO process achieves the lowest practical energy consumption by varying feed pressure to follow the osmotic pressure curve. Each process produces the same amount of water. The area under the feed pressure lines represent the majority of work done by the high-pressure pump (this diagram does not show the work required to overcome concentration polarization or frictional losses in either process).

with the salinity of the system. This process is balanced - the permeate flux is kept constant in time. In the ideal batch RO process the permeate flux would also be uniform over space, but this is not achievable in practice. Still, significant energy may be saved if the osmotic pressure (and thus flux) varies minimally along the length of a short membrane module.

1.2 Batch RO: background

A conceptual drawing of the batch RO process illustrates the essential characteristics of a batch RO system (Fig. 1-3). A net driving pressure is applied to produce a permeate flux. A high-pressure, variable-volume tank is required to accommodate the shrinking volume of salt water. Fluid movement is required to reduce the effects of concentration polarization at the membrane surface. In this conceptual illustration, the movement is supplied by the stirrer in a dead-end arrangment. A more practical batch RO system would be operated in a cross-flow arrangement and fluid movement

is supplied by a circulation pump.

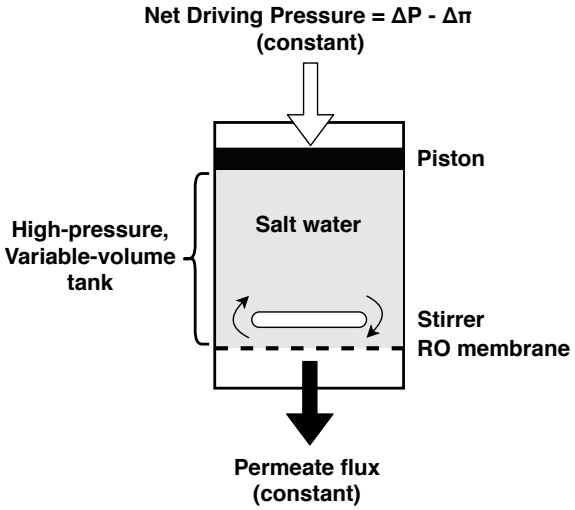

Figure 1-3: This drawing illustrates the essential characteristics of a true batch RO system.

Circulation pump

A circulation pump that produces crossflow serves as the stirrer in practical batch RO systems [6, 10]. Without the circulation pump, higher pressures would be required to drive the permeate flow because of salt accumulation at the membrane surface (i.e., concentration polarization). This addition is a significant difference from continuous RO systems - the circulation pump in a batch RO system presents an additional degree of freedom when it comes to system operation but also requires additional energy [11, 12], cutting into the potential energy savings of batch systems.

The use of a circulation pump in batch RO allows for flexibility in operating at different crossflow velocities and therefore different levels of concentration polarization [10]. In continuous RO, the maximum and minimum crossflow velocities are determined by the initial feed flow and the overall recovery ratio. In a batch RO system the maximum crossflow velocity is determined by the circulation pump flow rate, which can be adjusted independent of the initial feed mass and applied pressure. The minimum crossflow velocity occurs at the end of the membrane module, but should be close to the maximum crossflow velocity in batch RO systems since the per-pass

recovery ratio is relatively low.

True batch RO

The key challenge to implementing batch RO is the decreasing volume of pressurized saline water that remains in the system as permeate is produced (Fig. 1-3). Prior to the start of each cycle, a batch of feed is introduced into the system. During the batch RO process, permeate leaves the system through the membrane and the retentate circulates in a loop around the system. This retentate decreases in volume throughout the process since no new feed enters the system during permeate production. The retentate must stay pressurized to produce permeate, so a *true* batch RO system (also called "ideal" or "fully-pressurized" batch RO [11, 12]) requires a feed tank that can operate at high pressure while changing in volume.

One proposed batch RO design avoids the need for a variable-volume tank by using an energy recovery device (ERD) to allow the feed water to be stored in a tank at atmospheric pressure [11, 12]. The ERD is used to depressurize the retentate and recycle that energy to pressurize feed water before it enters the membrane module. To our knowledge, batch RO with ERDs has not yet been implemented. However, theoretical studies have shown that batch RO with ERDs consumes more energy than true batch RO in both BWRO and SWRO [11, 12]. Significant energy is lost as the feed repeatedly cycles through the ERDs, which are not perfectly efficient [13].

One way to implement true batch RO is with a rigid piston, which divides a pressure vessel into two compartments [14]. One compartment is filled with the feed that is to be treated during the batch RO process, while the other compartment starts out empty. A pump introduces make-up fluid (e.g., water) into the empty compartment in order to trigger permeate production. The make-up fluid accomodates the shrinking feed volume and does not interact directly with the membrane since it is separated from the feed by the piston. Since the pressure vessel is already completely filled, the pressure in both compartments will rise very rapidly on account of the near incompressibility of water. Once the pressure exceeds the feed osmotic pressure, permeate will leave through the membrane, the feed volume will decrease, and the piston

will move accordingly. In this manner, the flowrate of make-up fluid is approximately equal to the permeate flowrate.

Another proposed true batch design uses a flexible bladder to divide the pressure vessel into two compartments [15]. In this work, we have built and operated the first true batch RO prototype using a flexible bladder. The bladder design was preferable to the piston design because there is no sliding so the bladder easier to fabricate and less susceptible to leaks.

Batch RO cycle: phases of operation

The operation of a true batch RO system using a bladder is illustrated in Figure 1-4. During the permeate production phase (A1,A2), feed circulates in a loop around the system. At the beginning of the batch cycle (A1) the circulation loop is at its maximum volume and the bladder at its minimum volume. The permeate production phase ends (A2) when the desired amount of permeate is produced (typically but not necessarily when the bladder is full). The combined volume of the circulation loop and the bladder remains the same throughout the permeate production phase. Make-up fluid is pumped by the high-pressure pump into the bladder and, as the bladder expands, permeate exits the circulation loop through the membrane at a similar rate. The permeate flow rate thus approximately matches the high-pressure pump's flow rate.[1]

Following permeate production, the flush and recharge phases reset the system. At the end of permeate production (Figure 1-4A2) the circulation loop is filled with a concentrated brine solution. Brine is ejected from the system during the flush phase (Figure 1-4B). The circulation loop is broken (by opening and closing valves, not shown here) and new feed is introduced into the system. The incoming feed pushes brine out of the system and the system salinity reapproaches the feed salinity.

After the flush phase, the valves are opened or closed so that there is no outlet

[1]Pressure control is easily achieved if the high-pressure pump is a positive displacement pump (which operates close to the specified flow rate). The system pressure will automatically rise to maintain a constant flux as the system osmotic pressure increases. By design, no additional equipment is needed to control pressure.

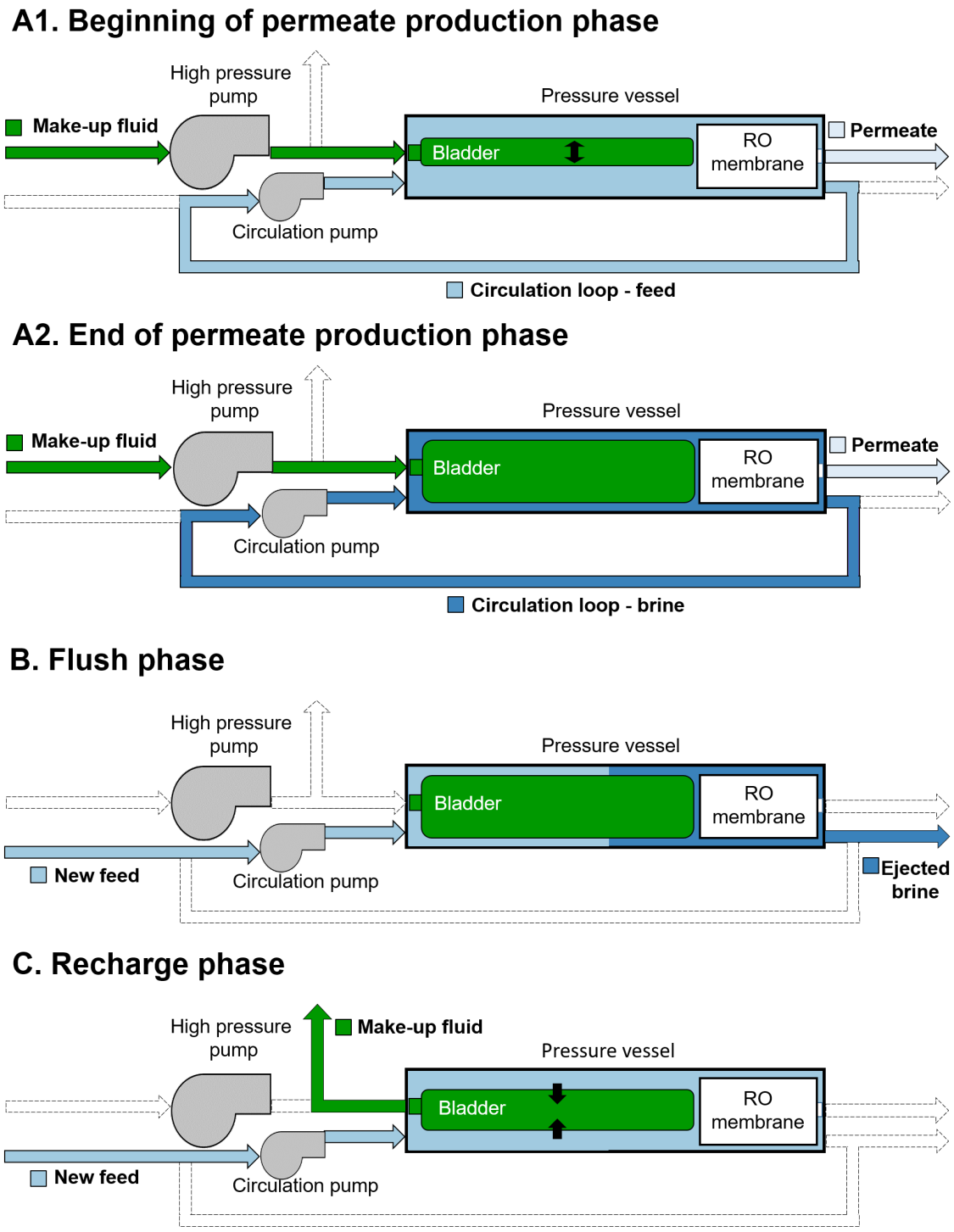

Figure 1-4: The batch RO cycle is composed of three phases, shown here as implemented in our true batch system with a bladder. During the permeate production phase (A1,A2), the circulation loop volume decreases but remains under pressure due to the expanding bladder. The flush and recharge phases (B,C) reset the system salinity and empty the bladder so that the batch cycle can be repeated. The make-up fluid is collected and reused. Dotted arrows indicate inactive flowpaths.

from the circulation loop. Instead, the valve blocking the bladder outlet is opened. During the recharge phase (Figure 1-4C) new feed is pumped into the system and the bladder is simultaneously emptied of make-up fluid. Once all make-up fluid has left the bladder, the recharge phase is complete and another batch cycle can restart with the permeate production phase.

1.3 Previous work

Two studies [11, 12] developed various models of RO processes and found that true batch RO consumes less energy than other RO processes. Closed-circuit RO (or semi-batch RO) energy consumption is higher because of continuous mixing (i.e., entropy generation) between fresh feed and brine during the permeate production phase. Batch RO with ERDs consumes more energy than true batch RO as a result of constant throttling of feed through the imperfect ERDs. These batch RO models included a circulation pump. The models mentioned above have not been validated with experimental results until now.

While numerous studies have used numerical models to investigate the potential benefits of batch RO systems [11, 12, 16], few systems have been built and operated. Davies et al. built and operated the first energy-efficient true batch RO system with a rigid piston [14]. They reported energy consumption lower than the minimum energy consumption of a single-stage continuous RO process (i.e., $SEC_{\mathrm{SSRO,ideal}} = \pi_f/[1-RR]$) at relatively high recoveries. These measurements included the hydraulic work of the high-pressure pump but not the circulation pump.

Swaminathan et al. investigated practical design aspects of batch RO for seawater desalination[17, 13]. They found that batch RO with an atmospheric tank is not energy saving as a result of the design constraints imposed by PX losses. Pressurized (true) batch RO designs could still save energy because designs with low per-pass recoveries are feasible. Warsinger et al. found that ultrapermeable membranes would increase the energy savings of batch RO, but those benefits might be outweighed by the cost of the new membranes [18].

Several studies have suggested that batch RO could reduce membrane scaling due to rapid salinity cycling [16]. These benefits have been attributed to other time-variant RO processes [19]. One study has disputed this benefit [20].

Alternate batch RO designs have been proposed. A double-acting design would reduce cycle downtime by combining the recharge phase with the permeate production phase [21, 22]. Davies et al. proposed a hybrid semi-batch/batch RO system to reduce the footprint of high recovery batch RO systems while maintaining low energy usage [23].

Salt retention has been studied in semi-batch and batch RO system. Cohen et al. measured salt retention in semi-batch RO systems and found that the energy penalty made these systems impractical [24]. Davies et al. measured salt retention in a batch RO system and determined that systems should operate at a flush time of unity to achieve the lowest energy consumption [6].

1.4 Structure of thesis

In this thesis, we further develop and investigate the batch RO technology to better understand its benefits and limitations. We started by building and operating the first batch RO system using a flexible bladder. We used this prototype to validate theoretical models of energy consumptio and water production.

Next, we investigated practical losses associated with batch operation: cycle downtime, salt retention, and water loss. We modeled these losses and validated our models with experimental measurements. Our models predict that today's batch RO designs are not practical due to the combined effects of salt retention and water loss.

We propose a new batch RO design which improves performance by limiting cycle downtime and water loss.

Finally, we investigate the economic feasiblity of batch RO systems. We identify a more promising value proposition for batch RO and identify initial markets for this promising technology.

Don't be afraid to turn on the pump.

2

Prototype

In this chapter we share details about the true batch RO prototype and its successful operation. We built the bench-scale prototype (shown in Figure 2-1) using off-the-shelf parts except for the custom-molded silicone bladder, which has operated for over 100 consecutive cycles with no issues.

I inherited the prototype from Emily & Ali [25].

2.1 Overview

The bladder and RO membrane are both housed inside a pressure vessel. As explained in Section 1.2, the bladder starts out empty at the beginning of the batch RO cycle. During the permeate production phase, a make-up fluid (water, in this case) is pumped into the bladder. A roughly equal amount of water leaves the pressure vessel as permeate through the RO membrane. We provide more details on the batch RO prototype in Section 2.4.

We collected pressure and flow data in order to measure the energy consumption and permeate production of the batch RO system. The pressure and flow data over the course of a single batch cycle are shown in Figure 2-2. The permeate production phase takes place over the first twelve minutes of the cycle. Once the high-pressure pump is turned on, the feed pressure takes about a minute to build up (see Section 2.7). The permeate flux rises along with the feed pressure until it reaches a steady-state value. The feed pressure rises slowly over the course of the permeate production phase

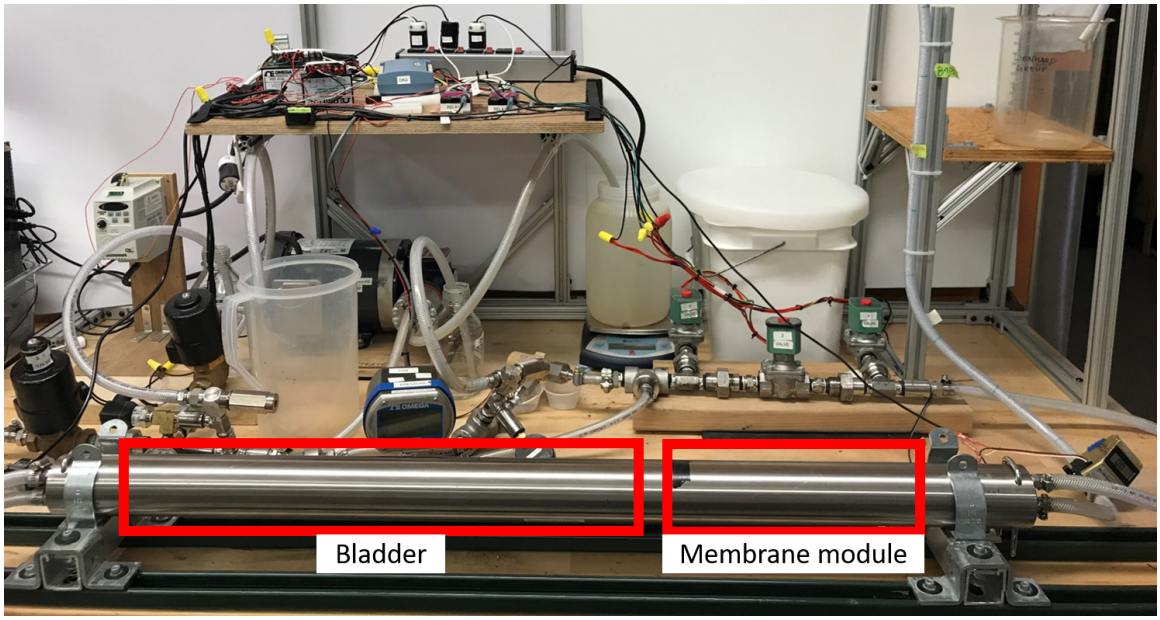

Figure 2-1: In our bench-scale batch RO prototype, a pressure vessel houses a custom-molded silicone bladder and a 2.5 in. (6.4 cm) spiral wound membrane element (Hydranautics ESPA-2514). We use five valves to switch between the phases of the batch RO cycle. We use LabVIEW to automate valve control and collect sensor data.

in order to drive a steady permeate flux (the system salinity increases gradually as permeate is produced). Once the desired amount of permeate is produced, the variable frequency drive (VFD) that drives the high-pressure pump is stopped and valves are opened in order to flush brine out of the system.

The beginning of the flush phase is marked by the rapid fall in feed pressure: the system depressurizes once valves are opened. This depressurization does not result in any significant change of internal energy (or temperature or entropy), because the liquid is essentially incompressible. During the flush phase, the circulation pump brings new feed water into the system and brine is ejected from the system. Once the desired amount of brine is flushed out of the system, valves open or close in order to start the recharge phase. The beginning of the recharge phase is marked by a rise in the circulation pressure and a fall in the circulation flow. The circulation pump is bringing new feed into the system but must push the make-up fluid out of the bladder. The added resistance to flow is due to the bladder. When the bladder is nearly empty, the circulation pressure rises rapidly and the circulation flow comes to

a halt. The recharge phase is complete when there is no more circulation flow. At that point, valves open or close to return back to the permeate production phase. The high-pressure pump turns back on and another batch cycle commences.

There are several practical concerns that arise during the flush and recharge phases, and some of these may be more problematic at higher salinities, as in seawater reverse osmosis (SWRO). Permeate quality can be worse in batch RO compared to continuous RO due to salt passage across the membrane during the flush and recharge phases. Permeate may also be lost due to osmotic backwash during the flush and recharge phases so the plant recovery ratio may be lower than the system recovery ratio.

2.2 Salt passage

Davies et al. observed that permeate quality was initially very poor at the beginning of the batch cycle but improved drastically after the "bad" permeate was flushed out [14]. We have also observed a similar phenomenon in our system. When the batch RO system is unpressurized (as when the system is off or during the flush and recharge phases), there is no water flux but salt continues to pass through the membrane from the feed channel to the permeate channel. Salt passage is driven by a concentration gradient across the membrane, independent of any pressure gradient. Thus, the permeate is relatively salty at the beginning of the next permeate production phase.

As shown in Table 2.1 permeate quality is worst when the permeate production phase is short (i.e. at low recovery ratios). All other factors held constant, if the permeate production phase is longer (i.e. at higher recovery ratios) the permeate quality improves since the additional fresh permeate can dilute the salty permeate. This problem may be mitigated in a batch RO plant which operates at high recovery ratios and continuously throughout the day.

We also observe permeate quality improving after the initial system start-up (lower portion of Table 2.1). When the system is left off there is a relatively long time (hours) for salt to pass through the membrane. Once the system is running in successive

Table 2.1: Permeate quality is worse at the beginning of the permeate production phase due to salt passage before the system is turned on or during the flush and recharge phases. As shown in the upper portion of this table, permeate quality improves at higher recoveries (i.e. longer permeate production phases) since the salty permeate gets diluted with more fresh permeate. Permeate quality is worse for the first batch RO cycle but improves on subsequent cycles due to the shorter time between cycles.

Cycle # [-]	Feed salinity [g NaCl/kg]	Recovery ratio [%]	Brine salinity [g NaCl/kg]	$\frac{t_{\mathrm{pp}}}{t_{\mathrm{cyc}}}$ [%]	Permeate salinity [g NaCl/kg]	Salt rejection [%]
1	2.0	29	2.8	72	0.31	87.0
1	2.0	48	3.8	81	0.19	93.4
1	2.0	52	4.1	86	0.14	95.5
2-5	2.0[1]	52	4.1[1]	81-86	0.08	97.5[1]

[1] The actual values for these quantities are expected to be higher than shown here due to salt retention between batch cycles. The salt rejection given here is taken as a lower bound on the actual performance. For more on salt retention, see Section 3.2.

cycles, there is only a shorter time (∼2 minutes) for salt to pass through the membrane during the flush and recharge phases. This phenomenon is not unique to batch RO; any RO membrane system will be subject to impaired start-up performance [26].

2.3 Osmotic backwash

We have observed osmotic backwash during the flush and recharge phases: permeate re-enters the membrane module through the permeate tube once the system is depressurized. Although the batch RO system consumed energy to produce this permeate, we were not able to actually collect the permeate. Osmotic backwash could lead to entrainment of air into the system, which may result in membrane contamination, dry-out, or fouling [26]. Osmotic backwash may be more problematic at higher salinities since the rate of backwash depends on the salinity difference across the membrane. We do not attempt to quantify the effects of osmotic backwash in the present study.

2.4 Experimental details

The pressure vessel (AMI PV2540SSAU-316) houses both the spiral wound membrane element (Hydranautics ESPA-2514) and the make-up bladder. The bladder was custom molded and is made of a duplication silicone (Zhermack Elite Double 22). The high pressure pump is a positive displacement pump (Hydra-Cell F-20) driven by an electric motor (Marathon 56T17F5322). The flowrate of the high pressure pump was controlled with a variable freqency drive (Automation Direct GS1). The circulation pump was a hot water circulation pump with a brushless motor (Yosoo DC 12V). Five valves were used to change flowpaths during each of the phases (Magnatrol 18A52-W and 18AR52-W, Asco 8210G030 and 8210G087). Valves were opened and closed through solid state relays controlled by a LabVIEW Virtual Instrument.

We measured feed pressure with a pressure transmitter (Wika A-10). We measured the pressure difference across the circulation pump with an digital pressure gauage (Omega DPG409-015DWU). We measured permeate and circulation flowrates with two flowmeters (permeate: McMillan G-111, circulation: McMillan 104). We measured feed, brine, and permeate conductivities with a conductivity probe (Hach CDC40101 IntelliCAL) and converted those values to concentrations via linear interpolation of experimental data [27, 28]. All these measurements were collected with a data aquisition unit (Omega OM-USB-1608GX) and processed using LabVIEW.

Previous studies have modeled the energy consumption of batch RO, but there has been no comparison to experimental data. We compared experimental measurements from our true batch RO prototype to a numerical model of batch RO. Our measurements agree with the model at the various feed salinities, recovery ratios, and fluxes tested. The high-pressure pump work is slightly overestimated in all cases. We believe that the newly-validated model can be used to predict batch RO performance under realistic operating conditions.

2.5 Experimental results

We calculated the hydraulic work (the product of flow rate and pressure rise, $Q\Delta P$) done by the high-pressure and circulation pumps using pressure and flowrate measurements. We assumed that the flow through the high-pressure pump is constant throughout the permeate production phase and equal to the steady-state permeate flow. We used these measurements to validate the energy predictions from an existing model [11], which we modified to account for concentration polarization and the recharge phase. The model predictions for specific energy consumption (SEC) agreed with the experimental measurements (largest error: -2.7%). In this section, we define the error as:

$$\text{Error} = \frac{\text{Model} - \text{Experiment}}{\text{Experiment}} \times 100 \tag{2.1}$$

We show the overall results from fifteen tests in Figure 2-3. We ran a single batch RO cycle for different combinations of feed salinity and flux at various recovery ratios. The model predictions for SEC agree with the experimental measurements, with the largest error (-2.7%) occurring at low recoveries where the cycle times are relatively short. The predicted SEC for low salinity and high flux (w_f = 2 g/kg, J_{sys} = 20 L m^{-2} h^{-1}) levels out at low recoveries (left side of the figure) since the osmotic pressure changes very little over the course of the cycle. The results agree well at higher recoveries, where we expect batch RO systems to be most beneficial due to higher variation in osmotic pressure.

We present the measured and predicted SEC in Table 2.2. The model consistently underestimates circulation pump work and consistently overestimates high-pressure pump work, so those errors partially offset each other. The model underestimates the circulation pump work due to non-zero start-up time (see Section 2.7). The model may overestimate the high-pressure pump work because it does not account for the pressure rise during start-up. At operating conditions higher than 10 bar (as in seawater RO), we expect the model to consistently overestimate the overall SEC, since the high-pressure pump work will be much greater than the circulation pump

work. The SEC figures listed here represent the hydraulic work and therefore do not reflect pump efficiencies, which are presumed to be low at the bench-scale compared to commercial-scale pumps.

Our experiments were limited to operating pressures below 10 bar and recovery ratios below 55%. The parameters used in the model validation are shown in Table 2.3. The osmotic pressure and density of aqueous sodium chloride solutions were calculated using a MATLAB implementation of the Pitzer equations [31, 32]. See Appendix 2.4 for more experimental details.

Concentration polarization

We adjusted the original model from Warsinger et al. [11] to account for concentration polarization (CP). The original model (without CP) consistently underestimated the high-pressure pump work (largest error: -3.35%). After adjusting the model to account for CP the predicted SEC rose in all cases and the model consistently overestimated the high-pressure pump work (largest error: 1.53%). This difference is as expected since higher pressures are required to overcome the elevated osmotic pressure difference at the membrane surface relative to the bulk.

The concentration at the membrane surface is calculated according to the film theory model of concentration polarization [33, 34]. The mass transfer coefficient is obtained via the Sherwood number, which we calculated using correlations from an experimental study on spacer-filled channels [35, 36]. The adjusted model is included in the accompanying data repository [37].

Membrane permeability

We calculated the membrane permeability, A, for each series of tests (with the same feed salinity and flux) according to the following equation:

$$A = \frac{J}{P_f - \mathrm{CP}\pi_\mathrm{f}} \tag{2.2}$$

Table 2.2: Experimental measurements and corresponding model predictions. We list the total specific energy consumption (Tot) in addition to the contributions from the high-pressure pump (HP) and circulation pump (C). Some numbers do not add up precisely due to rounding.

Feed salinity [g NaCl/kg]	Permeate flux [L m^{-2} h^{-1}]	Recovery ratio [%]		SEC_{model} [kW h m^{-3}]	SEC_{exp} [kW h m^{-3}]	Error [%]	% of SEC_{tot} [%]
2.0	20	28.7	HP	0.192	0.192	0.87	79
			C	0.048	0.052	−6.98	21
			Tot	0.242	0.244	−0.80	-
		38.3	HP	0.197	0.197	0.81	80
			C	0.046	0.049	−6.28	20
			Tot	0.244	0.245	−0.60	-
		43.1	HP	0.200	0.200	0.35	81
			C	0.048	0.048	−6.05	19
			Tot	0.245	0.248	−0.88	-
		49.8	HP	0.204	0.204	0.50	81
			C	0.044	0.047	−7.41	18
			Tot	0.249	0.251	−0.99	-
3.5	10	28.6	HP	0.168	0.168	0.18	65
			C	0.082	0.089	−8.20	35
			Tot	0.251	0.258	−2.66	-
		39.5	HP	0.177	0.177	0.17	68
			C	0.079	0.082	−3.84	32
			Tot	0.256	0.259	−1.21	-
		49.4	HP	0.185	0.185	0.92	70
			C	0.078	0.080	−3.03	30
			Tot	0.263	0.265	−0.44	-
		53.4	HP	0.188	0.188	0.62	70
			C	0.077	0.081	−4.16	30
			Tot	0.267	0.269	−0.57	-
3.5	15	29.7	HP	0.202	0.202	0.28	75
			C	0.062	0.066	−6.78	25
			Tot	0.264	0.268	−1.54	-
		39.6	HP	0.206	0.206	0.01	77
			C	0.059	0.062	−4.49	23
			Tot	0.268	0.268	0.24	-
		49.5	HP	0.217	0.217	0.68	79
			C	0.058	0.059	−2.59	21
			Tot	0.276	0.276	0.17	-
		52.3	HP	0.221	0.221	0.96	79
			C	0.057	0.059	−3.18	21
			Tot	0.280	0.280	−0.19	-
5.0	10	29.7	HP	0.210	0.208	1.33	70
			C	0.083	0.088	−5.48	30
			Tot	0.293	0.296	−0.69	-
		39.6	HP	0.221	0.218	1.16	72
			C	0.080	0.085	−5.63	28
			Tot	0.301	0.304	−0.75	-
		44.5	HP	0.227	0.223	1.53	73
			C	0.080	0.084	−4.73	27
			Tot	0.307	0.307	0.17	-

Table 2.3: Parameters used in validation of the batch RO model. We used a 2.5 in. (6.4 cm) spiral wound membrane element (Hydranautics ESPA-2514) in these experiments.

	Parameter	Note	Value	Units
Operational parameters	Intake feed salinity		2-5	g NaCl/kg
	Recovery ratios		29-53	%
	Operating flux		10-20	L m^{-2} h^{-1}
	Initial feed channel velocity		0.06	m/s
	Concentration polarization factor	calculated	1.07-1.14	-
	Maximum feed pressure		10	bar
	Circulation loop pressure drop		0.1	bar
	Circulation pump flowrate		2	L/min
	Permeate pressure		0.09	bar
Batch RO model inputs	Membrane element area		0.47	m^2
	Membrane water permeability		4.05-4.25	L m^{-2} h^{-1} bar^{-1}
	Batch RO system volume		2.8	L
	High-pressure pump efficiency		1	-
	Circulation pump efficiency		1	-

where J is the instantaneous permeate flux, P_f is the feed pressure, CP is the concentration polarization factor, and π_{f} is the osmotic pressure of the feed (as calculated according to the average system concentration). The calculated membrane water permeability was higher (4.25 ± 0.11 L m^{-2} h^{-1} bar^{-1}) for one set of tests ($w_f = 2$ g/kg, $J_{\mathrm{sys}} = 20$ L m^{-2} h^{-1}) compared to the other three sets of tests (4.07 ± 0.24, 4.06 ± 0.14, and 4.05 ± 0.21 L m^{-2} h^{-1} bar^{-1}). The reason for this 5% difference is unclear to us. Permeate flux could be a factor, but further investigation is needed. We also considered membrane compaction as a potential cause. However, there is no clear pattern in the calculated membrane permeability between successive tests.

Standard membrane compaction tests involve steady-state operation at test conditions (i.e., pressure and flux) with deionized water for hours at a time. Those tests may not be applicable to the batch RO process, because the membrane is regularly unpressurized during the flush and recharge phases. In lieu of membrane compaction tests, we operated the batch RO system for 28 hours prior to the model validation tests, using similar conditions (feed water, flux, and recovery). We used the same membrane element for all tests. There were no fouling or scaling agents in our feed

water, so we did not clean the membrane between tests. As future studies delve into fouling or scaling in batch RO, it will be important to develop a membrane compaction test appropriate to the batch RO process.

We used permeability data from the beginning of the permeate production phase (first twenty seconds after reaching the nominal permeate flux) since we expect the salinity of feed in the membrane module to be close to the average system salinity at that point, as opposed to towards the end. It was also important to avoid using data during the pressure and flux fluctuations that occured several minutes into some tests (see Section 2.7).

2.6 Experimental details

The pressure vessel (AMI PV2540SSAU-316) houses both the spiral wound membrane element (Hydranautics ESPA-2514) and the make-up bladder. We sealed off one end of the membrane module's permeate tube with a metal cap. The bladder was custom molded and is made of a duplication silicone (Zhermack Elite Double 22). During initial testing, we ruptured some bladders by filling them past capacity. This can be avoided by carefully keeping track of the volume of make-up fluid in the bladder at all times.

The high-pressure pump is a positive displacement pump (Hydra-Cell F-20) driven by an electric motor (Marathon 56T17F5322). The flow rate of the high-pressure pump was controlled with a variable freqency drive (Automation Direct GS1). The circulation pump was a hot water circulation pump with a brushless motor (Yosoo DC 12V) and was rated for operation up to 10 bar, which limited the system pressure. Five valves were used to change flow paths during each of the phases (Magnatrol 18A52-W and 18AR52-W, Asco 8210G030 and 8210G087). Valves were opened and closed through solid state relays controlled by a LabVIEW Virtual Instrument.

We measured feed pressure (taken to be net pressure at the membrane) with a pressure transmitter (Wika A-10). We measured the pressure difference across the circulation pump with an digital differential pressure gauge (Omega DPG409-015DWU).

We measured permeate and circulation flow rates with two flow meters (permeate: McMillan G-111, circulation: McMillan 104). Pressure and flow measurements were collected with a data acquisition unit (Omega OM-USB-1608GX) and processed by the same LabVIEW Virtual Instrument used for valve control. The relative locations of all instrumentation is shown in Figure 2-4.

The feed water was formulated in the lab using deionized water (Process and Water, Type II) and lab-grade sodium chloride (Sigma-Aldrich ACS reagent, $\geq 99.0\%$ purity). We measured feed, brine, and permeate conductivities with a conductivity probe (Hach CDC40101 IntelliCAL) and converted those values to concentrations via linear interpolation of experimental data [27, 28].

We believe that the dead volumes (shown in Figure 2-4) during flush contribute partially to salt retention. These dead volumes account for 2% of the total system volume. The dead volume by valve 4 could be reduced by replacing valves 3-5 with a three way valve or manifold. Another dead volume is next to the front end of the bladder; we believe the flow is reduced at this location because it is occluded from the feed inlet by the bladder's nozzle.

We designed our batch RO system to avoid entrainment of air into the system. We attached a length of tubing to the permeate outlet of the pressure vessel and secured the tubing to a vertical post, running it up about one meter above the pressure vessel. At the top of the post we bent the tubing into an arch so that the tubing outlet lay directly over a collection tub. During the permeate production phase the water level in the tubing would rise until it reached the apex of the arch and could drip into a collection tub. When the system depressurizes at the beginning of a flush phase, we visually observe the water level fall from the apex, rapidly at first but then at a steadier rate. During the recharge phase the water level would fall more slowly than during the flush phase. We made the tubing long enough such that the water level would still be above the pressure vessel at the end of the recharge phase (to avoid air entrainment).

Experimental procedure

For the model validation measurements (Fig. 2-3) it was important that the initial average system salinity at the beginning of the batch phase matched the nominal feed salinity (e.g., 2 g/kg). Prior to each test, we mixed up feed solution to the appropriate conductivity. We flushed the system of brine from the previous cycle by introducing the newly-mixed feed. Throughout this step we switched between batch mode and flush mode in order to flush brine remaining in dead legs. We measured the outlet stream's conductivity until it was within 2% of the feed solution's conductivity, and then emptied the bladder. At this point we switched to batch mode and began the test, running one complete batch cycle at the nominal recovery ratio. Each data point in Figure 2-3 is a single-sample observation. We ran five auxiliary tests at the same initial feed salinity, flux, and recovery ratio in order to assess the repeatability of our energy measurements and to calculate the 95% confidence intervals [29, 30].

In order to quantify the feed salinity elevation of our batch RO prototype (Fig. 3-5), we measured the initial average system salinity at the beginning of the batch phase once the system reached a steady state. We ran consecutive batch cycles, keeping relevant operating conditions (feed salinity, recovery ratio, and dimensionless flush time) constant[1]. The first batch cycle of each test started out at the nominal feed salinity (e.g., 2 g/kg), and increased in successive cycles due to salt retention. After each batch phase we measured the average conductivity of the rejected brine, which increased in successive cycles along with the initial system salinity. We ended the test once there were three consecutive cycles where the brine conductivity varied by less than 2%. In our tests, this happened within 5-10 cycles.

At the end of the each test, we measured the volume average system salinity. First, we allowed the feed in the system to recirculate for three passes so that the solution would be well-mixed. Next, we switched to the flush phase and collected five successive samples of the reject stream ($\sim$80 mL each). We measured the conductivity of each sample. The conductivities of the second and third samples varied by less

[1]We decreased the operating flux towards the end of the batch phase in later cycles in order to keep the pressure under 10 bar.

than 1%; we took the average of these measurements to be the average system salinity. The conductivities of the fourth and fifth samples were consistently lower than the first and second samples by up to $\sim 3\%$; we attribute this to osmotic backwash. The conductivity of the first sample was much higher than the rest of the samples. It was closer to the brine salinity at the end of the final batch phase because some of that solution was collected from the dead leg with low (or no) flow during the permeate production phase that immediately preceded the system outlet at valve 5 (Figure 2-4).

Each data point in Figure 3-5 represents a single-sample observation. We took eight auxiliary measurements in order to assess the repeatability of the measurement method described above and to calculate the 95% confidence intervals. We were able to take these measurements in concert with some of our steady-state tests because we expected the average system salinity at the end of the first batch phase to be the same in each of those tests, which started at the same initial feed salinity (2 g/kg) and operated at the same recovery ratio (52%). At the end of the first batch phase we turned off the high-pressure pump, but did not immediately switch to the flush phase. We allowed the remaining brine to recirculate for three passes and then measured five samples of the reject stream, as above. Again, we used the measurements of the second and third samples as proxies for the average system salinity. In this case, the first sample's conductivity was much lower than the rest of the samples (closer to the initial feed salinity at the beginning of the batch phase).

The raw experimental data and the data processing code are provided in the accompanying data repository [37].

2.7 Residual air

Despite our best efforts at de-airing the system, we believe that there was still residual air in the system throughout our tests. We attribute the system start-up time ($\sim$1 minute) and the pressure and flux fluctuations to residual air. The system pressure does not respond instantly to changes in flow, as we would expect if there were no air in the system.

System start-up

If all fluid contents in the batch RO system were perfectly incompressible (i.e., only filled with water) and the system components were perfectly rigid, then permeate production would start instantly once the high pressure pump is turned on, as shown in Figure 2-5 (model flux curve). In reality, we observe the pressure increase gradually, and there is a non-zero start-up time before the system flux is achieved. This shows that residual air remained in the system. Air is compressible, so when the high pressure pump introduces water into the empty bladder, the pressure does not rise as rapidly as it would if the system were only filled with water. In our experiments, t_{50}, the time that it takes for the permeate flux to reach 50% of the system flux, has ranged from 20-44 seconds. The circulation pump operates throughout this start-up time, so it consumes more energy than the model predicts.

We think that the start-up time can be reduced by eliminating dead space in the system. However, a gradual pressure build-up may be desirable in order to reduce mechanical stress on the membrane elements [26].

Pressure and flux fluctuations

In some tests, we observed pressure and flux fluctuations occur several minutes into the permeate production phase. We show some of these fluctuations in Figure 2-6. At point 1 the pressure departs from its gradual ascent and dips. This is followed by a sharp increase in the permeate flux, which peaks about twelve seconds later just before the pressure hits a local minimum at point 2, ten seconds afterwards. The pressure rises to another peak at point 3 (34 seconds after point 2) as the permeate flux falls to a local minimum and then sharply increases. The permeate flux hits another peak just before the feed pressure hits the last obvious dip at point 4 (23 seconds after point 2).

These fluctuations might be explained physically by the spatial variation in feed concentration. The dip in pressure at point 1 would occur when relatively less salty feed enters the membrane module. The drop in osmotic pressure would cause the

net driving pressure and permeate flux to increase. The lag in behavior between the permeate flux and the feed pressure suggests that there is air in the system. Assuming the high pressure pump flow is constant throughout the permeate production phase, this increase in permeate flux would be accompanied by a drop in pressure as the residual air in the system is allowed to expand (due to the net outflow of water). As the pressure drops (to a minimum at point 2), so does the permeate flux (to a minimum between points 2 and 3). As less water leaves the system, the residual air would compress and pressure rises again (to a peak at point 3) due to the net inflow of water.

These fluctuations do not appear in every single test. When they do appear, they do not start at the same time. Sometimes multiple fluctuations appear in a row, and other times only one fluctuation is apparent.

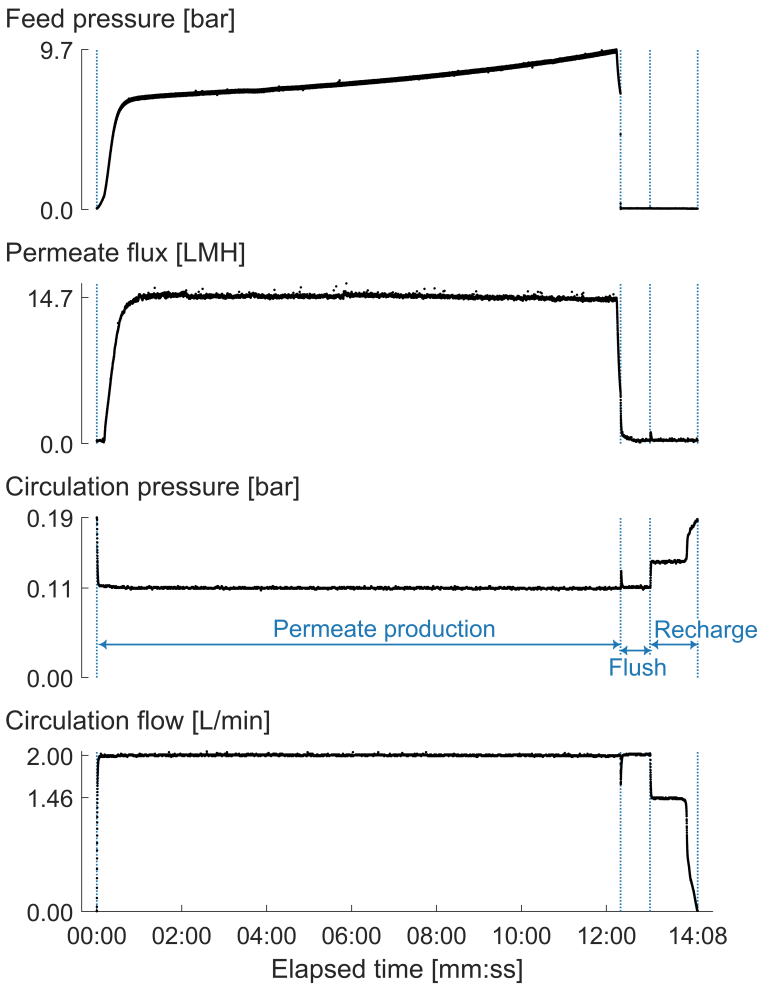

Figure 2-2: Pressure and flow data over the course of a single batch RO cycle. The feed pressure gradually rises over the course of the permeate production phase in order to drive a constant permeate flow. The circulation pressure and flow are relatively constant throughout the entire batch RO cycle. The circulation pressure is greater during the recharge phase since the bladder is being emptied. The system recovery ratio for this batch cycle was 49.5%.

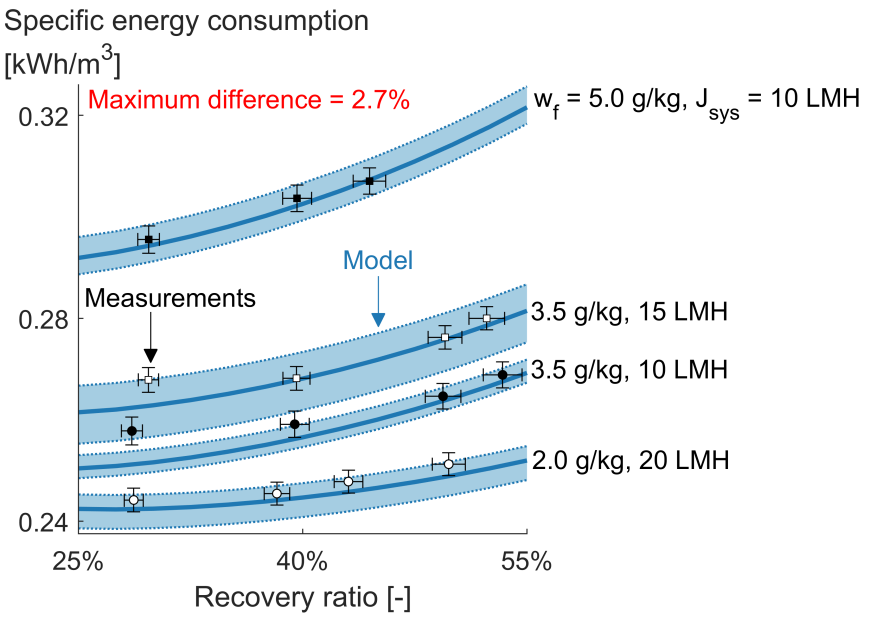

Figure 2-3: The model predictions for SEC agree with experimentally measured SEC (largest error: -2.7.%) at various feed salinities, fluxes, and recovery ratios. This model accounts for concentration polarization. Note that the y-axis does not start from zero. Error bars indicate 95% confidence intervals for the measured data [29, 30]. Dotted blue lines indicate upper and lower bounds on predicted energy consumption based on 95% confidence intervals of the measured membrane permeability.

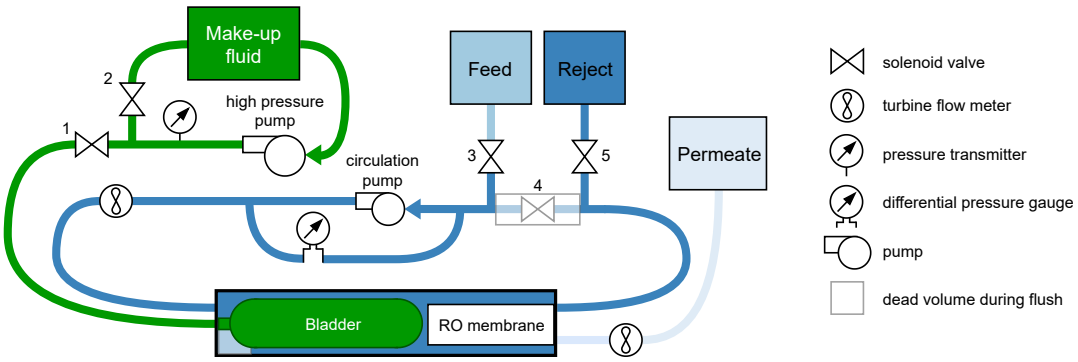

Figure 2-4: A small portion of salt retention is due to dead legs in the system during the flush phase. Here we show two dead legs: one by the brine outlet and one between the bladder and the pressure vessel.

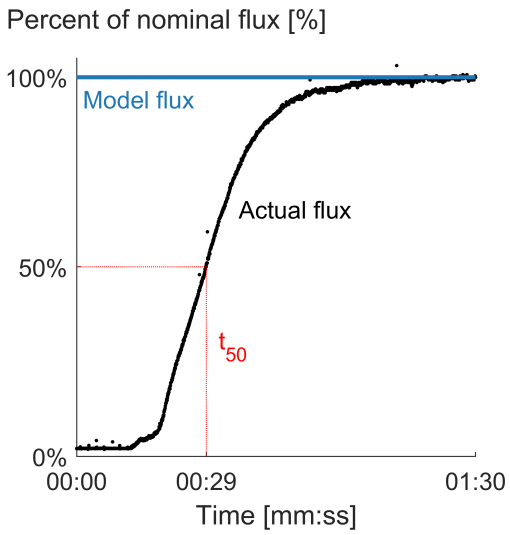

Figure 2-5: The model underestimates the circulation pump work since the batch cycle last longer than predicted. The model assumes permeate production starts instantly at the desired flux. In an actual system there is a non-zero start-up time, likely due to residual air in the system. Here, it takes 29 seconds for the permeate flux to reach 50% of the system flux.

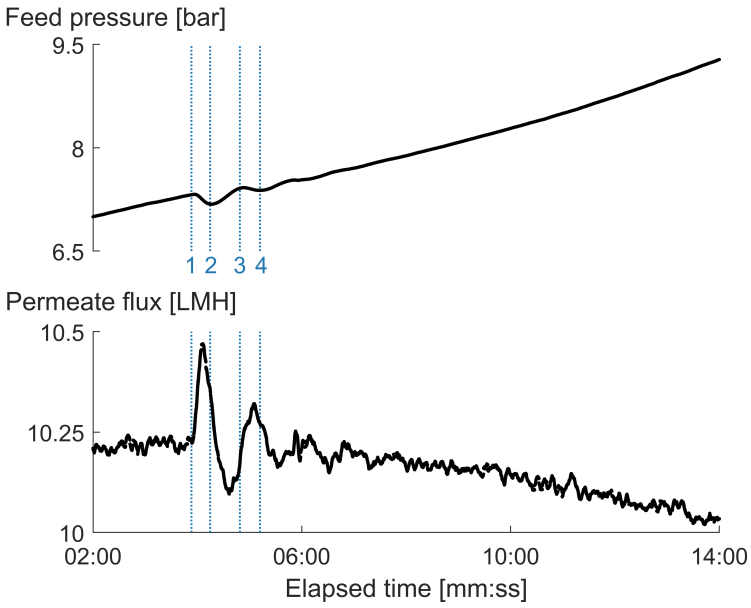

Figure 2-6: Pressure and flux fluctuations from one of the tests. Dotted blue lines mark the peaks and dips in pressure. The peaks and dips in permeate flux trail behind those of the pressure. We show the moving average of pressure and flux over a 5 second window (100 data points) for clarity.

3

Practical losses

We must be careful when comparing a new technology to the state-of-the-art. As many say, comparisons are not useful unless they are "apples-to-apples." One "apples-to-oranges" comparison serves as a cautionary tale. It is possible to reduce the energy consumption of a reverse osmosis plant significantly by operating at a lower system flux. However, the plant would be producing less water per unit area of membrane. In order to produce the same amount of water, more membranes and pressure vessels would be required. If that increase in capital costs are not accounted for, then the comparison is moot.

So how can we make a good "apples-to-apples" comparison? There is no universal prescription. However, a good comparison should consider three aspects: mass flows in and out of the system (feed, permeate, concentrate), energy requirements of the system, and the cost of the system (CAPEX, OPEX). Some of these aspects may be kept the same and others may differ. Where significant differences occur they ought to be acknowledged, if not accounted for.

Batch RO is subject to various practical losses as a result of its batch operation. One of these losses the "salt retention penalty." Due to incomplete flushing of brine, batch RO systems may operate at a feed salinity 10% greater than the feed intake salinity. This difference significantly increases the energy requirements of the batch RO process and cannot be ignored. The other practical losses affect the system flux and recovery ratio.

Throughout this chapter, we account for the above practical losses so that we can compare batch RO to other RO technologies on the following basis:

- Similarly sized plants (equal membrane area)
- Same feed intake (equal feed salinity and feed flow)
- Same freshwater production (equal system flux and recovery ratio)
- Differences in energy consumption (predicted by our models)
- Differences in CAPEX (accounted for in Chapter 5)

I could not have done this without Carson & Priscilla [25]. Emily pushed & pulled [38].

3.1 Cycle downtime

By its nature, a batch process must reset between treating successive batches. This introduces a recurring period of time when the system is not productive. As shown in Figure 3-1, a batch RO system might operate at a flux of 14.9 L m^{-2} h^{-1} during the permeate production phase, but the overall flux of the desalination plant (averaged over an entire batch cycle) is only 12.5 L m^{-2} h^{-1}. The system's operating flux is needed to calculate the energy consumption of a batch RO system, since the operating flux determines the feed pressures during the permeate production phase. On the other hand, the plant's overall flux corresponds to the desalination plant's revenues from selling fresh water since it accounts for the downtime in permeate production, to which a continuous RO plant would not be subject. A batch RO system must therefore operate at a higher flux than a corresponding continuous RO system in order to match the permeate production and revenue of the continuous RO plant (assuming equal membrane area).

In mathematical terms, to achieve a desired plant flux $\bar{J}_{\mathrm{pl}}$, a batch RO system must operate at an increased system flux $\bar{J}_{\mathrm{sys}}$ to compensate for the downtime in

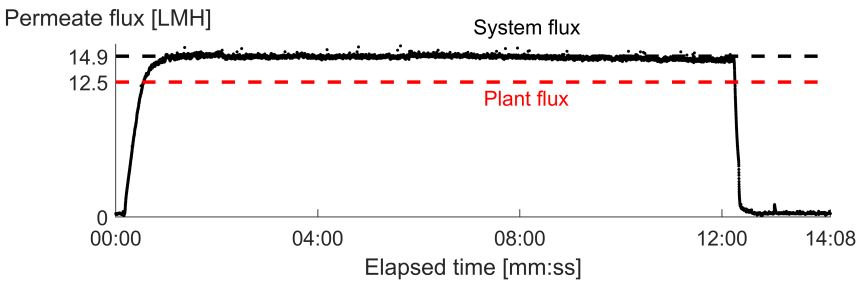

Figure 3-1: A batch RO system operates at a certain system flux during the permeate production phase. The plant flux is lower than the system flux because it accounts for the downtime in a batch cycle.

permeate production. The system flux is related to the plant flux by the ratio of the batch cycle time t_{cyc} to the permeate production time t_{pp}:

$$\bar{J}_{\text{sys}} t_{\text{pp}} = \bar{J}_{\text{pl}} t_{\text{cyc}} \rightarrow \bar{J}_{\text{sys}} = \bar{J}_{\text{pl}} \frac{t_{\text{cyc}}}{t_{\text{pp}}} \tag{3.1}$$

The system flux is always higher than the plant flux because the batch cycle time is greater than the permeate production time. The system flux can be reduced by minimizing the flush and recharge times t_{fl} and t_{re}:

$$\bar{J}_{\text{sys}} = \bar{J}_{\text{pl}} \frac{t_{\text{cyc}}}{t_{\text{cyc}} - (t_{\text{fl}} + t_{\text{re}})} = \bar{J}_{\text{pl}} \frac{1}{1 - \underbrace{\frac{\bar{J}_{\text{pl}} A_m}{V_p}}_{1/t_{\text{cyc}}} \underbrace{\frac{t^* V_b + V_p}{Q_{\text{circ}}}}_{t_{\text{fl}} + t_{\text{re}}}} \tag{3.2}$$

where Q_{circ} is the volumetric flow rate of the circulation pump during the flush and recharge phases. Maximizing the circulation pump flow rate during the reset phases is the most effective way to decrease system flux. Operating at a reduced value of dimensionless flush time t^* would also reduce the flush time but at the penalty of increasing the feed salinity as described above. V_p is the volume of permeate produced and V_b is the volume of brine remaining at the end of the permeate production phase. These volumes are presumed to be constrained by other factors along with the membrane area A_m.

A double-acting batch RO system would reduce, but not eliminate, the downtime of a batch cycle [21] by enabling permeate production during the recharge phase.

As described in the literature, a double-acting system would not produce permeate during the flush phase. The relationship between system flux and plant flux for double-acting batch RO is found as follows:

$$\bar{J}_{\text{sys}} t_{\text{pp}} = \bar{J}_{\text{pl}}(t_{\text{pp}} + t_{\text{fl}}) \rightarrow \bar{J}_{\text{sys}} = \bar{J}_{\text{pl}} \frac{t_{\text{pp}} + t_{\text{fl}}}{t_{\text{pp}}} \tag{3.3}$$

$$\bar{J}_{\text{sys}} = \bar{J}_{\text{pl}} \frac{t_{\text{pp}} + t_{\text{fl}}}{(t_{\text{pp}} + t_{\text{fl}}) - t_{\text{fl}}} = \bar{J}_{\text{pl}} \frac{1}{1 - \frac{\bar{J}_{\text{pl}} A_m}{V_p} \frac{t^* V_b}{Q_{\text{circ}}}} \tag{3.4}$$

A double-acting system reduces the required system flux to achieve a desired plant flux. However, double-acting systems still operate at elevated feed salinities, which increases the required work input.

3.2 Salt retention

A batch RO system will operate at a feed salinity higher than the plant's intake feed salinity. This results in an energy consumption penalty due to the increased osmotic pressure of the feed. This may also have implications for membrane scaling. This elevated feed salinity occurs due to incomplete flushing of brine from the system. This phenomenon, which takes place during the flush phase, is illustrated in Figure 3-2. At the beginning of the flush phase, the system is full of brine. In the ideal (and unrealistic) case, plug flow occurs and the incoming feed would perfectly displace the brine. At the end of the flush phase, all brine would be ejected and the system salinity would match the feed salinity [6, 24].

In reality, mixing occurs between the incoming feed and the outgoing brine. At the end of the flush phase, a mixture of feed and brine remains in the system. The initial feed salinity at the beginning of the next batch cycle is greater than the incoming feed salinity because salt is retained in the system between successive batch cycles. This substantially increases the energy consumption of the batch RO system.

This phenomenon can be explained by Taylor dispersion [39], shown in Figure 3-3. The fluid in the middle of a channel will travel faster than the fluid near the walls

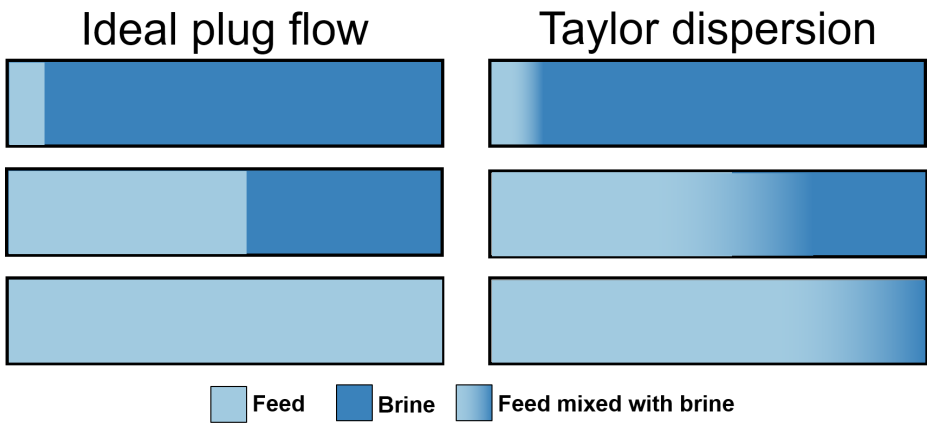

Figure 3-2: A batch RO system will operate at an elevated feed salinity compared to the plant's intake as a consequence of incomplete flushing of the brine. In ideal plug flow, the incoming feed would perfectly displace the outgoing brine. In reality, mixing occurs between feed and the brine (Taylor dispersion) and some brine remains in the system.

(due to friction). Over time, a region of mixing develops.

In a continuous RO plant, the initial feed salinity seen by the RO module is roughly equal to the intake feed salinity. However, in a batch RO plant the initial feed salinity at the beginning of a batch cycle will be higher than the intake feed salinity. A proper comparison between batch RO and continuous RO plants must take feed salinity elevation into account.

3.2.1 Theory

Here we derive the expressions for feed salinity elevation. We have calculated these expressions for both ideal plug flow conditions (unrealistic) and realistic conditions (Taylor dispersion). In both cases we are interested in the steady-state feed salinity of the batch RO system. When a batch RO system is first started, the system feed salinity will initially be the same as the plant feed salinity. After the first batch cycle, the system feed salinity will rise a bit due to incomplete flushing of brine. The system feed salinity will eventually reach a steady-state value. We are interested in this steady-state feed salinity since we expect that batch RO desalination plants will operate for many cycles consecutively.

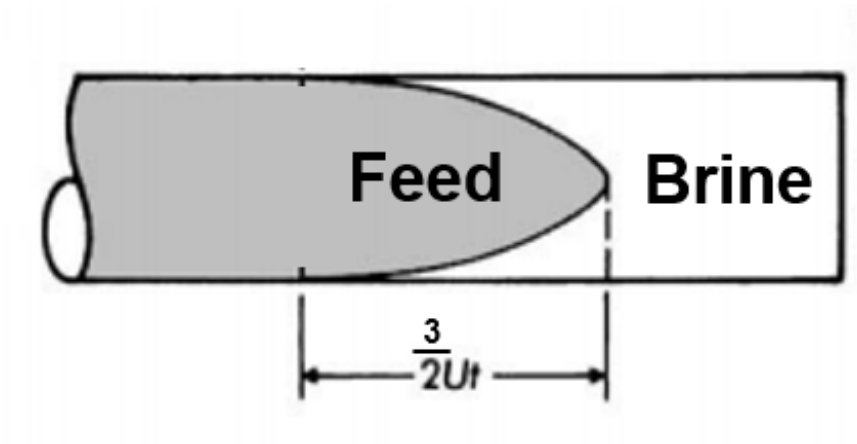

Figure 3-3: The salt retention penalty is explained by Taylor dispersion. Figure adapted from Probstein [40].

Dimensionless quantities

It is useful to introduce a dimensionless feed salinity elevation Θ:

$$\Theta = \frac{w_{f,\mathrm{sys}} - w_{f,\mathrm{pl}}}{w_{b,\mathrm{pl}} - w_{f,\mathrm{pl}}} \tag{3.5}$$

where $w_{f,\mathrm{sys}}$ is the system feed salinity, $w_{f,\mathrm{pl}}$ is the plant feed salinity, and $w_{b,\mathrm{pl}}$ is the initial brine salinity. The numerator of this equation is simply the feed salinity elevation of the batch system. The difference in the initial brine salinity and the plant feed salinity characterizes the mixing that occurs during the flush phase so we normalize by that quantity.

We also introduce the dimensionless flush time t^*:

$$t^* = \frac{t_{\mathrm{fl}}}{V_b/Q_{\mathrm{circ}}} = \frac{t_{\mathrm{fl}}}{t_{\mathrm{fl,plug}}} \tag{3.6}$$

where t_{fl} is the duration of the flush phase, V_b is the volume of brine in the system (membrane module, pressure vessel, and piping) at the end of the permeate production phase, and Q_{circ} is the flow rate of the circulation pump during the flush phase. $t_{\mathrm{fl,plug}}$ would be the flush time required to reject all of the brine (but no feed) from the system under ideal plug flow conditions.

For both of these derivations, we are interested in the volume average system feed

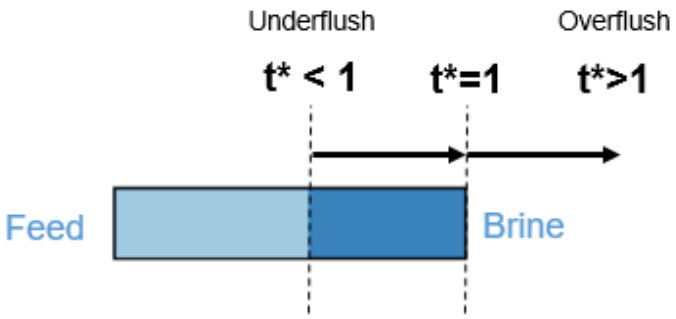

Figure 3-4: When the dimensionless flush time is unity, the system is flushed perfectly under plug flow conditions.

salinity at the beginning of the permeate production phase. This value will reach a steady-state value when the amount of salt that leaves the system is equal to the amount of salt that enters the system between each cycle:

$$m_{\text{salt,in,fl}} + m_{\text{salt,in,re}} = m_{\text{salt,out,fl}} \tag{3.7}$$

where $m_{\text{salt,in,fl}}$ and $m_{\text{salt,in,re}}$ are the masses of salt that enter the system during the flush and recharge phases, respectively and $m_{\text{salt,out,fl}}$ is the mass of salt that exits the system during the flush phase. Zero salt flux into the permeate is assumed.

Ideal plug flow

Under ideal plug flow conditions, Equation 3.7 is readily expressed in terms of the incoming and outgoing concentrations and mass flows:

$$w_{f,\text{pl}}\left[m_{\text{sol,in,fl}} + m_{\text{sol,in,re}}\right] = w_{b,\text{sys}}\left[m_{\text{sol,out,fl}}\right] \tag{3.8}$$

where $m_{\text{sol,in,fl}}$, $m_{\text{sol,in,re}}$, and $m_{\text{sol,out,fl}}$ are the masses of solution that enter and exit the system in the appropriate phases. $w_{f,\text{pl}}$ is the plant intake feed salinity and $w_{b,\text{sys}}$ is the system brine salinity when operating under steady-state conditions. Neglecting the effects of osmotic backwash, we assume the mass of feedwater entering the system is equal to the mass of brine exiting the system during the flush phase. We rearrange this equation and put it in terms of RO operating parameters:

$$w_{b,\mathrm{sys}} = w_{f,\mathrm{pl}}\left[1 + \frac{m_{\mathrm{sol,in,re}}}{m_{\mathrm{sol,out,fl}}}\right] = w_{f,\mathrm{pl}}\left[1 + \frac{RR}{t^*(1-RR)}\right] \tag{3.9}$$

where RR is the system operating recovery ratio and t^* is the dimensionless flush time. We are interested in the system feed salinity rather than the brine salinity. We make a simplifying assumption that salt does not enter the permeate channel to express the system brine salinity (from Eq. 3.9) in terms of the system feed salinity:

$$w_{f,sys} = w_{b,sys}(1-RR) = w_{f,\mathrm{pl}}\left[1 - RR + \frac{RR}{t^*}\right] \tag{3.10}$$

where $w_{f,sys}$ is the system operating feed salinity (the quantity we are interested in). It is useful to express the feed salinity elevation as a dimensionless quantity, so we substitute the equation above into Equation 3.5:

$$\Theta = (1-RR)\left(\frac{1}{t^*} - 1\right) \tag{3.11}$$

where Θ is the dimensionless feed salinity elevation. As expected, the feed salinity elevation is zero when t^* is unity.

Realistic conditions - Taylor dispersion

Under realistic conditions, there is convective mixing between the incoming feed and the outgoing brine. Calculating the mass of salt that leaves the system during the flush phase is not as simple as in the case of plug flow. The concentration at the system outlet varies over time so we must integrate over the duration of the flush phase t_{fl}:

$$w_{f,\mathrm{pl}}\left[m_{\mathrm{sol,in,fl}} + m_{\mathrm{sol,in,re}}\right] = \int_{t=0}^{t=t_{\mathrm{fl}}} w_{\mathrm{exit}}(t)\dot{m}_{\mathrm{sol,out,fl}}\,\mathrm{d}t \tag{3.12}$$

where $w_{\mathrm{exit}}(t)$ is the concentration of the feed/brine mixture at the exit of the system at any time t. $\dot{m}_{\mathrm{sol,out,fl}}$ is the mass flow rate of solution exiting the system and is assumed constant throughout the flush phase. At this point we recognize that it takes time for the incoming feed to travel to the system exit. Towards the beginning of the

flush phase the concentration at the system exit will simply be the brine salinity:

$$w_{f,\mathrm{pl}}\left[m_{\mathrm{sol,in,fl}} + m_{\mathrm{sol,in,re}}\right] = w_{b,\mathrm{sys}}\dot{m}_{\mathrm{sol,out,fl}}t_{\mathrm{tr}} + \dot{m}_{\mathrm{sol,out,fl}}\int_{t=t_{\mathrm{tr}}}^{t=t_{\mathrm{fl}}} w_{\mathrm{exit}}(t)\,\mathrm{d}t \tag{3.13}$$

where t_{tr} is the (dimensional) transition flush time, which depends on the flow velocity profile throughout the system. We assume that the system concentration is uniform ($w_{b,\mathrm{sys}}$) at the beginning of the flush phase in order to simplify the analysis.

At this point, we assume that the mixing is purely convective, as is valid at high Peclet number [39, 40, 6]. In purely convective mixing, the concentration profile in time and space simply depends on the flow velocity profile. We can write an expression for the outlet concentration as long as we keep track of the leading edge of the interface between the incoming feed and outgoing brine. The concentration at the system exit is:

$$w_{\mathrm{exit}}(t) = w_{b,\mathrm{sys}}\left[1 - \frac{r(t)}{a}\right] + w_{f,\mathrm{pl}}\left[\frac{r(t)}{a}\right] \tag{3.14}$$

where a is the width of the entire channel and $r(t)$ is the width of the channel that is occupied by feedwater. We rearrange the terms in this equation:

$$\frac{w_{\mathrm{exit}}(t) - w_{f,\mathrm{pl}}}{w_{b,\mathrm{sys}} - w_{f,\mathrm{pl}}} = 1 - \frac{r(t)}{a} \tag{3.15}$$

We model the flow as laminar flow through a flat channel, which approximates the flow through the membrane channel. Qiu and Davies found that it is reasonable to neglect the spacer's effect on dispersion [6]. The expression for $r(t)$ is known [39, 6]:

$$\frac{r(t)}{a} = \sqrt{1 - \frac{2}{3t^*}} \text{ for } t^* \geq t^*_{\mathrm{tr}} \tag{3.16}$$

where t^* is the dimensionless flush time and t^*_{tr} is the dimensionless flush transition time. This expression shows us that $t^*_{tr} = 2/3$ for laminar flow through a flat channel, which matches our experimental measurements. We evaluated the integral in

Equation 3.13 numerically with MATLAB's `integral` function. We also calculated results for laminar flow through a circular pipe (as in the circular tubing), but our experimental data agreed much better with the flat channel expression.

3.2.2 Experimental validation

When a batch RO system is starting up, the feed salinity at the beginning of the first batch cycle will match the plant feed salinity. However, during the flush phase the incoming feed and outgoing brine will mix (Taylor dispersion)[6]. The feed salinity (averaged over the system volume) at the beginning of the second batch cycle will be greater than the first cycle. After several batch cycles the system feed salinity reaches a steady-state value.

We calculated the dimensionless feed salinity elevation Θ as a function of the dimensionless flush time t^* assuming ideal plug flow and Taylor dispersion through a flat channel [39, 40, 6]. At steady-state, the salt entering the system during the flush and recharge phases matches the salt exiting the system during the flush phase. The salt entering the system is a function of the plant feed salinity. The salt exiting the system depends on the steady-state system feed salinity and can be calculated since we can find the concentration profiles under plug flow and Taylor dispersion conditions.

We also measured the feed salinity elevation of our batch RO prototype. We ran successive batch cycles while keeping all operating parameters constant until the system reached a steady-state (see Section 2.4).

Our calculations and measurements are shown in Figure 3-5. The measured curve lies close to the calculated curve for $t^* \leq 1$. We expect most batch systems to operate in this region to avoid throwing out pretreated feed. At larger values of t^*, the discrepancy between the measurements and the calculations increase. We believe this is due to residual brine in piping dead legs, where there is no flow during the flush phase: no matter how long we flush the system, that brine will always remain in the system for the next batch cycle. Dead legs during the flush phase account for 2% of the total system volume.

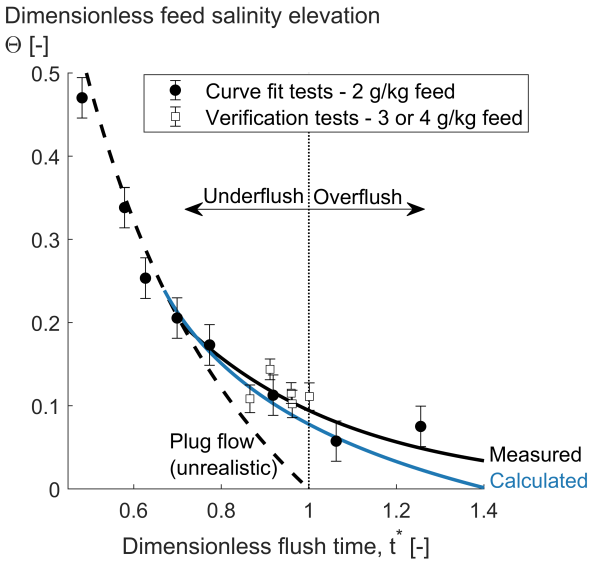

Figure 3-5: Feed salinity elevation decreases as the flush time increases. The measured feed salinity elevation is close to the elevation calculated according to Taylor dispersion in a flat channel. The plug flow curve is shown here for reference but is not achievable in reality. Error bars indicate 95% confidence intervals.

Note that the plug flow curve and Taylor dispersion curve coincide at relatively low values of t^*. When t^* is less than the dimensionless transition flush time t^*_{tr}, the flush phase does not last long enough for any of the incoming feed to make it out of the system. If the feed/brine mixture does not leave the system, the elevated feed salinity ends up being the same as in the plug flow case. Assuming a laminar velocity profile in a flat channel (an approximation of flow through the membrane module) $t^*_{\mathrm{tr}} = 2/3$ since the mean velocity is two thirds the maximum velocity (at the middle of the channel) [6]. We observe a transition flush time close to the expected value from theory: $t^*_{tr} \approx 0.71$ for our system.

The measured curve was obtained by running batch cycles with a plant feed salinity of 2 g/kg, as indicated by the circular data points. We expect this curve to predict the elevation for any plant feed salinity since the mixing is purely convective. In order to verify the predictive ability of the measured curve, we ran additional tests at feed salinities of 3 and 4 g/kg (square data points) but could not go much higher in view of limits on the operating pressure. The results from these tests lie close to the measured curve. In our system, the Péclet number is large enough (80,000) that the

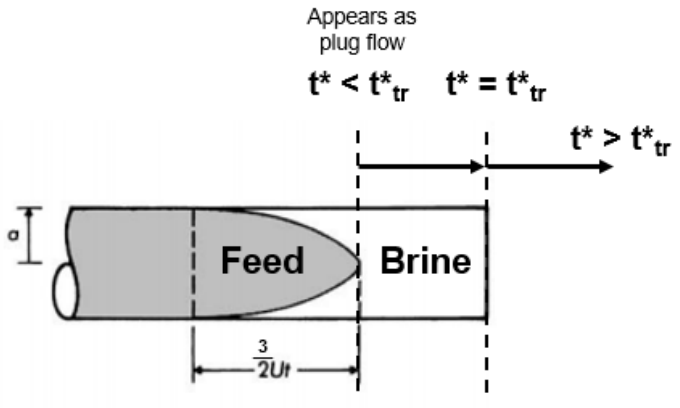

Figure 3-6: In real-life, feed begins to exit the system when the dimensionless transition flush time is equal to unity.

effects of diffusion are entirely negligible [39, 40]. We expect other batch RO systems to also operate at high Péclet numbers during the flush phase to minimize the flush time.

Our batch RO prototype has a maximum recovery ratio of 53%, but other batch RO systems will operate at higher recoveries. Figure 3-5 is only applicable at a recovery ratio of 52% (all tests were run at that recovery). We combine the calculated curve for ideal plug flow with the measured curve to form a general piecewise function for feed salinity elevation:

$$w_{f,\mathrm{sys}} = \begin{cases} w_{f,\mathrm{pl}}\big[1 + RR_{\mathrm{sys}}(t^{*-1} - 1)\big] & \text{for } t^* \leq t^*_{\mathrm{tr}} \\ w_{f,\mathrm{pl}}\big[1 + RR_{\mathrm{sys}}(t^{*-1}_{\mathrm{tr}} - 1)e^{-C_F(t^* - t^*_{\mathrm{tr}})}\big] & \text{for } t^* > t^*_{\mathrm{tr}} \end{cases} \tag{3.17}$$

where RR_{sys} is the system recovery ratio and C_F is the system's flushing effectiveness coefficient. For $t^* \leq t^*_{\mathrm{tr}}$, the measured feed salinity coincides with the plug flow curve. For $t^* > t^*_{\mathrm{tr}}$, the feed salinity elevation curve departs from the ideal plug flow curve. We chose to fit the data to an exponential function; fitting the data to a power function yields similar results. Feed salinity elevation is greater at higher recovery ratios (all other factors held equal) because the brine salinity increases with recovery ratio. From our experimental data, we obtained fitted values of $C_F = 2.57$ and $t^*_{\mathrm{tr}} = 0.71$ for our true batch RO prototype.

We can form a simplified (but not general) expression for the feed salinity elevation

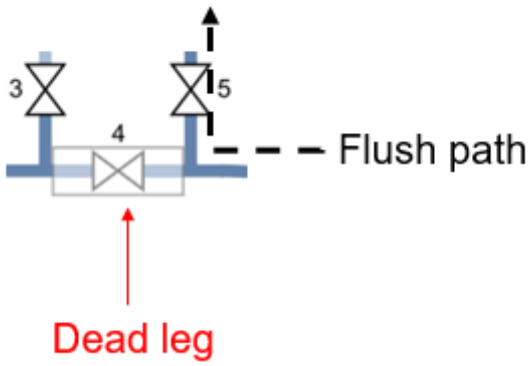

Figure 3-7: Brine within a dead leg does not get flushed out, so remains in the system during the next cyclel, further elevating the feed salinity.

of a batch RO system that has similar system characteristics (i.e., C_F and t^*_{tr}) as our prototype and operates at $t^* = 1$:

$$w_{f,\text{sys}} = w_{f,\text{pl}}\left[1 + 0.19RR_{\text{pl}}\right]$$

3.2.3 Salt elevation due to Taylor dispersion

We have shown that salt retention has a significant on batch RO energy consumption. The salt retention we observed can be divided into different components: a) salt retention due to Taylor dispersion; and b) salt retention due to dead legs in the piping [41]. While the first component cannot be practically avoided, the second component may be minimized by reducing the volume of dead legs in the system.

In Figure 3-8 we have calculated the dimensionless feed salinity elevation due to Taylor dispersion for a range of recovery ratios and flush times. This represents the minimum salt elevation that is to be expected in any batch-type RO system. Additional salt elevation is to be expected but the quantity will depend on the exact piping configuration of the system.

We expect many batch RO systems to operate with a dimensionless flush time of unity to avoid overflushing. In that case, the dimensionless feed salinity elevation can be predicted with the following equation, obtained via curve-fit:

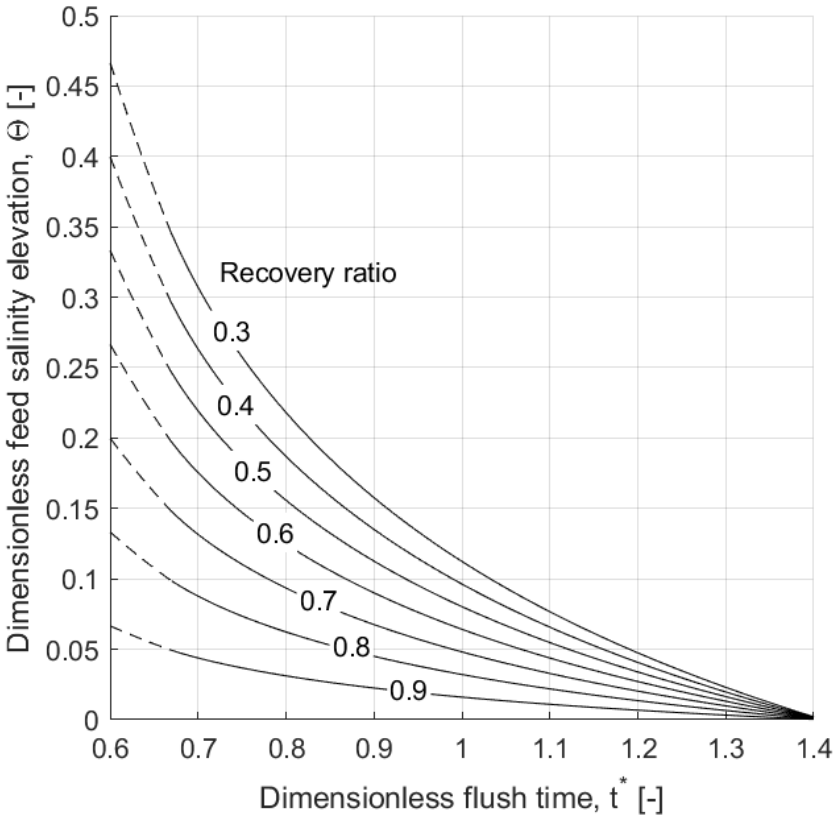

Figure 3-8: Salt elevation resulting from Taylor dispersion in batch RO systems as a function of recovery ratio and flush time. These values are expected to be the minimum amount of salt elevation with the severity of additional losses dependent on system design. Dotted lines indicate predicted salt elevation for plug flow (as expected for $t^* < t^*_{\mathrm{tr}}$.)

$$\Theta_{Td} = -0.16RR + 0.16 \tag{3.18}$$

3.3 Recovery ratio

It is important to have an accurate assessment of a batch RO plant's recovery ratio. The effective recovery ratio reflects the freshwater that is being produced by the plant. The recovery ratio of the batch RO system (along with the elevated feed salinity) will determine the final brine osmotic pressure, impacting energy consumption. A batch RO plant's recovery ratio is affected by operating settings (flush volume) and by a practical loss (osmotic backwash during the reset phases).

3.3.1 Flush volume

During the permeate production phase, a batch RO system recovers a volume of permeate V_p from the initial system volume V_{sys}. The expression for a batch RO system recovery ratio RR_{sys} is:

$$RR_{\text{sys}} = \frac{V_p}{V_{\text{sys}}} = \frac{V_p}{V_b + V_p} \tag{3.19}$$

where V_b is the volume of brine remaining in the circulation loop at the end of the permeate production phase. The system recovery ratio is relevant to calculating the energy consumption of a batch system. However, RR_{sys} does not necessarily reflect the amount of feed water that is taken in by the desalination plant. The plant recovery ratio RR_{pl} accounts for this:

$$RR_{\text{pl}} = \frac{V_p}{V_{\text{f,fl}} + V_{\text{f,re}}} \tag{3.20}$$

where $V_{\text{f,fl}}$ and $V_{\text{f,re}}$ indicate the volume of feed that enters the system during the flush and recharge phases, respectively. The plant recovery ratio should be used when calculating pretreatment and brine disposal costs, since it is the ratio of permeate produced by the batch system to the feed water taken in by the desalination plant.

$V_{\text{f,fl}}$ and $V_{\text{f,re}}$ correspond to $t^* V_b$ and V_p,[1] so we can relate the system recovery ratio to the plant recovery ratio:

$$RR_{\text{pl}} = \frac{V_p}{t^* V_b + V_p} = \frac{RR_{\text{sys}}}{t^*(1 - RR_{\text{sys}}) + RR_{\text{sys}}} \tag{3.21}$$

where t^* is the dimensionless flush time, introduced above. Since the system volume is equal to the sum of the brine and permeate volumes, the system recovery ratio is the same as the plant recovery ratio when t^* is unity. When $t^* > 1$, the plant recovery ratio is smaller than the system recovery ratio: feed water is thrown out of the plant without being desalted.

3.3.2 Water loss

When operating our prototype, we observed significant osmotic backwash during the reset phases. In our prototype, the system is depressurized during the flush and recharge phases. The freshwater in the permeate channel flows across the membrane back into the feed channel. This "water loss" effectively decreases the overall recovery ratio and is accounted for by modifying Equation 3.21:

$$RR_{\text{pl}} = \frac{V_p}{t^* V_b + V_p} - V_{ob} = \frac{RR_{\text{sys}}}{t^*(1 - RR_{\text{sys}}) + RR_{\text{sys}}} - LR \tag{3.22}$$

where V_{ob} is the volume of osmotic backwash and LR is the (water) loss ratio. This water loss must be accounted for when operating a batch RO plant in order to meet permeate production requirements.

3.3.3 Measurements

We measured the the water loss in the batch RO prototype. The prototype discussed in Chapter 2 was modified with a second flowmeter on the permeate line to measure the rate of backwash (McMillan S-111). We also added a new circulation pump (Wanner Hydra-Cell M03) in order to control the circulation and flushing flowrates. We used a DOW TW30-2514 membrane element for these experiments. The membrane

[1] This assumes that airspace in the system is negligible. See Section 2.7.

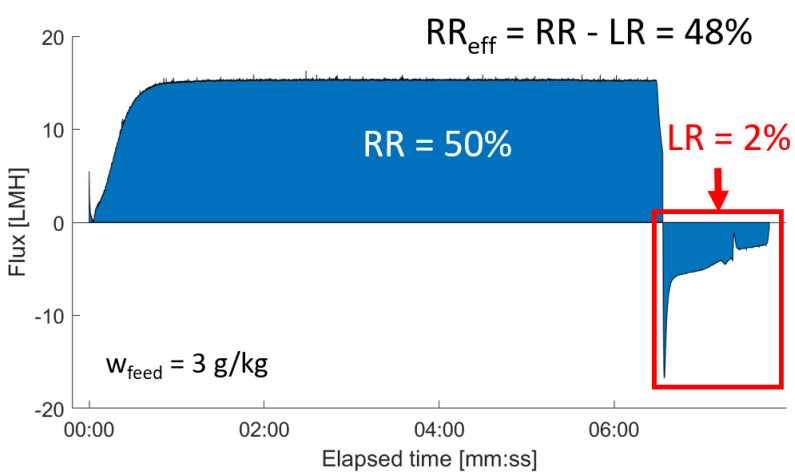

Figure 3-9: Water loss occurs during the flush and recharge phases because the system is depressurized. This reduces the effective water recovery.

was housed in its own 14 in. (35.6 cm) pressure vessel. We manufactured a larger bladder to occupy the entire length of the pressure vessel from the first prototype – increasing the maximum recovery ratio to 65%.

Water flux data from one batch RO cycle is shown in Figure 3-9. The effective recovery ratio is reduced due to osmotic backwash during the flush and recharge phases.

3.3.4 Model

We wrote and validated a model of osmotic backwash in batch RO systems. The validated model was then used to predict the extent of water loss in batch RO systems operating on seawater feeds.

Methods

Modeling osmotic backwash requires a 2D transient model of the convection and diffusion within the feed channel. Our model is based off the model described by Ramon et al. which was validated by comparison to measurements from literature [42]. The computational domain and boundary conditions used to model osmotic backwash are shown in Figure 3-10.

We used FVTool, a simple finite volume solver for MATLAB [43] to build the os-

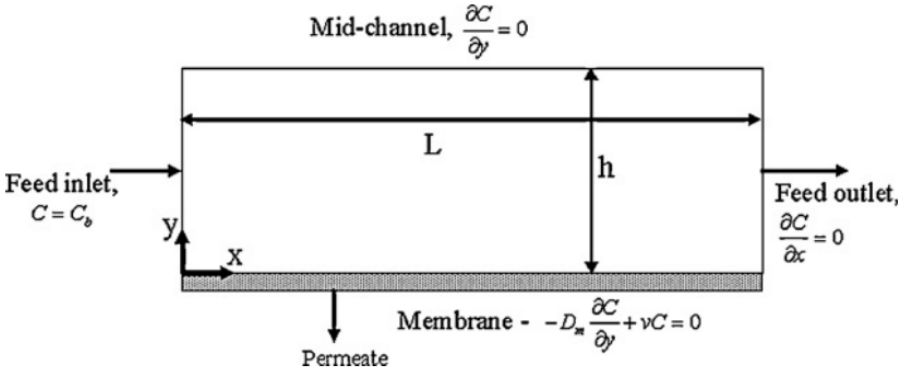

Figure 3-10: We model the feed channel of an RO membrane as shown by Ramon et al. We used the same domain and boundary conditions. Some boundary conditions were adjusted for the recharge phase. Figure from [42].

motic backwash model. One file ("createFaceVariable.m") was modified to accommodate a non-uniform flow field. Our model solves the 2D unsteady advection-diffusion equation:

$$\frac{\partial c}{\partial t} + u\frac{\partial c}{\partial x} + v\frac{\partial c}{\partial y} = D_m\left(\frac{\partial^2 c}{\partial x^2} + \frac{\partial^2 c}{\partial y^2}\right) \tag{3.23}$$

where c is space and time-dependent concentration field, D_m is the solute molecular diffusion coefficient. u and v are the axial and transverse components of the velocity field. We assume fully developed laminar flow, and the transverse velocity component throughout the domain is calculated according to the water flux equation (Equation 3.1).

We modify the boundary conditions and flow field for the recharge phase. In our batch RO prototype, feed does not flow through the membrane during the recharge phase, so the axial velocity component is set to zero. We also modify the boundary condition at the feed inlet to remove the constant concentration condition and replace it with a symmetry condition.

Our model of water flux accounts for the concentrative internal concentration polarization (ICP) that occurs within the support layer. This well-documented phenomenon reduces the water flux by increasing the apparent salinity on the permeate side of the active layer [44]. We model the effects of ICP with the following implicit

equation:

$$v(x) = J_w(x) = A[\pi_{F,m} - \pi_{p,b}e^{J_w K}] \tag{3.24}$$

where $v(x)$ is the tranverse velocity component, J_w is the water flux, A is the membrane water permeability, $\pi_{F,m}$ is the membrane osmotic pressure (feed side), $\pi_{p,b}$ is the bulk osmotic pressure (permeate side), and K is the solute resistivity of the porous support layer [44]. THe water flux, feed side membrane osmotic pressure, and permeate side bulk osmotic prssure vary along the length of the membrane. The appropriate value of J_w is determined iteratively, as described in earlier work [9].

transient –> steady-state

It takes some time for internal concentration polarization to develop. We model this development with a simple logistical growth model:

$$K(t) = \frac{K_{\text{nom}}}{1 + e^{-t}} \tag{3.25}$$

We also accounted for the evolving permeate salinity. During the reset phases, permeate gets saltier as salt diffuses across the membrane without an accompanying water flux. This increase in permeate salinity has been observed in our own measurements as well as in other batch RO systems [45]. We use a simplified model of salt transport to the permeate channel. The volume of the parcel of permeate close to the membrane surface ($\frac{1}{10}$ of the permeate channel volume) is a parameter fitted to one batch RO cycle and used for all other cycles.

$$J_s = B(w_{F,m} - w_p) \tag{3.26}$$

where J_s is the salt flux, B is the membrane salt permeability, $w_{F,m}$ is the feed salinity at the membrane surface, and w_p is the permeate salinity.

Finally, we accounted for the entrance of fresh feed into the membrane, which reduces the rate of water loss. Fresh feed begins to enters the membrane after a certain time t_{mem}:

Table 3.1: Computational parameters for the osmotic backwash model.

Symbol	Parameter	Value	Unit	Note
L	Membrane length	0.3	m	
H	Channel half-height	3.5×10^{-4}	m	symetrical across mid-channel
t	Simulation time	64-106	s	flush and recharge phases
N_x	number of x cells	100	-	per membrane
N_y	number of y cells	90	-	smaller towards membrane
dt	timestep	1	s	

$$t_{mem} = \frac{V_{sys}(1 - RR) - V_{mem}}{\frac{3}{2}Q_{fl}} \tag{3.27}$$

where V_{mem} is the volume of fluid within the membrane element's feed channel and Q_{fl} is the flushing flowrate.

We show the evolution of the concentration field in Figures 3-11-3-13. Similar to past results from literature [42], the concentration polarization layer is quickly swept away and replaced by a dilution layer during the first several seconds of the flush phase (Figure 3-11). We have modeled the entrance of fresh feed (Taylor dispersion) which flushes brine out of the membrane (Figure 3-12). There is no axial velocity during the recharge phase so the dilution layer diffuses upwards away from the membrane (Figure 3-13).

In Table 3.1 we show the computational parameters used to obtain the results throughout the rest of this chapter. Our choice of computational parameters was informed by a grid convergence study, shown in Figure 3-14. We divided the feed channel vertically into three different sections, with the height of the cells in each section getting exponentially smaller as they approach the membrane.

Validation

We compare the predictions from our model with experimental measurements. Ultimately, the quantity of interest is the water loss during the flush and recharge phases. The water loss is highly affected by salt passage across the membrane throughout the reset phase. Salt passage is a function of various membrane properties, which

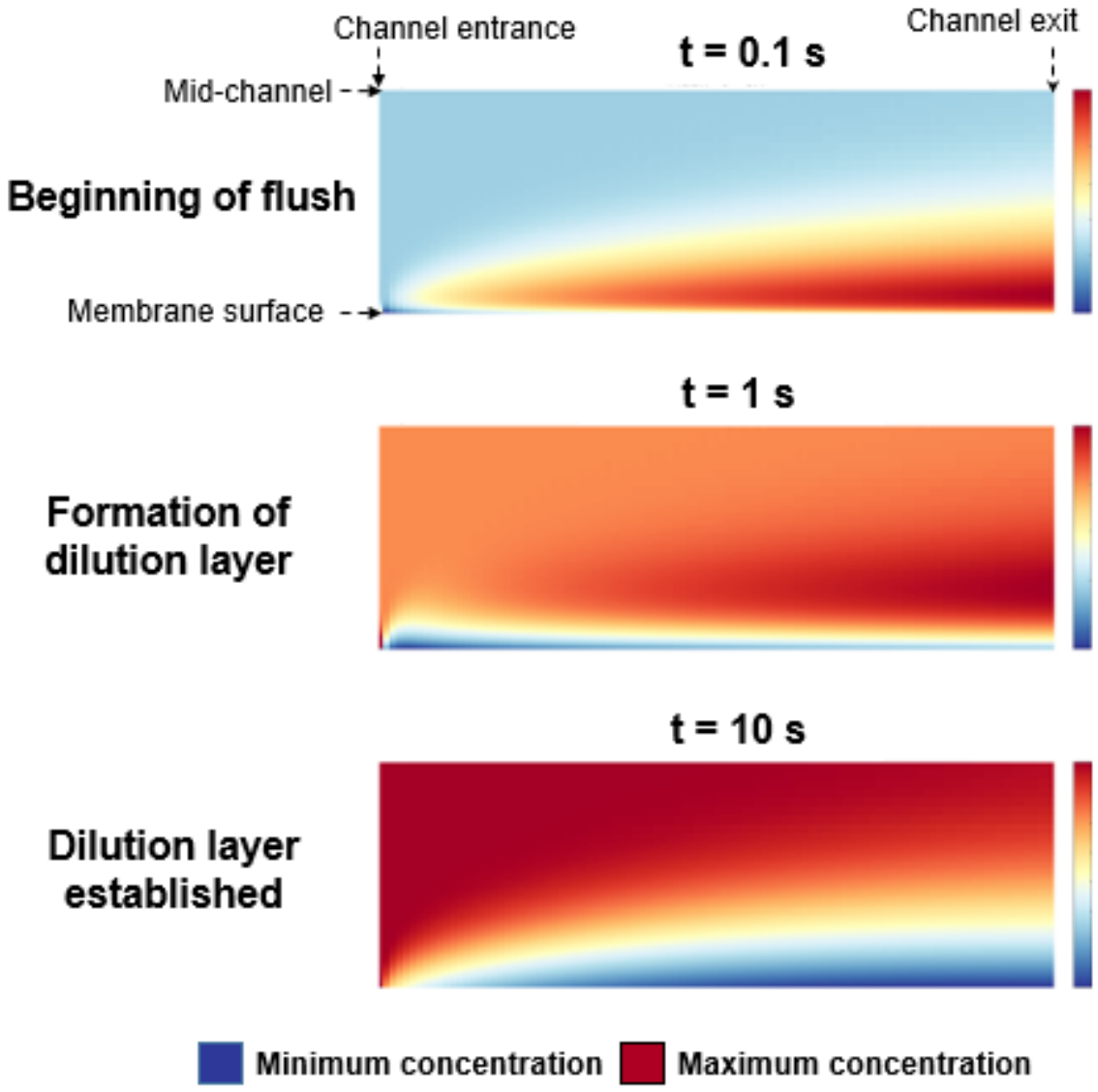

Figure 3-11: At the begininng of the flush phase, there is a concentration polarization layer at the membrane surface, as in regular RO. Once the system is de-pressurized, permeate rapidly enters the feed channel and dilution layer begins to form. The dilution layer replaces the concentration polarization layer within ten seconds. The range of concentrations within the domain decreases with time, but the colorbar is reset at each timestep to enhance visibility.

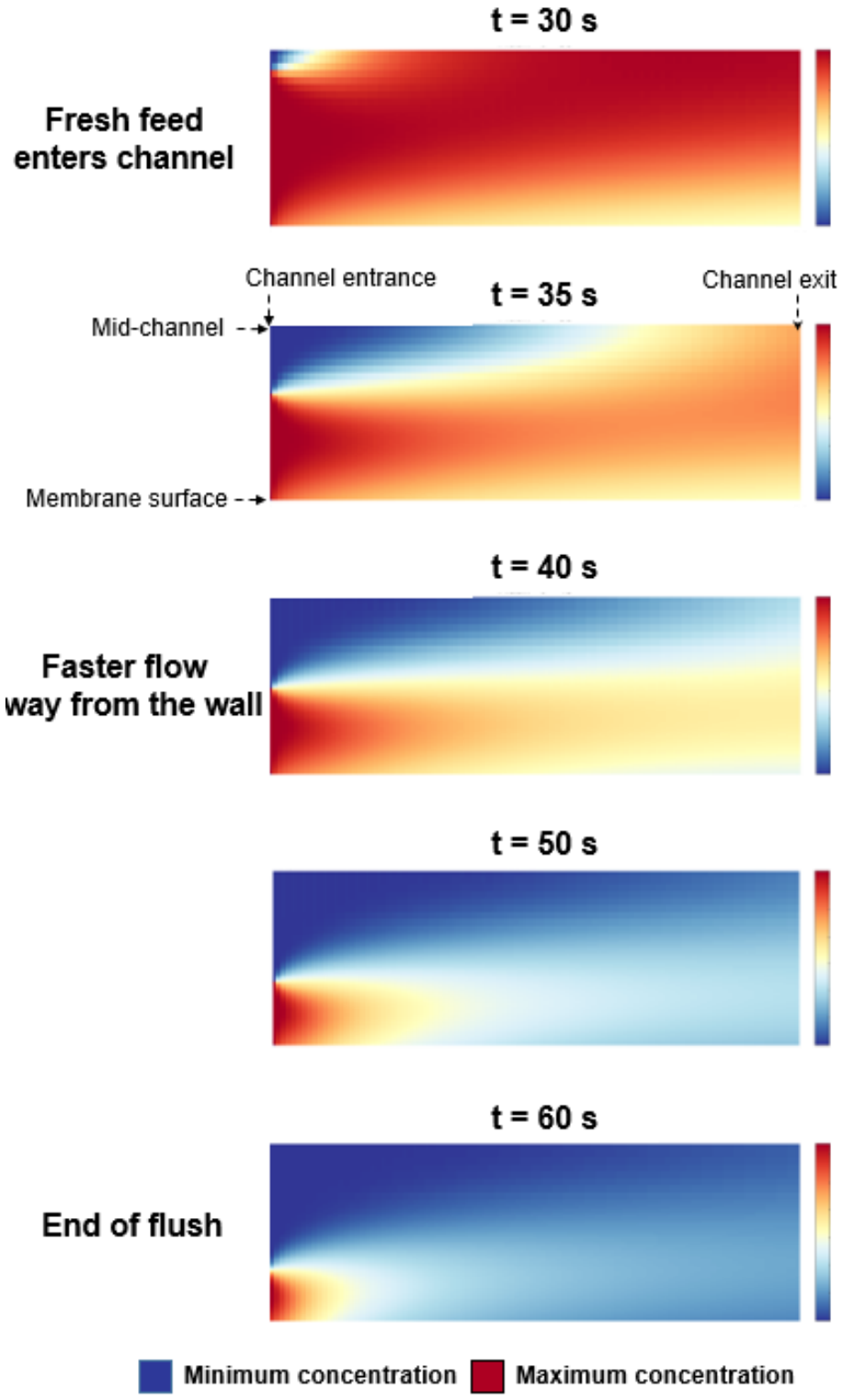

Figure 3-12: Here we can see the effects of Taylor dispersion. Fresh feed begins to enter the feed channel at thirty seconds. The flow is faster at the middle of hte channel away from the membrane surface. The feed flushes out the brine. At the end of the flush phase, the channel is mostly filled with feed except for the fluid in the lower left-hand corner (i.e. at the membrane surface, where the flow is slowest. The range of concentrations within the domain decreases with time, but the colorbar is reset at each timestep to enhance visibility.

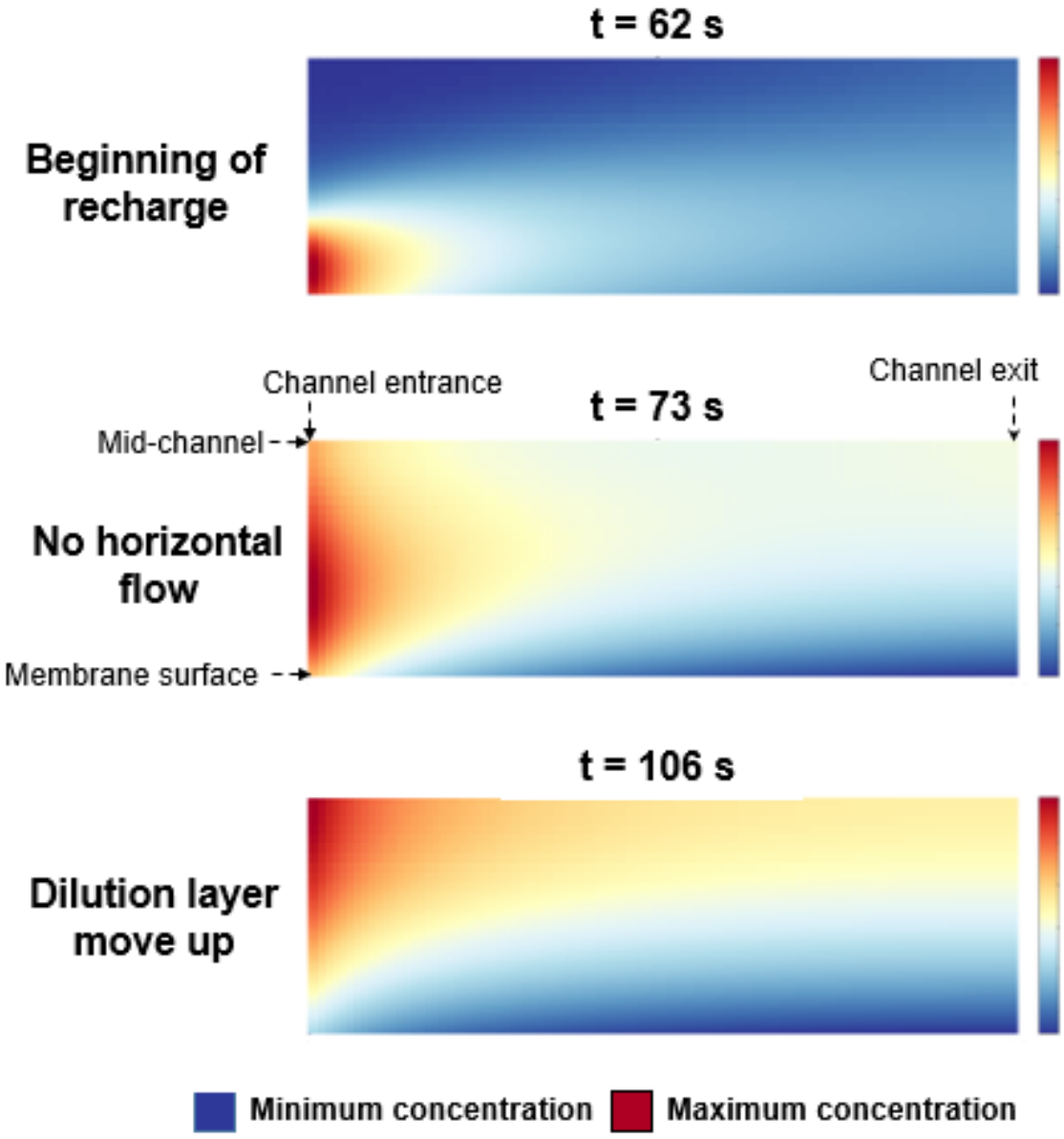

Figure 3-13: In our prototype there is no horizontal flow through the membrane module during the recharge phase. Permeate continues to enter the feed channel through the membrane The range of concentrations within the domain decreases with time, but the colorbar is reset at each timestep to enhance visibility.

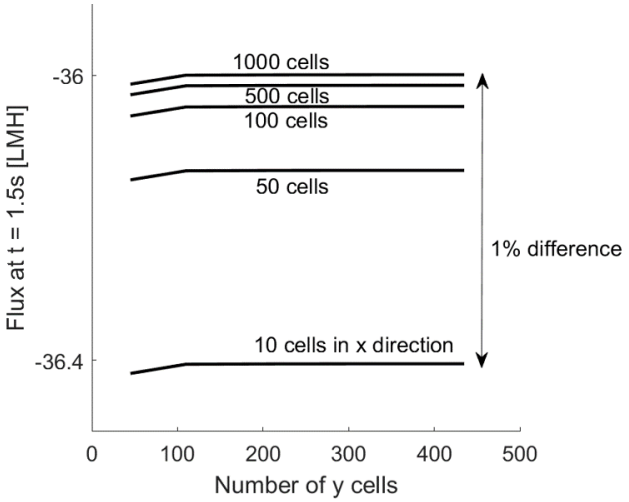

Figure 3-14: We ran a grid convergence study to determine how to discretize the domain. 10 cells in the x direction was sufficient to get within 1% of the baseline value ($N_x = 1000$). We consider the value of the average flux when it is rapidly changing at the very beginning of the flush phase.

were fitted to one measurement and applied to all other tests. The parameters for the osmotic backwash model (Table 3.2) were kept fixed for each of the 15 tests. The model is able to predict water loss to a reasonable degree of accuracy, within 20%. This level of accuracy was sufficient for the present work. To obtain a higher level of accuracy, more sophisticated modeling of the permeate salinity throughout the reset phase would be required.

We show the model predictions and measurements from one batch RO measurement in Figure 3-15. During the first ∼10 seconds of the flush phase, the water flux starts at its largest magnitude and quickly tapers off. This trend is caused by both the removal of the concentration polarization layer and also the development of internal concentration polarization as salt diffuses across the support layer, as modeled by Equation 3.25. The change in flux tapers off by $t = 10$ s but then increases from $t = 15$-30 s. This is attributed to the entrance of fresh feed into the membrane module – decreasing the driving force for osmotic backwash (Eq. 3.27).

There is an upward spike in flux at the moment when the system switches from the flush phase to the recharge phase. This spike likely results from a spike in the feed pressure. The circulation pump is continuously pumping fresh feed into the

Table 3.2: Parameters used to model osmotic backwash in our prototype.

Symbol	Parameter	Value	Unit	Note
A_m	Membrane area	0.7	m^2	
H_f	Feed channel height	7×10^{-4}	m	
L_m	Membrane length	0.3	m	
A	Membrane water permeability	5	L/m^2-h-bar	measured
V_{sys}	System volume	3.56	L	measured
ϕ	Feed channel porosity	0.9	-	assumed
B	Membrane salt permeability	0.2	kg/m^2-h	[46]
K	Solute resistivity, support layer	6×10^5	s/m	[47]
H_p	Permeate channel height	3×10^{-4}	m	
PC	Permeate channel multiplier	0.1	-	fitted

system. Meanwhile the brine outlet valve is closing and the bladder outlet valve is opening. Evidently, both valves are closed for a split-second, while the feed continues to drive the system. This pressure spike can be modeled by manually adjusting the feed pressure during this switch, but we have left that modification out for the sake of simplicity.

Throughout the entire duration, the permeate salinity is gradually increasing as salt diffuses from the feed channel into the permeate channel. The increasing permeate salinity has a significant impact on the water flux because the apparent salinity on the permeate side of the active layer ($w_{p,m}$) is several times greater as a result of concentrative ICP within the support layer. We attribute the error in our model mostly to inaccuracies in predicting $w_{p,m}$.

The water loss ratio in our experiments was generally between 2-4% (Figure 3-16). The model consistently overestimates water loss. We calculated the error in water loss according to the following equation:

$$\text{Error} = \frac{\text{Model} - \text{Experiment}}{\text{Experiment}} \times 100 \tag{3.28}$$

In Figure 3-17 we show the error in water loss from each of our tests. The maximum error is 20% and the model overestimates water loss in each case. The figure shows significant correlation between the error and the duration of the reset phases. In most tests, the model underestimates the magnitude of the water flux during the

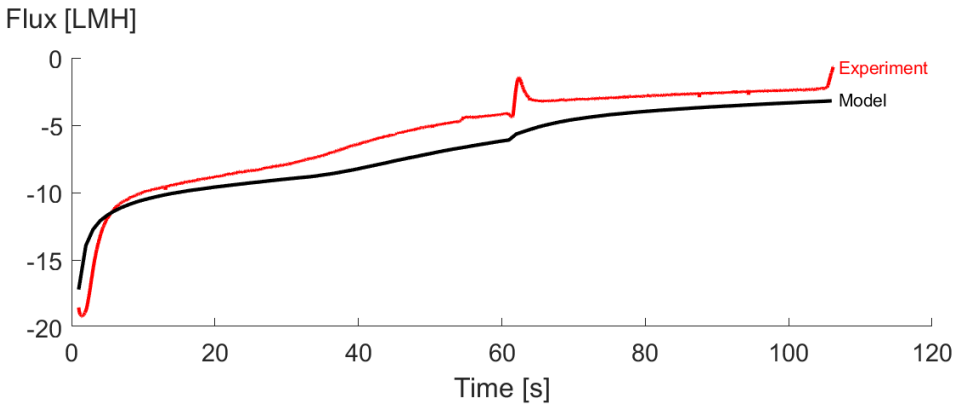

Figure 3-15: A comparison of the measured flux to the flux predicted by our model. Our model captures several key aspects of the measured water flux – development of ICP, introduction of fresh feed, and increasing permeate salinity.

Table 3.3: Parameters used to model osmotic backwash in our full-scale seawater desalination.

Symbol	Parameter	Value	Unit	Note
A_m	Membrane area	37	m^2	
H_f	Feed channel height	8×10^{-4}	m	
L_m	Membrane length	1	m	
A	Membrane water permeability	3	L/m^2-h-bar	measured
V_{sys}	System volume	36-200	L	measured
ϕ	Porosity	0.9	-	assumed
B	Membrane salt permeability	0.1	kg/m^2-h	[46]
K	Solute resistivity, support layer	6×10^5	s/m	[47]
H_p	Permeate channel height	3×10^{-4}	m	
PC	Permeate channel multiplier	0.1	-	fit

first ∼5 seconds of the flush phase and then overestimates the magnitude of the water flux for the remainder of the flush and recharge phases. This error accumulates over the course of the flush and the recharge phases. The open-faced symbols only account for water loss during the flush phase, as would be the case for a double-acting system. When considering only the flush phase, the error in water loss decreases. In some cases, water loss is underestimated by less than 5%.

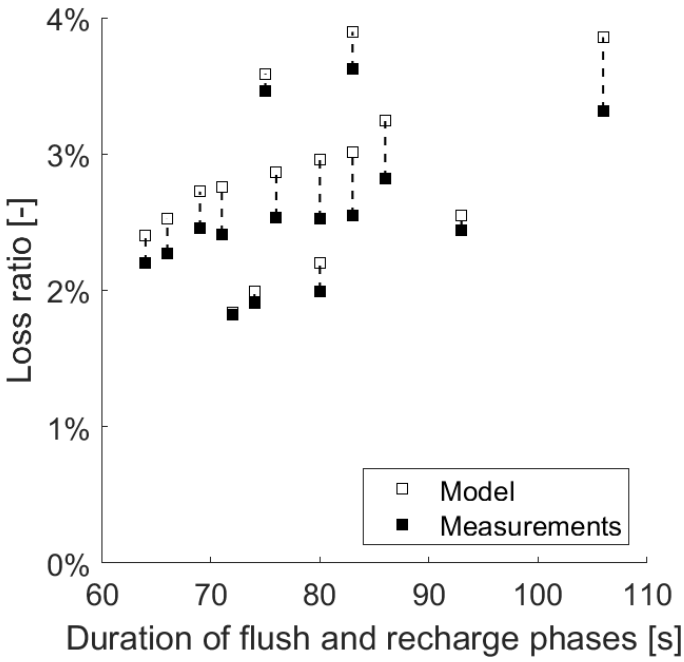

Figure 3-16: The water loss ratio in our experiments (brackish conditions) was always less than 4%. The model generally overestimates water loss.

3.3.5 Analysis

Here we use the validated model to predict water loss in seawater batch RO. The obvious shortcoming in this analysis is the lack of experimental data at seawater conditions. The permeate salinity is a key factor to predicting water loss. Here, we use a simple model of the permeate salinity and fit to the experimental data (i.e. the permeate channel multiplier). This approach might also work for seawater data. If not, a more sophisticated model of permeate salinity might be required to predict water loss in seawater batch RO. One option is to model the concentration field within the permeate channel and couple that domain with the feed channel domain used in this work.

In lieu of experimental measurements, we run the model using a wide range of membrane parameters. In each case, the general conclusion is the same: water loss is significant in seawater batch RO. Table 3.3 shows the parameters used to analyze full-scale batch RO systems throughout this chapter. In Figure 3-18 we show the predicted water loss for double-acting batch RO system operating on a seawater feed

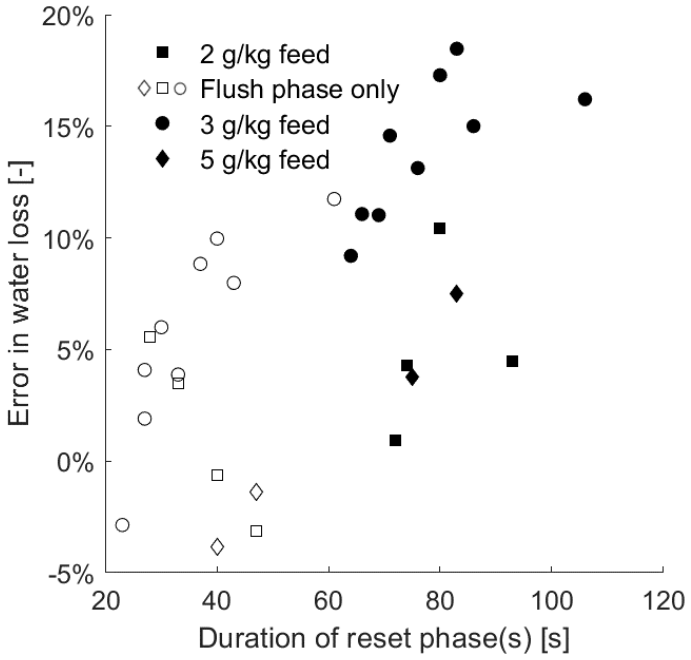

Figure 3-17: Error in predicted water loss for all 15 measurements across a range of feed salinities, dimensionless flush times, and flush speeds. The error generally increases with the duration of the reset phases because the model generally overestimates water flux. The closed symbols reflect water loss across both the flush and recharge phases, while the open symbols only consider water loss during the flush phase (i.e. a double-acting system).

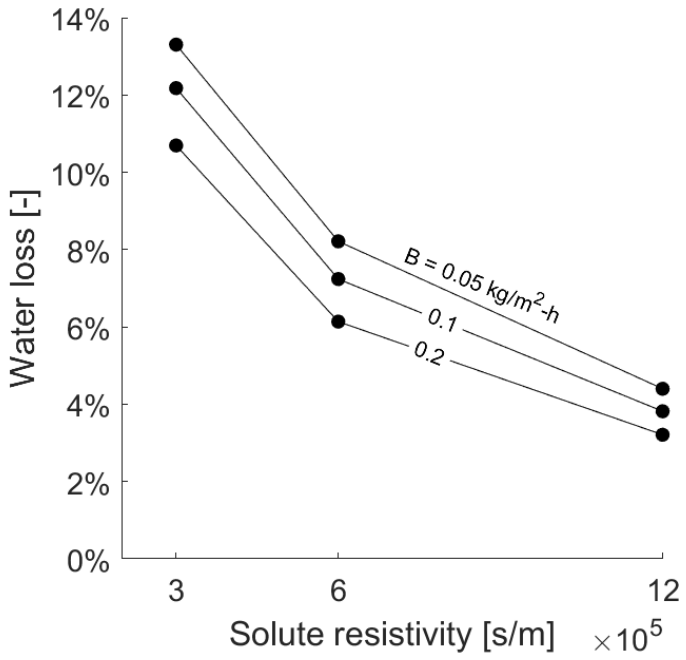

Figure 3-18: The impact of membrane properties on water loss in seawater RO. The support layer solute resistivity has the biggest impact on water loss, so increasing the structural parameter is desirable to enhance the concentrative ICP and reduce water loss. Increased salt permeability is helpful to a lesser extent and will affect permeate quality.

at 50% recovery. The nominal solute resistivity K is 6×10^5 s/m and the nominal salt permeability B is 0.1 kg/m^{-2}-h is representative of today's SWRO membranes. In order to investigate the effects of membrane properties on water loss in seawater conditions, we vary the nominal values of the membrane properties by a factor of two in each direction. The low value of solute resistivity (3×10^5 s/m) is typical of FO membranes. To the best of our knowledge, the high value of solute resistivity (1.2×10^6 s/m) is not found in today's membranes. This value could be approached with new membranes that tune support layer parameters (thickness, tortuosity, porosity).

In conventional RO processes, ICP does not arise over the course of normal operation so not much attention is paid to the structural parameter ($S = KD$). ICP reduces water flux in processes like forward osmosis (FO) or pressure-retarded osmosis (PRO), so those membranes have been optimized to reduce the structural parameter. In batch RO, ICP is helpful in retarding water loss, so a larger structural parameter is

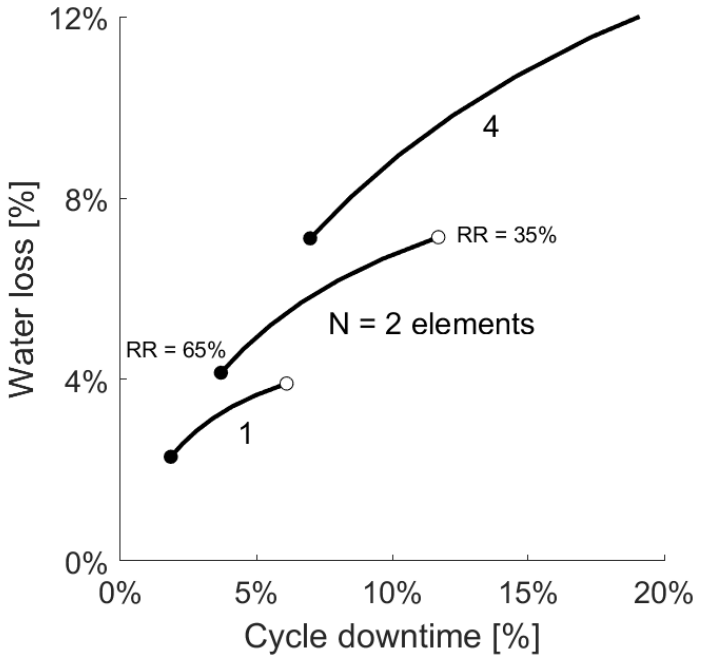

Figure 3-19: Water loss increase with cycle downtime. Here we show the water loss for batch RO systems of three different sizes (N = 1-4 membrane elemetns) operating at recovery ratios from 35-65%. Water loss is greater at lower recovery ratios because there is more brine to flush. Longer systems lose more water because they take longer to flush.

actually desirable in batch RO. The beneficial effects of ICP are further enhanced by salt passage across the membrane. Thus, the salt permeability coefficient might be increased to help reduce water loss, so long as water quality is not compromised. There is an opportunity to tune membrane parameters (water permeability, salt permeability, structural parameter) to tailor the batch RO process for specific applications.

Figure 3-19 demonstrates two design factors which influence the magnitude of water loss in a batch RO system. First, we see that water loss actually decreases with recovery ratio. This result is somewhat surprising given that the brine salinity at $RR = 65\%$ is nearly double the brine salinity at $RR = 35\%$. To understand this effect, we must consider the system volume. The required volume of a batch RO system can be calculated according to the following equation:

$$V_{sys} = V_{br} + V_{bl} = \underbrace{(V_{mem} + V_p + V_{ex})}_{V_{br}} \left(1 + \frac{RR}{1 - RR}\right) \tag{3.29}$$

where V_{sys} is the system volume, V_{br} is the brine volume, V_{bl} is the bladder volume, V_{mem} is the free volume in the membranes, V_p is the volume of the piping, V_{ex} is excess volume, and RR is the recovery ratio. The summation of volumes is equal to the volume of brine remaining at the end of the permeate production phase. In this analysis, we assume that $V_{ex} = 0$, such that the batch RO system is precisely sized to operate at a certain recovery ratio, i.e. the minimum required system volume.

For a fixed number of membranes, the brine volume is constant with recovery ratio, whereas the system volume increases. Because the brine volume is fixed, the duration of the flush phase is constant. The volume of osmotic backwash increases slightly with recovery ratio due to the higher brine salinity. However, the water loss (relative to the system volume) is smaller. Water loss can therefore be reduced by "oversizing" a batch RO system beyond the minimum volume described above. At some point, this will become impractical once the resulting plant density (m^3/day-acre) becomes too low.

We also see that water loss increases with the number of membranes in the system. At a fixed recovery, the ratio of system volume to brine volume is constant. This trend is due to the ratio of the flush phase relative to the batch RO cycle, i.e. the cycle downtime. At $RR = 50\%$, the cycle downtime can vary between 4% (1 element) and 12% (4 elements). The longer the flush phase (relative to the entire cycle), the more water lost.

Water loss affects both seawater and brackish water RO. However, the magnitude of water loss is greater in seawater roughly due to larger driving forces (higher brine salinities). The implications of this water loss are also greater in seawater desalination because of practical limitations on peak pressure and brine salinity. In either case, a batch RO system must operate at a greater recovery ratio to compensate for the water loss. This increase will increase the energy consumption in seawater desalination, which is already at a premium. In brackish water desalination, energy consumption

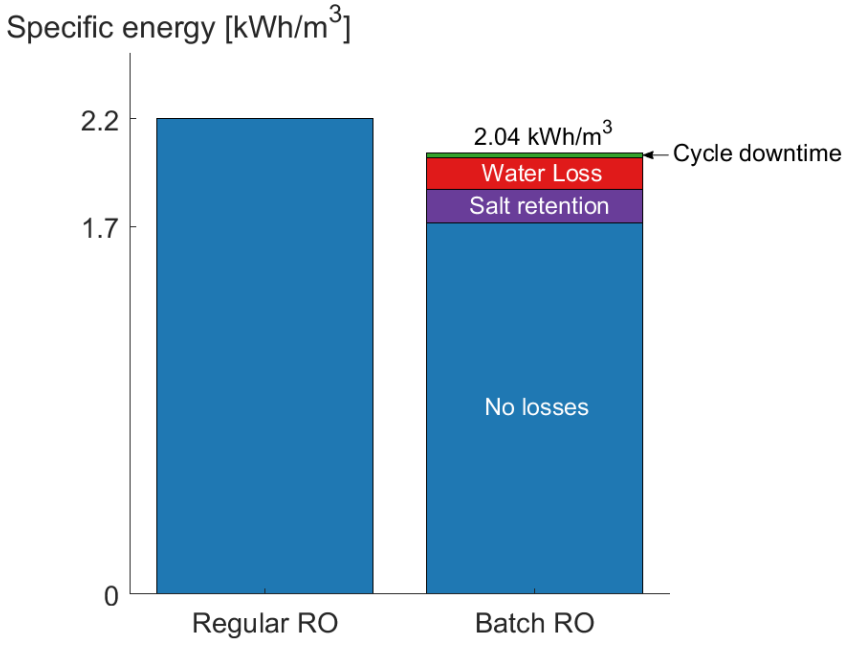

Figure 3-20: The impact of practical losses on seawater batch RO energy consumption. Salt retention and water loss have a bigger impact on energy than cycle downtime. These results are for a double-acting system that operates with a dimensionless flush time of unity.

is less of a concern.

3.4 Conclusions

In this chapter, we have investigated practical losses associated with batch RO: cycle downtime, salt retention, and water loss. In Figure 3-20, we show the individual and cumulative effects of these losses on a double-acting seawater batch RO system (35 g/kg feed, 50% recovery, 15 LMH). Cycle downtime has the smallest impact on energy consumption. Salt retention and water loss each increase energy consumption by roughly 10%. After accounting for the three losses, we find that batch RO saves less energy (7%) than previously expected (22%).

Good things happen in the RK lab.

4

Improved design

In this chapter we discuss an improved batch RO design which minimizes the practical losses discussed in the previous chapter. When batch RO is implemented at full-scale in seawater desalination, we believe this design will be used because it is simple and effective.

One obstacle to rapidly flushing a batch RO system (or any membrane system) is the membrane's maximum feed flowrate. Our design minimizes cycle downtime by decoupling the RO membranes from the rest of the system. This allows us to rapidly flush the system, minimizing cycle downtime and reducing water loss.

I gathered the pieces... Andrew put them together [48, 38].

The bottleneck

In a standard batch RO design, the system is flushed in series with the RO membranes. The flushing flowrate is limited by the membrane manufacturer's maximum recommmended flowrate. Exceeding this flowrate may damage the membranes.

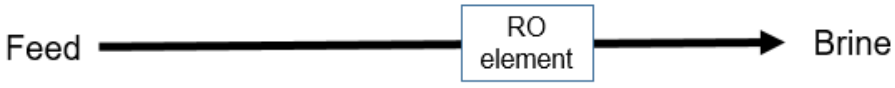

Figure 4-1: The membrane is the bottleneck that prevents us from rapidly flushing normal batch RO systems.

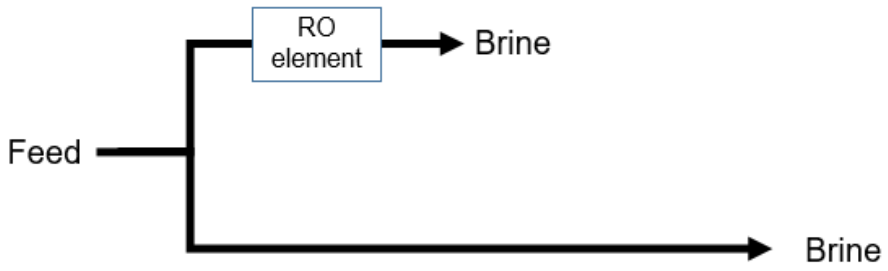

Figure 4-2: In our new design, we branch out to isolate the bottleneck and enable faster flows through the other branch.

Branch out

We branch out to remove the bottleneck. The membrane goes into its own branch, and the rest of the hydraulic circuit goes to another branch. The membrane branch must still stay below the maximum recommended flowrate, but its volume is less. With the bottleneck removed, the main branch can flush in the same time as the membrane branch by increasing flowrates. The two branches are flushed in parallel and the cycle downtime is reduced.

4.1 Design overview

We compare a regular double-acting system to a double-acting system with rapid flushing in Figure 4-3. At the beginning of the flush phase, the system is filled with brine from the permeate production phase. This brine must be flushed out and replaced with fresh/new feed to reset the system for the next cycle. Pumps (not shown here) must bring new feed into the system while pushing old brine out of the system. In the regular double-acting system (Figure 4-3a) the flushing flowrate is constrained by the maximum allowable flowrate ($\sim$ 16 m^3/h for Dow 8" elements) through the membranes, so it can take about half a minute (7% of the cycle time) to flush the system.

In the rapid flushing design (Figure 4-3b), the membranes (the bottleneck) are decoupled from the main branch and the two branches are flushed in parallel. The feed flow must be spit (via valves, not shown here) to provide water to both branches.

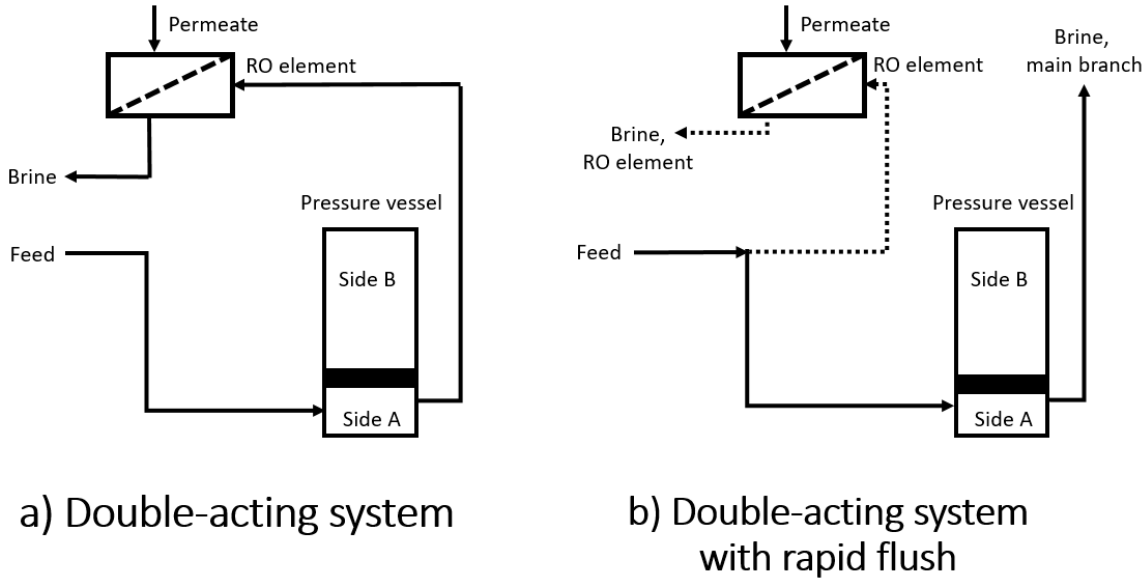

Figure 4-3: In a standard double-acting batch RO system (a) the flushing flowrate is limited by membrane manufacturer specifications. In these systems, the cycle downtime may be ∼7% of the whole cycle, resulting in significant water loss (10%). Our new design (b) rapidly flushes the system while staying within the specific maximum flowrates. The membranes are separated from the rest of the system. This simple improvement greatly reduces cycle downtime (1%) and water loss (3%).

Here, the membranes are flushed at the maximum allowable flowrate. The volume in the main branch is greater than the volume in the membranes (∼3 times greater in our reference system), so it must be flushed three times faster in order to match the membrane flushing time. By parallelizing the bottleneck with the rest of the system, the system can be flushed much faster (1% of the cycle time).

4.1.1 Further parallelization

In the above example, the membranes were the bottleneck that prevented the flush time from being reduced further. After decoupling the membranes from the main branch, another bottleneck remains. The membrane portion may continue to impose a minimum flush time. The main branch could become the limiting factor, if the high flowrates would lead to excessive energy consumption due to increased pressure drop. Whatever the case, it is possible to take the design further by decoupling the next bottleneck and parallelizing it with the rest of the system. We illustrate this in

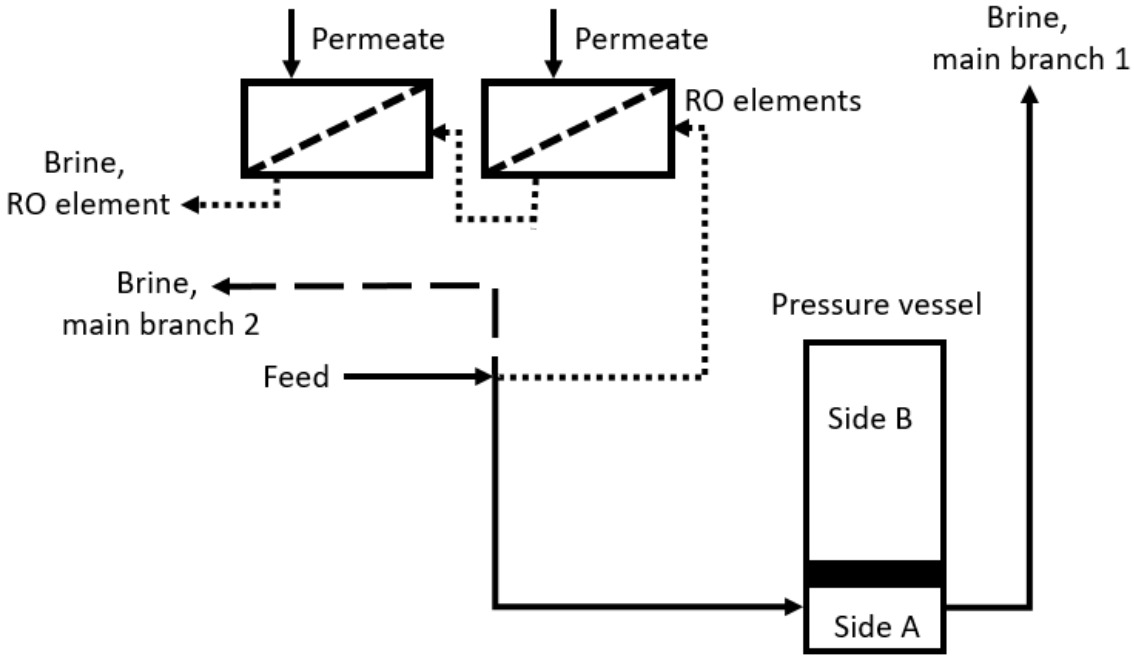

Figure 4-4: This design principle can be extended by identifying the next bottleneck and further parallelization. Here, we split the main branch into two smaller branches. The entire system can be flushed in the same amount of time but with lower flowrates (and pressure drop) throughout the main branches. The membrane branch could also be subdivided in a similar manner (not shown here).

Figure 4-4 by splitting up the main branch into two smaller branches. This would allow for the same rapid flushing but with lower flowrates through both of the main branches. The same concept could be applied to the membrane branch by splitting it up further. This can be repeated until it is no longer practical to further reduce the flush time.

4.1.2 Pump configurations

Several different pump configurations may be used to implement this design.

In one configuration (Figure 4-5a) the high-pressure pump must serve two functions: during permeate production it must deliver high pressures (30-80 bar) at low flowrates (18 L/min) and during flush it must deliver high flowrates (260 L/min) at low pressures (friction within the elements: $\sim$1 bar). The T100 Hydra-Cell pumps (Wanner Engineering, MN, USA) may work, but this unusual mode of operation will

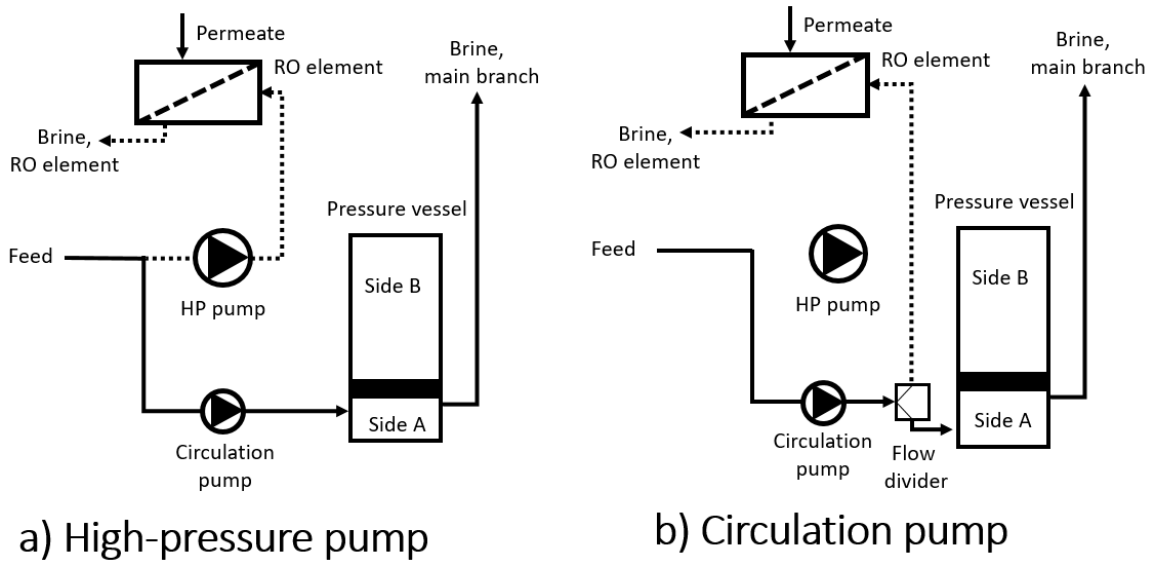

Figure 4-5: There are several possible pump configurations for this design: (a) the high pressure pump could used to flush the membrane, but pump reliabilty may be a concern; (b) the circulation pump could be used with a flow divider to flush both branches. The circulation pump would need to be rated for the combined flow of both branches. Another possibility (not shown here) is to add a new pump to flush either branch.

need to be tested and long-term reliability of the pump would be a concern.

In an alternative design (Figure 4-5a), the circulation pump paired with a flow divider could provide flow to both the membrane branch and the main branch. The circulation pump would need to be rated for the combined flow of both branches and the flow divider would be a new component, both increasing the cost of the system.

In yet another design (not shown here), a new pump could be added to flush either the membrane branch or the main branch. This design might make the most sense in a very large plant with many batch RO systems. The new pump could be shared amongst multiple batch RO skids if their operation were staggered so that the flush phases did not overlap. In this case, the cost of the new pump and the piping to each of the skids would be relevant.

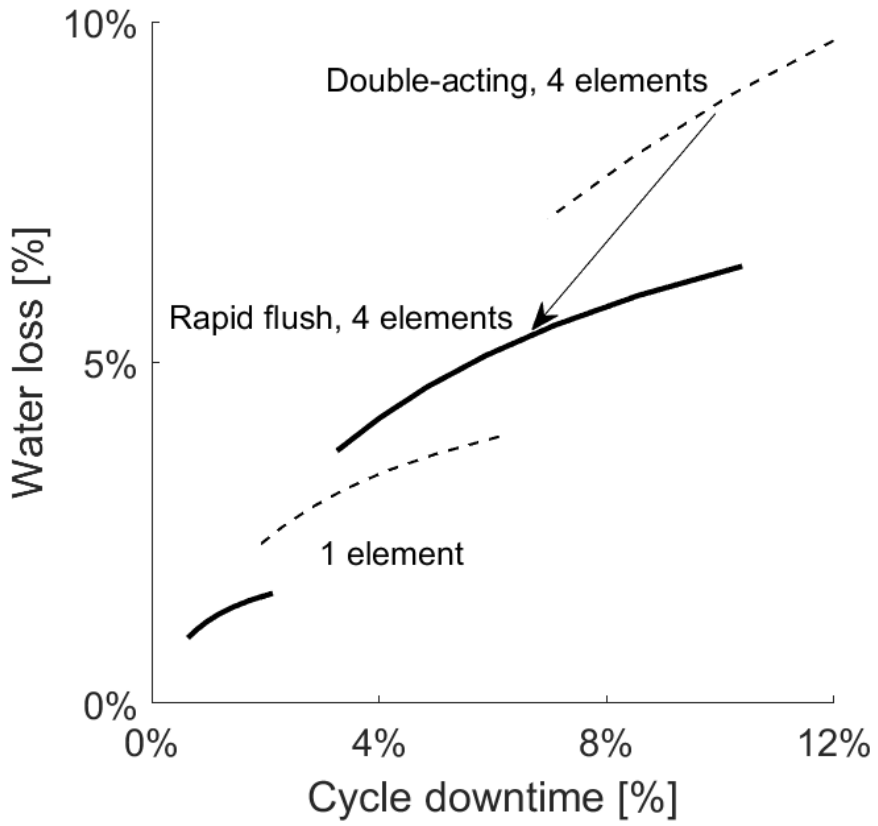

Figure 4-6: The rapid flushing improvement substantially decreases the cycle downtime and thus reduces water loss.

4.2 Performance comparison

In Chapter 3, we found that the combined effects of salt retention and water loss significantly degraded batch RO performance. Despite reducing water loss, a double-acting system does not provide significant energy savings in seawater desalination. We find that a rapid-flushing double-acting batch RO system provides significant energy savings (13%) by minimizing cycle downtime and water loss (Table 4.1). The amount of water loss is further reduced because the membrane is filled with fresh feed much quicker than in the other systems.

Table 4.1: A double-acting batch RO system with rapid flush outperforms other designs by minimizing water loss. In this comparison, each system has the same membrane area and operates on a 35 g/kg feed at flux of 15 LMH and at 50% overall recovery. The continuous RO system is single-stage with isobaric ERDs ($\eta = 92\%$).

		Continuous RO	Batch RO		
			Single-acting	Double-acting	
					Rapid flush
Cycle downtime	[%]	-	10%	7%	1%
Water loss	[%]	-	13%	10%	3%
Energy usage	[kWh/m^3]	2.20	2.29	2.04	1.94
Energy savings	[%]	-	+(4%)	-7%	-12%

4.3 Alternate designs

We considered several alternate designs to reduce water loss in batch RO before arriving at the rapid flushing design. The first two were not as effective. The last design effectively limits water loss with a check valve, but has significant practical limitations.

4.3.1 Pressurized Flush

In this design, the system would stay pressurized during the flush phase in order to reduce backwash. If the hydraulic pressure precisely matched the osmotic pressure, there would be no flow in either direction. The hydraulic pressure could exceed the osmotic pressure in order to produce permeate – essentially acting as a continuous RO system during the flush phase. This scheme has been used by Desalitech with a side conduit to reduce downtime in their CCRO/semi-batch RO systems [19].

In the case where hydraulic pressure precisely matches the osmotic pressure, the energy consumption increases dramatically from 2.29 kWh/m^3 to 4.05 kWh/m^3. This is because the entire brine volume is being pressurized while no additional permeate is being produced, akin to a continuous RO system without energy recovery devices.

This design does not seem practical due to its high energy consumption or need for energy recovery devices. It seems unlikely that anyone would want to deal with both a batch RO bladder/piston and an energy recovery device when simpler designs

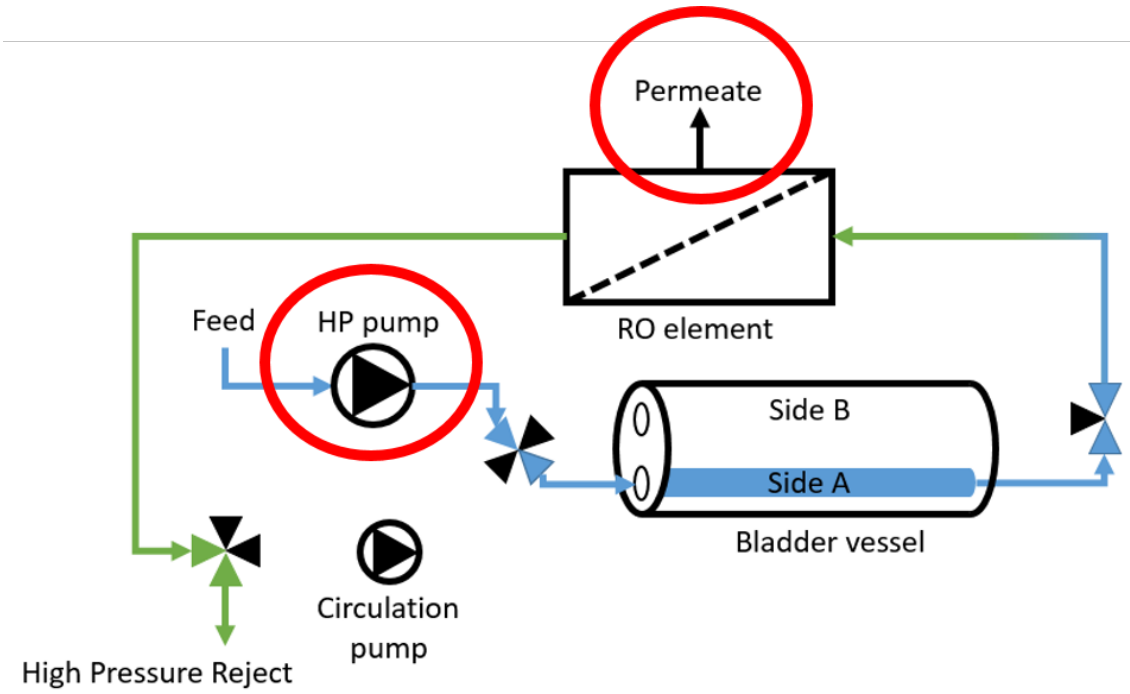

Figure 4-7: One way to eliminate backwash is to pressurize the brine while it is being flushed out of the system. This hybrid batch-continuous RO system can avoid water loss but requires a significant amount of energy to pressurize the brine stream.

are available.

4.3.2 Isolate membrane

Another option is to isolate the RO membrane from the rest of the system, as shown in Figure 4-8. In a standard batch RO system, water backwashes into the system during the reset phases because water is flowing through the system. In this design, the RO membrane would be sealed off from the rest of the system. As backwash occurs, the pressure would ramp up significantly due to the incompressibility of water (neglecting airspace).

This design is effective in limiting water loss, but results in a further salt retention penalty. The brine within the membrane element remains in the system during the next cycle and elevates the feed salinity, on top of the salt retention discussed in Section 3.2. We find that this design reduces batch RO energy from 2.29 kWh/m^3 to 2.14 kWh/m^3. Performance might be further improved by optimizing the system

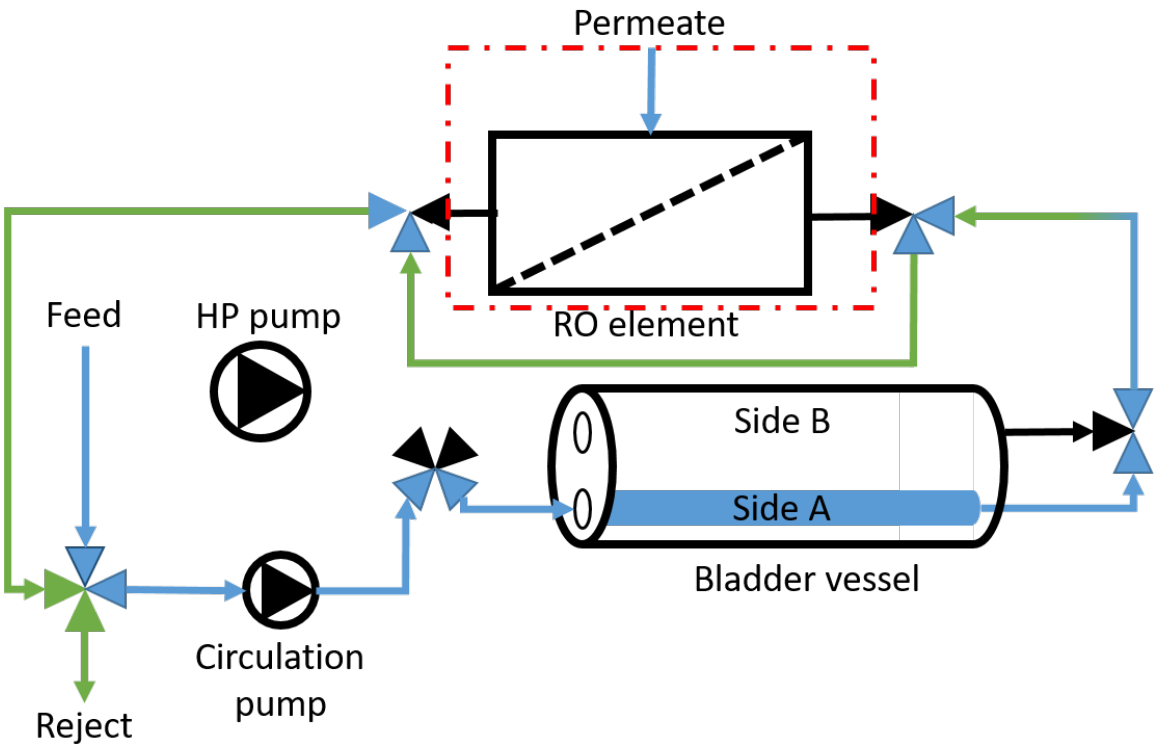

Figure 4-8: In this design, the membrane is isolated from the rest of the system. Water loss should be minimal because the membrane is a closed volume. However, the brine in the membrane remains in the system and further elevates the feed salinity (on top of Taylor dispersion).

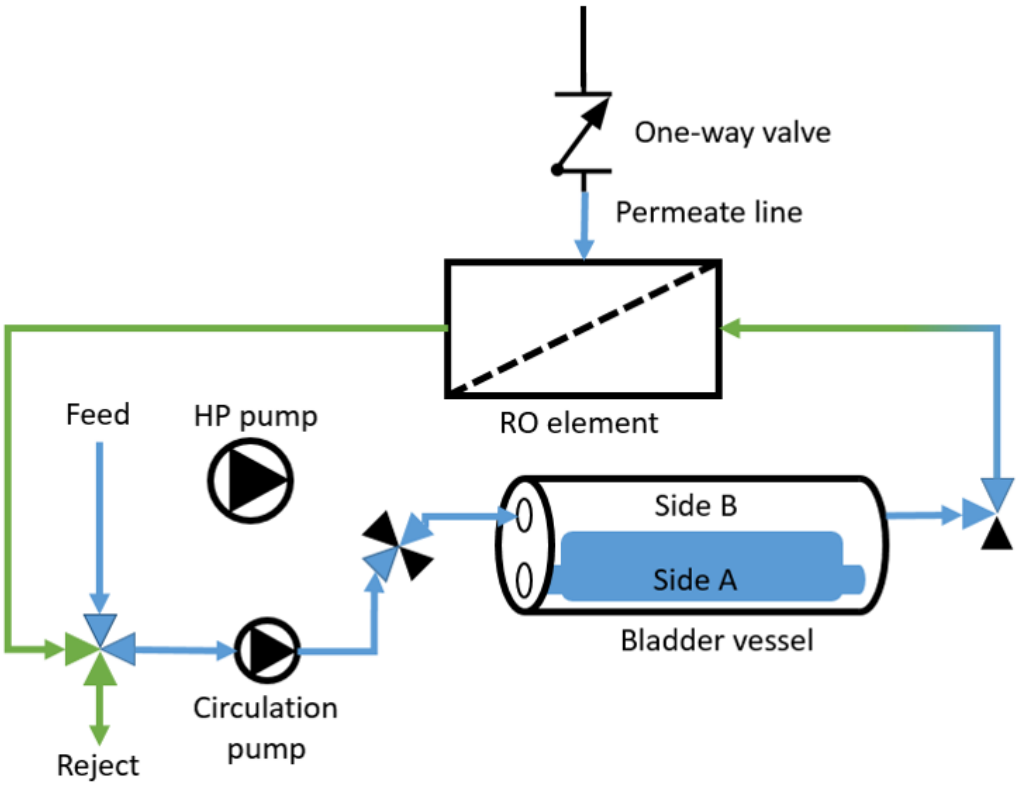

Figure 4-9: In this design, a check valve is used to limit the amount of osmotic backwash. Water in the permeate line between the check valve would re-enter the feed channel and expose the membrane to vacuum, which may be problematic.

design (minimizing membrane volume relative to system volume) but would require larger system footprints.

4.3.3 Check-valve

Another idea is to limit osmotic backwash by placing a check valve on the permeate line Figure 4-9. The maximum amount of backwash would be limited by line volume between the valve and the membrane. In our design, we assume water loss is still 1%, resulting in an energy consumption of 1.99 kWh/m^3, down from 2.29 kWh/m^3.

In theory, this idea is the most promising. However, there are several practical challenges to its implementation. As backwash occurs, a vacuum will be drawn inside of the permeate line. It is not clear how membranes will react to this periodic exposure to vacuum – water permeability and salt rejection may be adversely affected if the support layer is dried out. Membrane manufacturers may not cover this atypical

usage of their membranes in their warranties.

Another challenge is selecting a check valve that will reliably behave as expected: allowing permeate flow during permeate production and blocking back flow during the reset phases. Poppet check valves have finite cracking and reseal pressures that must be accounted for in designing these systems. One could place two check valves in series to minimize the effective reseal pressure.

4.4 Conclusions

A new, rapid flush concept has been developed for batch RO. This design holds the potential for significant performance improvement. With this design, batch RO energy savings in seawater desalination (35 g/kg, 50% recovery, 15 LMH) nearly double (Figure 4-10). This improvement is not only applicable to batch RO. We can easily imagine that this idea could be used to rapidly flush a semi-batch RO system or a batch osmotically assisted RO (also counterflow RO) system.

Generally speaking, this design is a simple way to rapidly flush a membrane-based system. We can drastically reduce the flushing time by taking the "bottleneck" and flushing it in parallel with the rest of the system. We imagine that this improvement will be most useful in batch-type systems where the system is being flushed regularly. This design essentially minimizes the cycle downtime and any losses associated with the flush phase (i.e. water loss in batch and semi-batch RO).

Whatever the technology, the benefits of reducing flush time will have to be weighed against the costs (e.g. valves) of implementing this design. We have presented several different design options (pump configuration, further parallelization). The exact implementation will be case-specific: what is most practical and cost-effective?

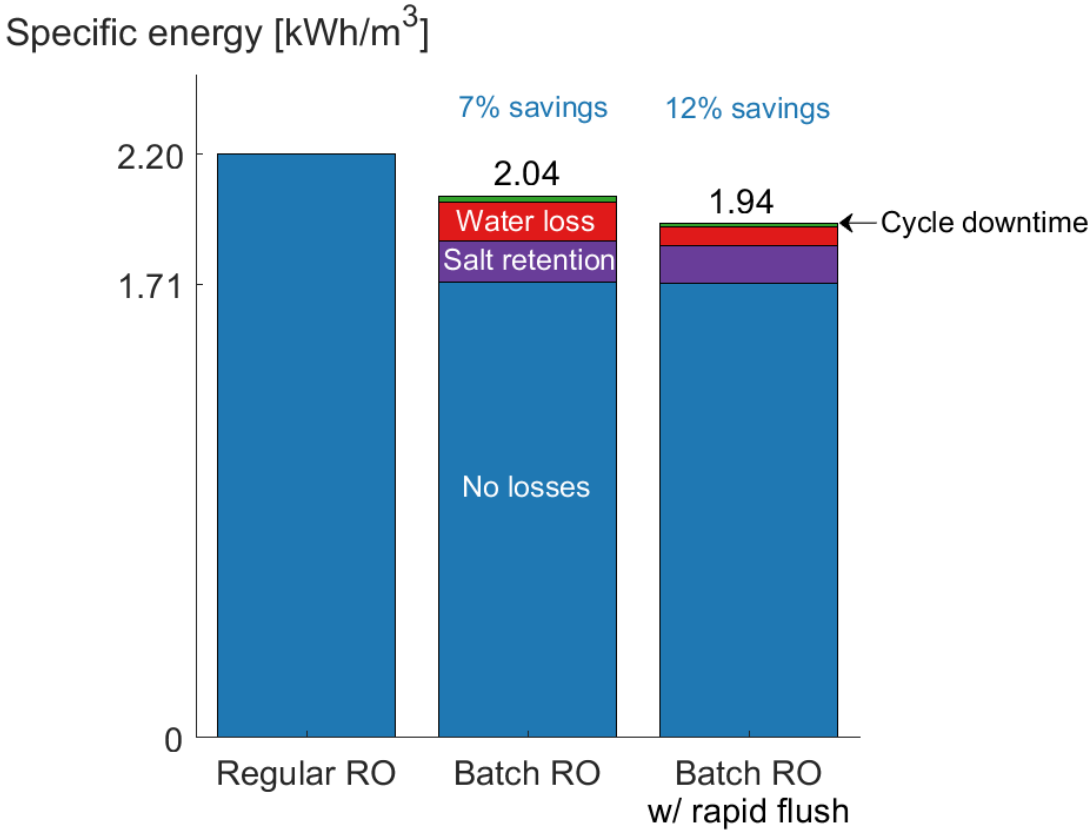

Figure 4-10: In this design, a check valve is used to limit the amount of osmotic backwash. Water in the permeate line between the check valve would re-enter the feed channel and expose the membrane to vacuum, which may be problematic.

"... a school of industrial science
aiding the advancement, development and practical application of science
in connection with arts, agriculture, manufactures, and commerce."

Acts and Resolves of the General Court
Relating to the Massachusetts Institute of Technology, 1861

5

Techno-economic analysis

Will batch RO make desalination more affordable? To answer that question, we perform an integrated techno-economic analysis, considering the economic realities of our world alongside the performance of the technology. We also consider practical limitations of today's RO membranes and pressure vessels.

I got lucky. Then I told Grace & Sahil [49].

5.1 Seawater desalination with batch RO

5.1.1 Less energy

Batch RO can be used to reduce the energy consumption of a desalination plant. Under typical seawater conditions, we expect batch RO save about 10% relative to a continuous RO plant with pressure exchangers. However, a batch RO plant will cost more than a regular RO plant if membrane area and plant capacity are fixed.

In Table 5.1 we consider both the cost and benefits of using batch RO to reduce energy consumption. At an electricity price of \$0.10/kWh, it would take 17 years[1] for the energy savings to offset the additional CAPEX. For desalination plants with 20-30 year lifespans, this is not a compelling proposition.

[1]This "ideal" payback period neglects the time value of money and is still too long.

Table 5.1: The energy savings achieved with batch RO are relatively small compared to the additional CAPEX required to implement the process, here assumed to be 10% of regular RO's CAPEX.

		Value		Unit
Plant capacity		100,000		m^3/day
CAPEX - regular RO		120M		$
Energy consumption - regular RO		2.2		kWh/m^3
Energy consumption - batch RO		2.0		kWh/m^3
Uptime		95%		-
Electricity cost	0.05	0.10	0.20	$/kWh
Annual energy savings	0.35M	0.7M	1.4M	$/year
CAPEX premium - batch RO		12M		$
Real discount rate		0%		-
Ideal payback period	34	17	8.5	years
Real discount rate		3%		-
Realistic payback period	100+	25	11	years

5.1.2 More water

What if we used batch RO to produce more water? As shown in Figure 5-1, we could operate a batch RO system at a higher flux (20 LMH) while keeping energy consumption the same as continuous RO (15 LMH). While water loss and salt retention are purely parasitic, when we operate at higher fluxes we receive more water in exchange for the additional energy (Figure 5-2).

Flux distribution in RO systems

Why don't regular RO systems operate at higher fluxes?

In a regular RO system the flux distribution is uneven: flux is high at the end of the system and low at the end (Figure 5-3). The peak flux, the flux in the first element, is more than double the average system flux (15 LMH) and exceeds the manufacturer's maximum recommended flux [26]. This is because regular RO systems recover all the water (50%) along the length of the system in one pass. In batch RO systems, water is recovered in multiple passes. A batch RO system can achieve the same recovery (50%) and flux (15 LMH), but the recovery across the membrane module at any instant is lower (21% here).

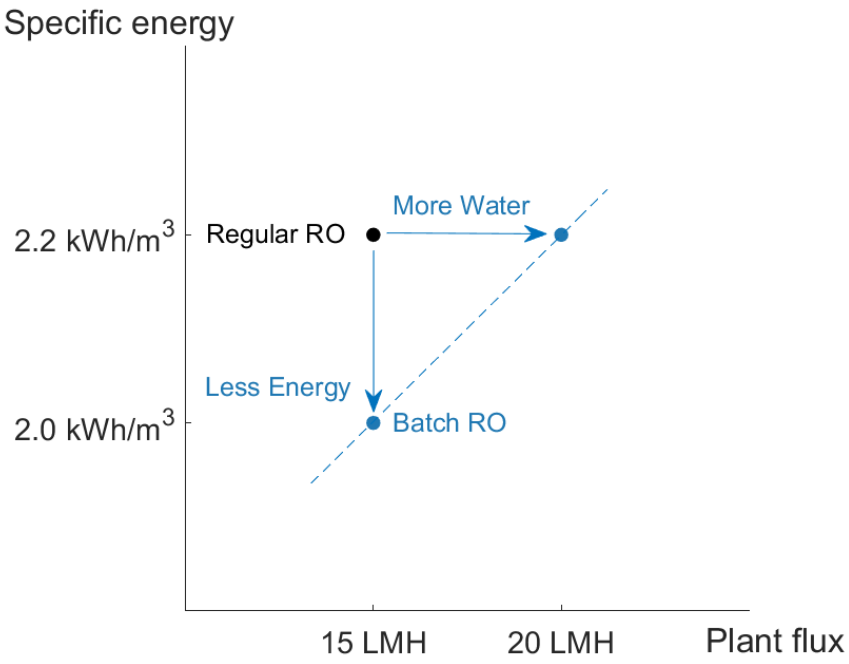

Figure 5-1: Batch RO can be used to produce more water (per membrane area) instead of using less energy.

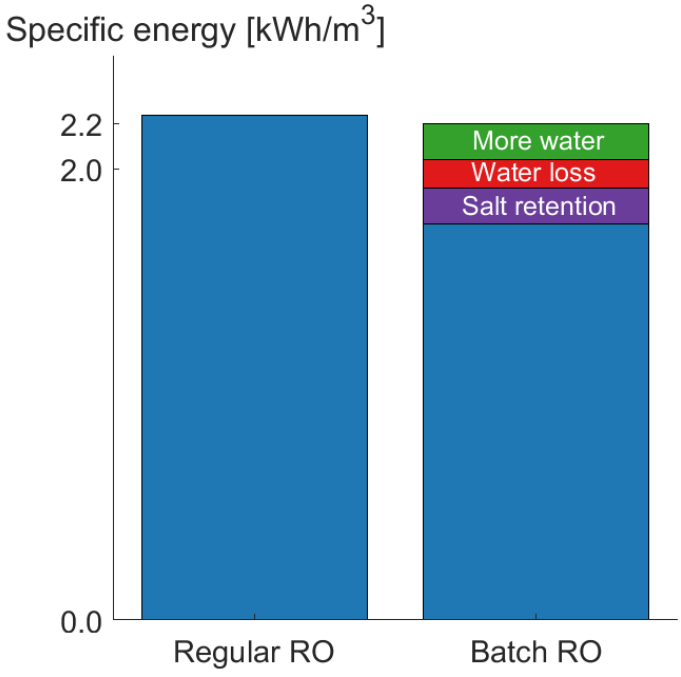

Figure 5-2: Operating at a higher flux results in an energy penalty, but also generates a valuable product. There is no benefit to the salt retention and water loss penalties.

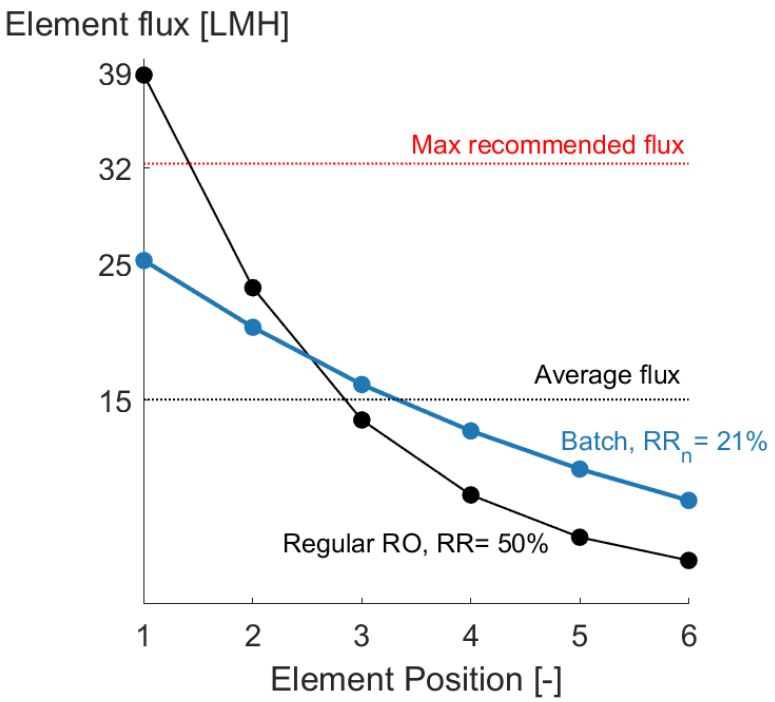

Figure 5-3: The flux distribution in batch RO systems is more even than in regular RO systems. Here, a batch RO system is able to achieve the same average flux (15 LMH) while keeping the peak flux below the manufacturer's maximum recommended flux. Flux values were calculated with the Q+ RO Projection Software (LG Water Solutions).

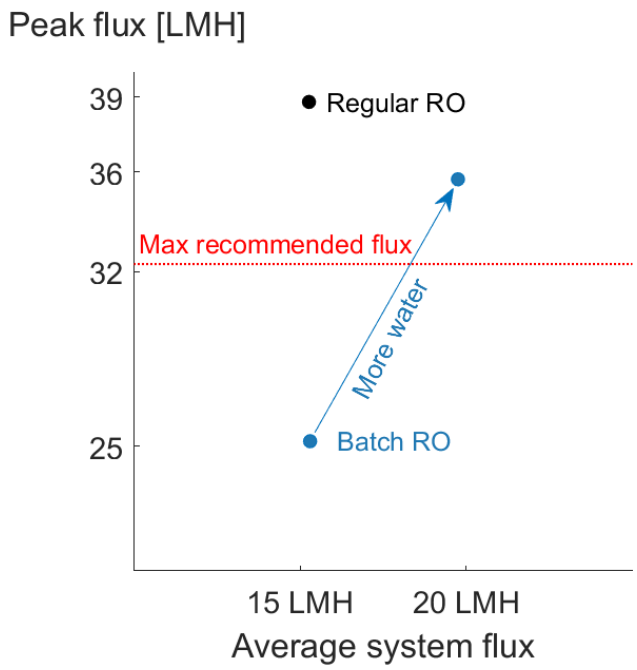

Figure 5-4: We can take advantage of batch RO's flux distribution to produce more water with the same sized system ($n = 6$) or reduce the size of the system ($n = 3, 4$) while keeping the peak flux the same as or below that of a regular RO system.

We can take advantage of the flux distribution in batch RO to increase the productivity of RO plants without compromising membrane life (Figure 5-4). With batch RO, we can expand the capacity of existing plants and build smaller plants.

Plant expansion

In this illustrative example, we upgrading an existing RO plant with the batch RO process so that it can operate a higher average flux without additional membrane area (Figure 5.2). With an expanded capacity, the plant can sell more water. The plant must also use more energy to produce that water, but the net benefit is six million dollars, an order of magnitude greater than the energy savings from before.

It is notable that the net benefit is independent of electricity price. The energy costs contribute to the cost of water, so the additional water revenue increases and decreases along with the price of electricity. The net benefit reflects the fact that besides energy, all other cost components (CAPEX, OPEX, labor) are being used to produce more water than before.

Table 5.2: The energy savings achieved with batch RO are relatively small compared to the additional CAPEX required to implement the process, here assumed to be 10% of regular RO's CAPEX. We acount for the time value of money and financing terms when calculating the cost of water. Some values are rounded.

	Value	Unit
Membrane area	280,000	m^2
Flux - regular RO	15	L/m^2-h
Flux - batch RO	20	L/m^2-h
Energy consumption	2.2	kWh/m^3
Capacity - regular RO	100,000	m^3/day
Capacity - batch RO	130,000	m^3/day
CAPEX - regular RO	120M	$
Uptime	95%	-
Electricity price	0.10	$/kWh
Additional water revenue	8.3M	$/year
Additional energy cost	2.3M	$/year
Net benefit	6M	$/year
CAPEX premium - batch RO + higher flow	50M	$/year
Interest rate	6%	-
Equity yield	12%	-
Loan repayment	25	years
Debt equity split	75%	-
Capital recovery factor - interest	9%	-
Capital recovery factor - equity	17%	-
Net capital recovery factor	0.10	-
Cost of water - regular RO	0.76	$/$m^3$
Cost of water - batch RO	0.73	$/$m^3$

In this case we have assumed a higher CAPEX premium because the plant has higher flowrates (feed, brine, and permeate) than the original plant. If the CAPEX premium is 40%, the levelized cost of water decreases by 3% due to the increase in plant productivity.

In this analysis OPEX costs (excluding energy) were kept constant. Batch RO might require less chemicals or membranes but we cannot quantify this benefit based on currently available research.

Smaller plant

Now we consider building a "smaller" batch RO plant with the same capacity (100,000 m^3/day) as a regular RO plant. In this example the feed, brine, and permeate

Table 5.3: An educated guess at the relative costs of implementing batch RO instead of regular RO.

Component	Relative Cost	Reason
Pressure vessels	2	Bladder
Piping, High-grade alloy	1.5	More piping, higher pressures
Civil costs	1.3	Increased plant footprint or density
Equipment and materials	1.1	Valves, bladders, VFDs, etc.
Pumps	1	Smaller pumps but more moving parts
Energy Recovery Devices	0	Replaced by bladder

flowrates are equal. Therefore, the costs associated with those flowrates are assumed to be constant. This allows us to perform a simple estimate of the capital costs of the batch RO plant.

We list the costs which we expect to be directly affected by batch RO in Table 5.3. We started with baseline component costs for a 100,000 m^3/day plant from DesalData and scaled those costs appopriately. If the batch RO plant has the same membrane area and flux (15 LMH), the CAPEX premium is 15% (not shown in the table).

However, if we operate at higher flux (20 LMH), we can use less membranes to produce the same amount of water. We consider membrane area because cost components scale with the number of membranes. We scaled another set of costs (membranes, pressure vessels, civil costs, equipment, piping) to account for the resulting reduction in membrane area (Table 5.4). The result is a plant that is a little less expensive.

The precise numbers shown here are not important, and the actual numbers will certainly differ. But this analysis illustrates an important idea. At first appearance, batch RO is more expensive than regular RO. However, the CAPEX premium can be offset by building more productive plants (process intensification). We anticipate this idea will become particularly attractive during desalination "booms," when demand for new membranes exceeds global supply [50].

Increasing recovery

Batch RO can also be used to operate at higher recovery ratios than regular RO while keeping energy consumption relatively low. By increasing recovery ratio, we

Table 5.4: An educated guess at the capital costs of a batch RO plant with the same capacity as a regular RO plant. The batch RO plant has 75% the membrane area because it operates at a higher flux. Associated costs (membranes, pressure vessels, civil, equipment, piping) are scaled by the membrane area. When these numbers are applied to the plant expansion (as above) – the CAPEX premium is 42%. Baseline costs for regular RO are from the DesalData cost estimator.

Component	Regular RO 15 LMH	Batch RO 20 LMH	Relative cost
Equipment and materials	27	22	0.8
Civil costs	21	21	1
Piping, High-grade Alloy	16	18	1.1
Pumps	10	10	1.1
Pretreatment	10	10	1
Installation services	10	10	1
Intake/Outfall	9	9	1
Design costs	7	7	1
Membranes	6	4.5	0.75
Pressure vessels	2	3	1.5
Energy Recovery Devices	1	0	0
Legal and professional	1	1	1
Total	120	116	0.97

can reduce capital costs associated with the feed and brine flowrates (i.e. intake, pretreatment, piping, pumps, outfall). One limiting factor in pushing up recovery is the peak pressure of batch RO systems (Section 5.2.3).

5.2 Practical considerations

5.2.1 Space requirements

The space requirements of a regular RO system are due to the pressure vessels holding the membranes. A batch RO system with equal membrane area will therefore have a greater volume due to the additional pressure vessels needed to hold the bladders:

$$\text{RV} = \frac{\text{Bladder PV} + \text{membrane PV volumes}}{\text{Membrane PV volume}} \tag{5.1}$$

We can intentionally increase the size of a batch RO system. The minimum volume of a batch RO system assumes that the tank is empty at the end of the permeate

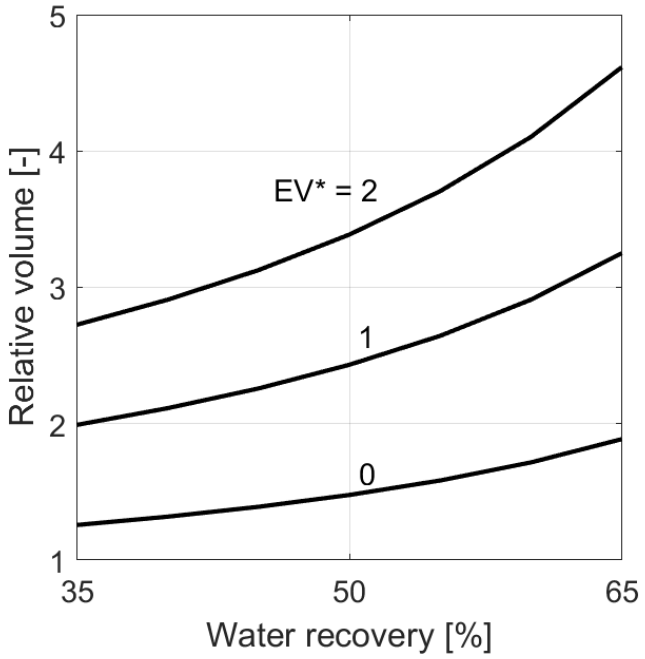

Figure 5-5: Batch RO systems get bigger depending on design (EV*) and operation.

production phase. We normalize the excess volume of an oversized system by the feed channel volume in the membrane module:

$$\text{EV*} = \frac{\text{Excess volume}}{\text{Feed channel volume}} \tag{5.2}$$

We show the relative volumes according to recovery ratio and excess volume 5-5. Relative volumes increase as recovery ratio increases (bigger bladders). In Figure 5-6 we see that increasing EV* reduces cycle downtime (and water loss). Thus, in selecting the size of a system (EV*) one must weigh the trade-offs between cost (RV) and performance (water loss).

While batch RO plants require more space, it does not follow that they will be bigger and more expensive. There is a wide range range in desalination plant densities (9,000-34,000 m^3/day-acre) [51]. There is much room for plant designers to squeeze equipment into a confined footprint (e.g. second stories or going underground). Plant density does not seem to correlate with cost. The Tuas III and Tuaspring plants in Singapore have similar plant densities (20,000 m^3/day-acre) but the capital require-

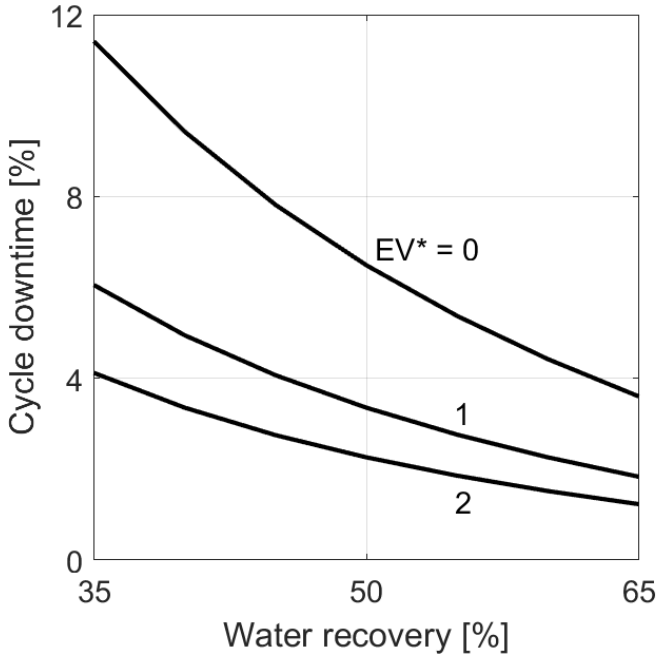

Figure 5-6: Increasing EV* reduces cycle downtime (and water loss) because the length of the permeate production phases increases while the flush time remains the same.

ments were roughly 50% greater for Tuaspring[2].

We can calculate how much extra space batch RO requires. Figuring out the extra cost associated with that space is less tractable.

5.2.2 Membrane train length

The ideal batch RO system would be vanishingly short. With no spatial variation in osmotic pressure, such a system could achieve the lowest possible energy consumption [8]. Actual systems consume more energy because the osmotic pressure and flux varies across the length the system [13]. The spatial variation in osmotic pressure is quantified by the per-pass recovery ratio.

The per-pass recovery ratio is the permeate flow divided by the circulation flow [25]. Thus, we can reduce the per-pass recovery by increasing the circulation flowrate. However, at some point we hit the maximum feed flowrate as specified by membrane

[2]Adjusted for inflation and normalized by plant capacity.

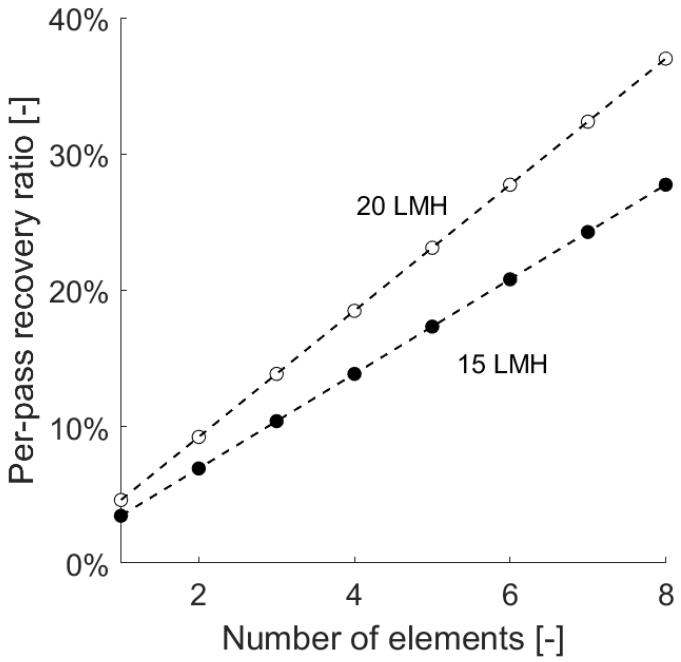

Figure 5-7: For a given number of elements and membrane flux, the minimum achievable per-pass recovery ratio is imposed by the membrane's maximum feed flowrate. Per-pass recovery and energy consumption increase with flux and membrane length.

manufacturers. Once a system is operating with the maximum circulation flowrate, the per-pass recovery will necessarily increase when permeate flow is increased by operating at higher flux or adding more membranes (Figure 5-7).

Shorter batch RO systems consume less energy than longer batch RO systems, but also require more pressure vessels to house the same amount of membrane area. There is a trade-off between energetic performance and capital expenditures.

5.2.3 Peak pressure

For a given intake feed salinity and recovery ratio, a batch RO plant will reach higher peak pressures than regular RO plants due to salt retention and water loss. If batch RO plants operate at high enough recoveries, equipment costs will increase step-wise once they exceed the pressure ratings of standard RO equipment. Right now, most RO membranes are rated for up to approximately 80 bar [26]. There are specialty high-pressure membranes and pressure vessels rated up to approximately 120 bar [52,

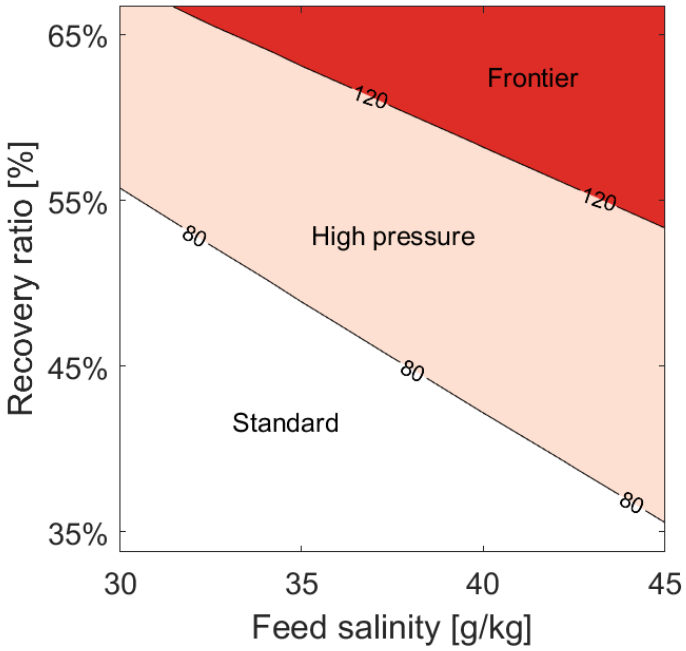

Figure 5-8: Batch RO plants with a peak pressure below 80 bar can use standard RO membranes and pressure vessels. Beyond 80 bar, more expensive high-pressure equipment must be used. High-pressure RO membranes are rated up to 120 bar. The precise locations of the boundaries between these regimes can change based on system design and operation.

53]. In Figure 5-8 we show the pressure regimes of a batch RO plant depending on the intake salinity and recovery ratio. This analysis assumes that the batch RO systems at constant flux throughout the permeate production phase. One could reduce the flux towards the end of the cycle in order to reduce the peak pressure. Batch RO plants might require thicker piping to withstand the higher pressures.

5.3 Beachhead markets

The previous analyses assessed the viability of batch RO at full-scale, neglecting the fact that it is currently an immature technology. Even if a plant owner wanted to use batch RO in a full-scale desalination plant today, they would have to pay a penalty incurred by their financer due to the risk of using an unproven technology [54].

Because of this technology risk, a new technology may not enter the market with just an incremental cost savings. It must solve a thorny problem or create an oppor-

tunity in order to secure first adopters and leap from the lab to the market.

5.3.1 Less brine for POU

One key advantage of batch RO (and semi-batch RO) is the decoupling of the feed flow rate from the recovery ratio. Throughout each batch, feed recirculates around the system multiple times until the desired recovery ratio is achieved. Basically, a single membrane system is capable of achieving any recovery ratio desired[3]. A regular RO system with a single membrane is limited to low recoveries in order to stay above the minimum concentrate flow (in concert with the restriction on local flux).

This makes batch RO an attractive process for any application where high recovery is required in a compact footprint. This may include household water purifiers, commercial purifiers for use in restaurants, cafes, offices, or remote localations (e.g. oil rigs).

5.3.2 Less brine for BWRO

One challenge in brackish water deslination is brine disposal [55]. Many BWRO plants are located inland, so plants must resort to evaporation ponds, deep injection wells, or brine concentrators to treat discharge in compliance with local regulations.

Batch RO may be able to achieve higher recoveries than conventional RO methods due to rapid salinity cycling [16]. A standalone batch RO plant would have less brine disposal costs than a regular RO plant that produces more brine. However at high recovery ratios, the relative volume of the batch RO plant can become very high (Figure 5-9). Many inland deslination plant are located in remote locations, so the high relative volumes may not be cost prohibitive. A hybrid semi-batch/batch RO system could also be used to reduce the space needed for a standalone batch RO plant [41].

Alternatively, a batch RO brine reducer could be used to concentrate brine from an existing RO plant. The add-on batch RO system would operate at lower recovery ratios (40-80% rather than 90-98%) and would have lower relative volumes. In Figure

[3]Due to the size of the bladder, recovery in batch RO might be limited by footprint constraints.

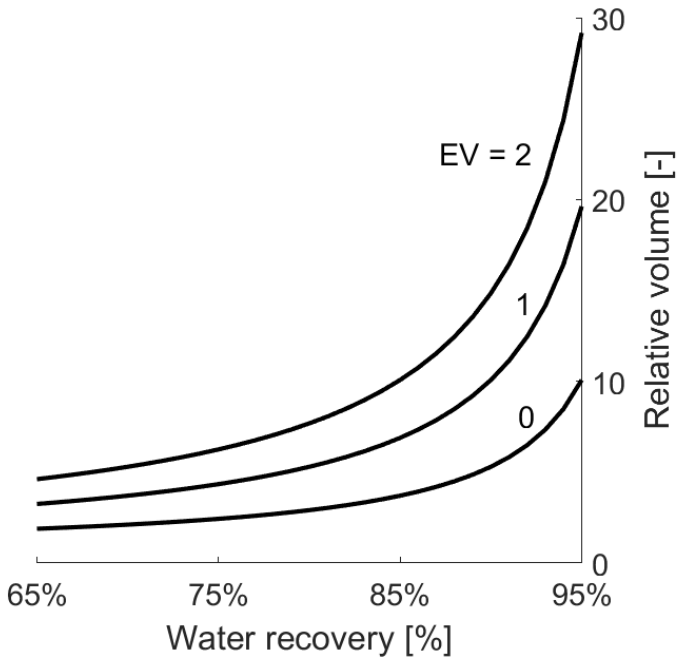

Figure 5-9: Relative volume of batch RO systems at high recoveries. At the highest water recoveries (e.g. 95%) the relative volume of a batch RO system can be 10-30 times greater than a regular RO system.

5-10 we consider adding a batch RO brine reducer to a 10,000 m^3/day plant operating at 80% recovery. We quantify the effectiveness of the batch RO system with the brine reduction ratio BRR:

$$\text{BRR} = \frac{V_{br,\text{old}}}{V_{br,\text{new}}} \tag{5.3}$$

where $V_{br,old}$ is the volume of brine without the reducer and $V_{br,new}$ is the volume of the brine with the reducer. A 1,000 m^3/day brine reducer would reduce the brine volume by a factor of two and cost about $2M.

The annual savings shown here are compelling, particularly when brine disposal is expensive ($10/$m^3$). However, the scaling resistance of batch RO has not been quantified or demonstrated experimentally. More work must be done if these benefits are to be realized.

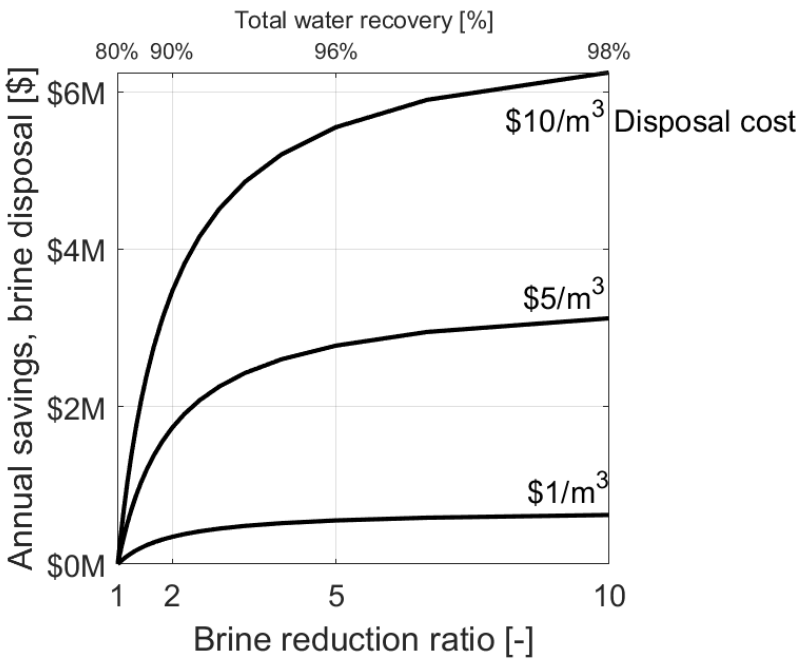

Figure 5-10: Brine disposal savings become increasingly difficult to obtain as the concentrations ramp up. A 1,000 m^3/day batch RO system would reduce the brine volume by a factor of two and cost about $2M.

5.3.3 Less energy for old SWRO

In Section 5.1.1 we looked at the reduction in energy costs for a modern RO plant with best-in-class energy consumption. However, old RO plants consume more energy because of inefficient pumps or lack of energy recovery.

In Figure 5-11 we consider the savings achieved by converting an old seawater RO plant (1,000 m^3/day capacity, relatively small) into a batch RO plant. The annual energy savings depend on the old plant‘s energy consumption and the price of electricity. The energy savings can be attributed both to the batch RO process and to the improved efficiency of the new pumps. The retrofit is assumed to cost $250-500k [56].

5.3.4 Fewer batteries for off-grid RO

Designing an off-grid desalination system is a thorny problem with many variables to consider. How can we provide a steady supply of water when the power source is

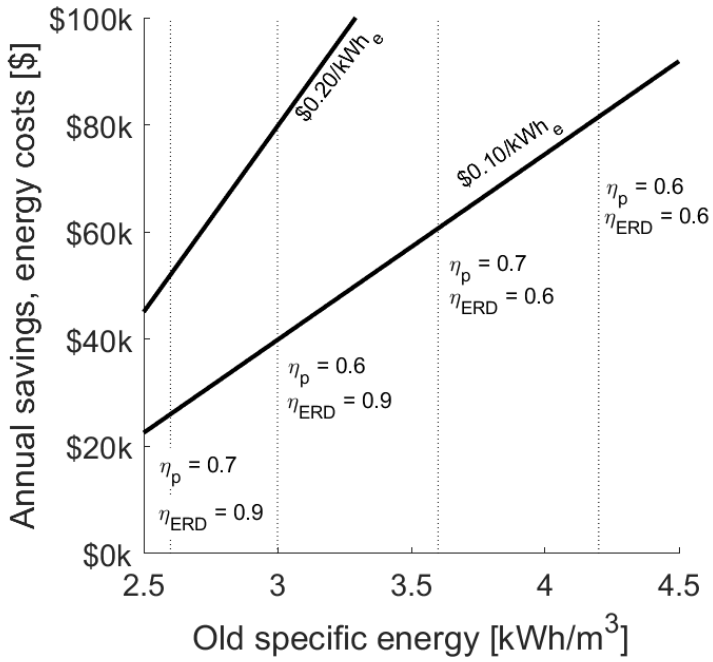

Figure 5-11: Annual savings in energy costs by converting an old RO plant to a batch RO plant. Example combinations of pump and ERD efficiencies are highlighted.

intermittent and stochastic, all while keeping costs low? Designers of such systems have a tough job and have to weigh trade-offs and make value judgements[4].

One strategy is to use excess power to produce water to be stored for later use. Water tanks are cheaper than batteries, so the system cost can be reduced without sacrificing reliability. This strategy has been demonstrated on an solar-powered electrodialysis system [57, 58].

Batch RO can adjust its power consumption and water production more flexibly than continuous RO by adjusting flux and recovery. In this example 5-12, we consider solar-powered RO systems. We have kept the photovoltaic (PV) panel area constant. Both regular RO and batch RO have the same available power, modeled by the sine function over the course of a 12-hour day. We assume batch RO can operate at a higher maximum flux (20 LMH) than regular RO (15 LMH). If both RO systems have the same membrane area, batch RO can operate at higher power consumption and water production rates than the regular RO system (Max power = Max flux $\times$

[4]The users should be involved in these conversations.

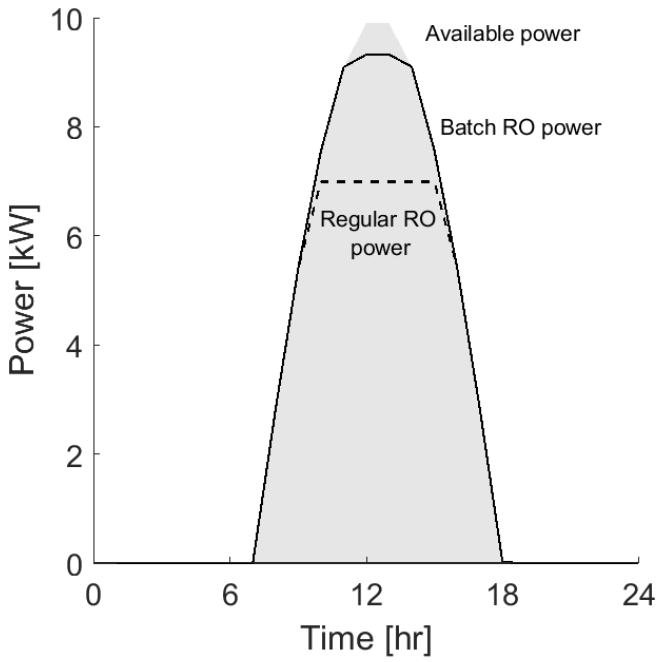

Figure 5-12: Batch RO can ramp up its power consumption to take more advantage of the peak in solar availability. This might allow designers to reduce the cost or improve the reliability of off-grid desalination systems.

Specific energy × Membrane area). The batch RO system is able to use up more of the available power by operating at higher fluxes to produce more water.

This capability will give designers more flexibility to vary the amount of PV area, membrane area, or battery capacity. Perhaps batch RO can make off-grid desalination cheaper or more reliable.

5.4 ÷

Cost of water is defined as:

$$\text{COW} = \frac{\text{Total costs}}{\text{Total water production}} \tag{5.4}$$

This is a tricky concept to visualize. Less energy? One piece of the pie shrinks a bit while the other grows. The net effect is difficult to discern.

There's nothing new here. We just flipped things around.

$$\text{POW} = \frac{\text{Total water production}}{\text{Total costs}} \tag{5.5}$$

Afterword

This was the story of three penalties.
Simple to complex. Boring to interesting. First to last.
But that story did not satisfy.

Funny how focus can blind.
How truths can mislead.
How trivial can transform.

This is the story of resources.
Count resources. Value resources. Use resources (fully)

Connect the dots!
To connect the dots, you have to collect the dots...
Where are the dots?

maybe this is the story of entropy

The Question

Can batch reverse osmosis make desalination more affordable and sustainable?

Quantum Wei's PhD Thesis Defense
Lienhard Research Group
May 3, 2021

Department of Mechanical Engineering
Massachusetts Institute of Technology

The Answer

Yes, it can

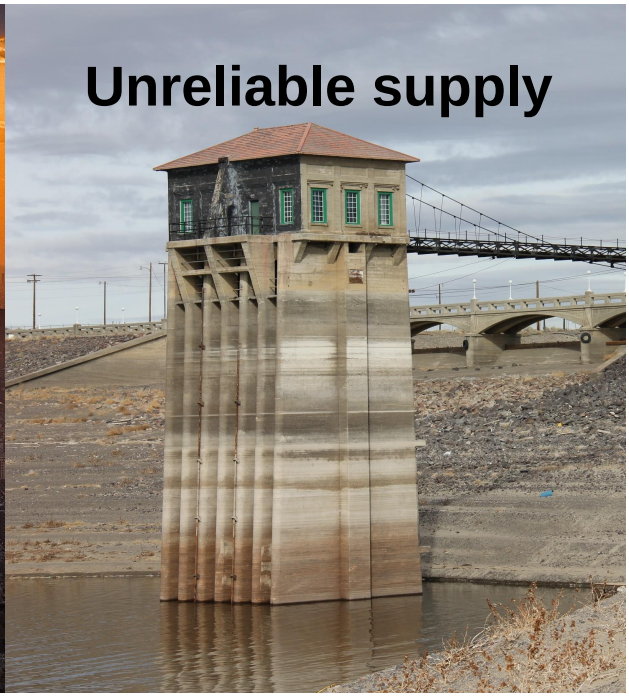

When it doesn't rain, we can desalinate

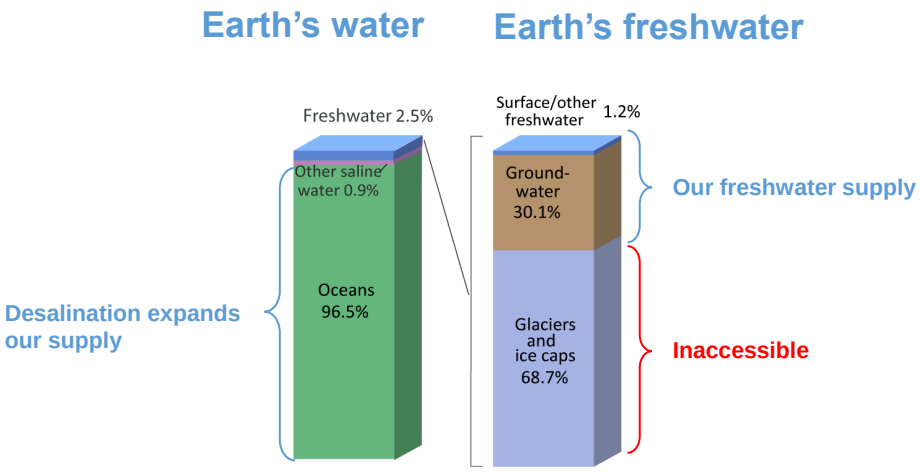

Source: Igor Shiklomanov's chapter "World fresh water resources" in Peter H. Gleick (editor), 1993, Water in Crisis: A Guide to the World's Fresh Water Resources. (Numbers are rounded).

Reverse Osmosis (RO) is the state-of-the-art

Carlsbad Desalination Plant, CA / AP

Seawater RO cost: ~⅓ energy

Brine disposal is expensive

Membranes clog

More water

Motivation

- Reverse osmosis (RO)
- Batch RO

Practical Losses
Improved Design
Techno-economics
Conclusions

Water flow

$$J \propto (\Delta P - \Delta\pi)$$

Hydraulic pressure

$$\Delta P = P_Y - P_S = 0$$

Osmotic pressure

$$\Delta\pi = \cancel{\pi_Y}^{\,0} - \pi_S = -\pi_S$$

$$J \propto (\Delta P - \Delta\pi)$$

$$0 \quad -\pi_S$$

$$J > 0$$

Water flows from yolk to salt

America's Test Kitchen

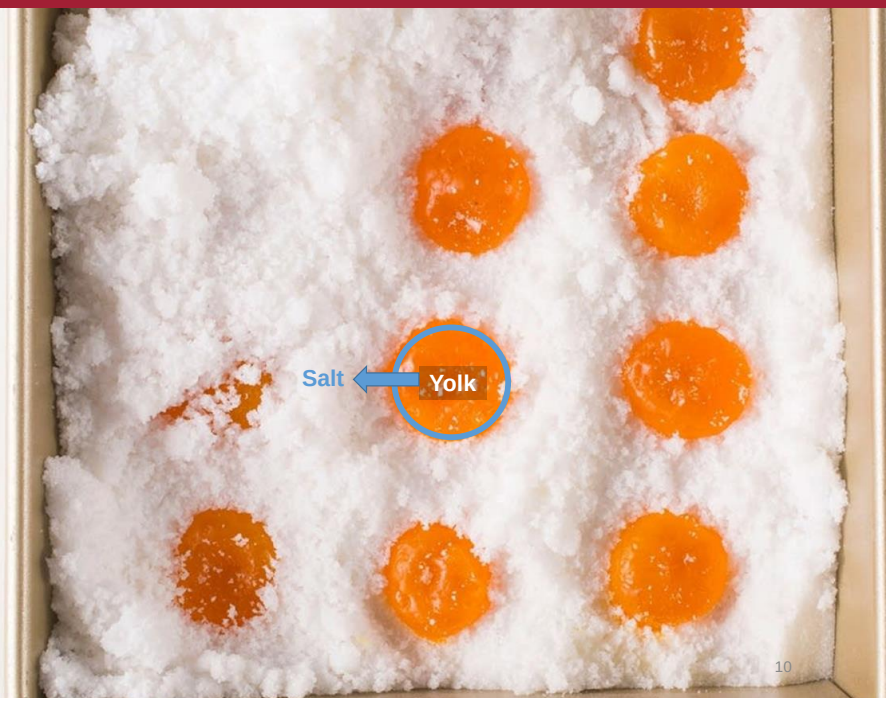

To produce freshwater, apply pressure

Permeate flux

$$J_v = A(\Delta P - \Delta\pi)$$

Driving force

Membrane water permeability

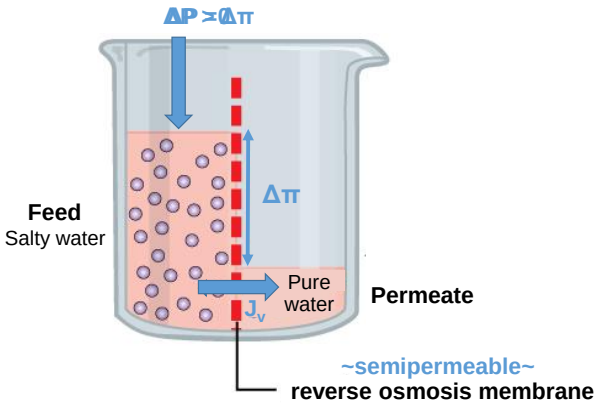

OpenStax, "Osmosis", *WikiMedia Commons*

Harmony Desal, "More Water, Less Energy"
MIT Clean Energy Prize (2020)

Regular RO is a continuous process

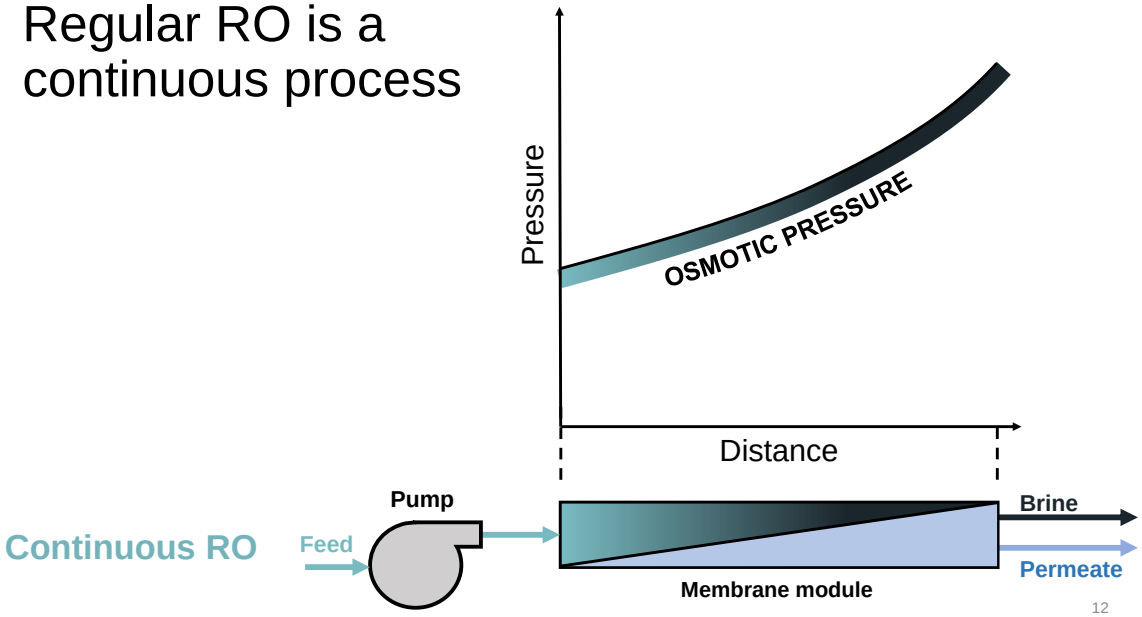

Continuous RO wastes energy
by over-pressurizing the system

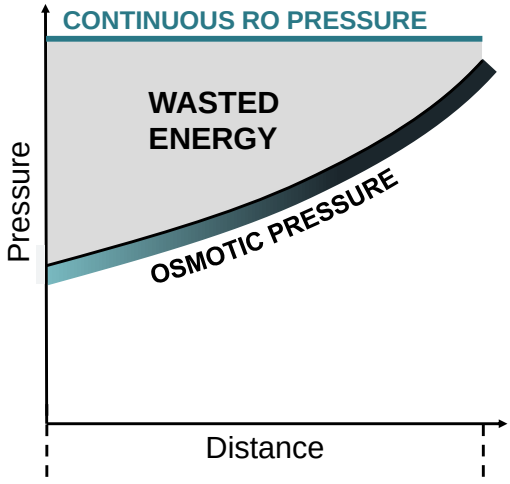

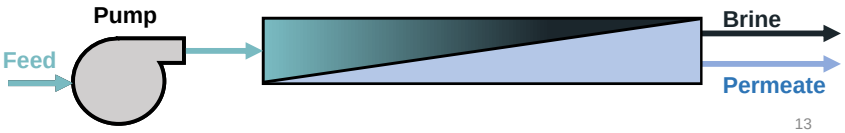

Continuous RO

Batch RO saves this energy
by tracking osmotic pressure over time

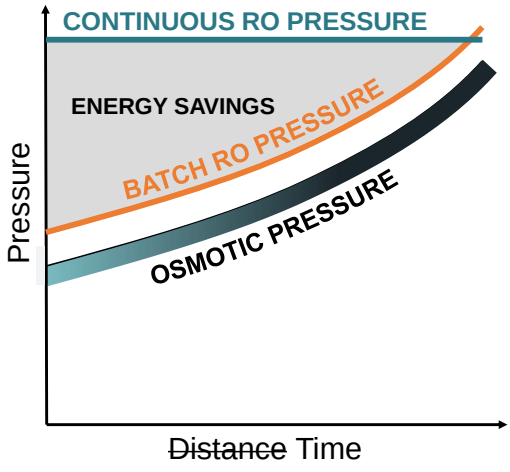

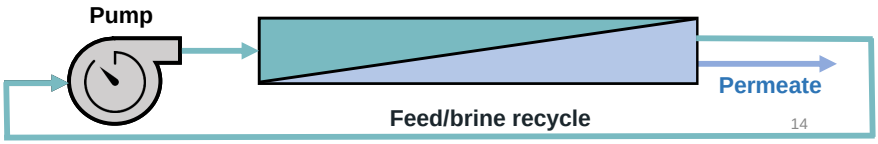

Batch RO

Energy models

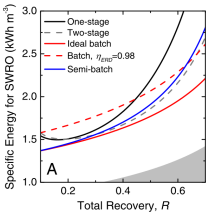

Werber & Deshmukh…, *Desalination* (2017)
Warsinger & Tow…, *Water Research* (2016)

Prototype w/ a piston

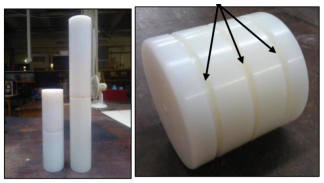

Davies et al. *Desalination & Water Treatment* (2016)

Salt retention

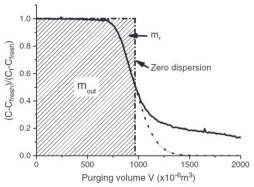

Qiu & Davies, *Desalination* (2012)
Cohen et al. *DWPR Report No. 179*

Optimal design

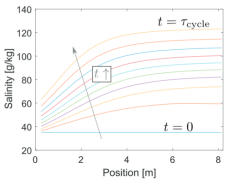

Swaminathan et al., *Desalination* (2019)

Scaling resistance

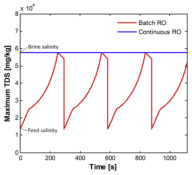

Warsinger et al., *Water Research* (2018)

New designs

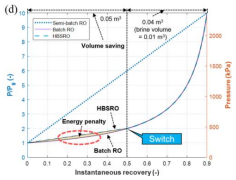

Park & Davies, *Desalination* (2021)

Batch RO with a bladder

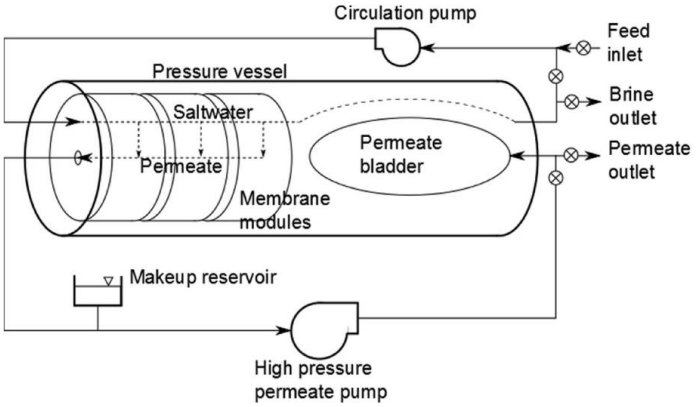

Warsinger et al., *Batch Pressure-Driven Membrane Desalination*… US Patent #10,166,510 (2019)

Batch RO system operates on a cycle

1 START OF PERMEATE PRODUCTION

2 END OF PERMEATE PRODUCTION

3 FLUSH

4 RECHARGE

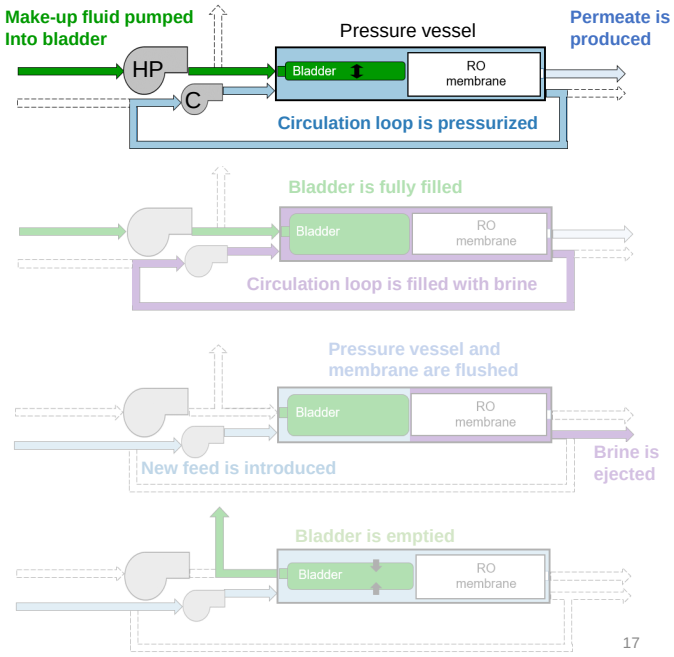

Wei, **Shah**, Lienhard, BoR Pitch-to-Pilot submission (2020)

Batch RO system operates on a cycle

1 START OF PERMEATE PRODUCTION

2 END OF PERMEATE PRODUCTION

3 FLUSH

4 RECHARGE

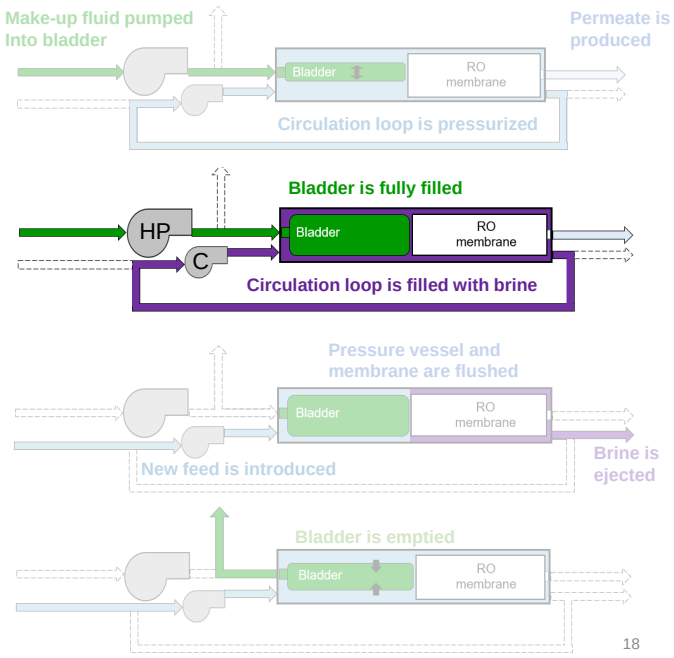

Batch RO system operates on a cycle

1 START OF PERMEATE PRODUCTION

2 END OF PERMEATE PRODUCTION

3 FLUSH

4 RECHARGE

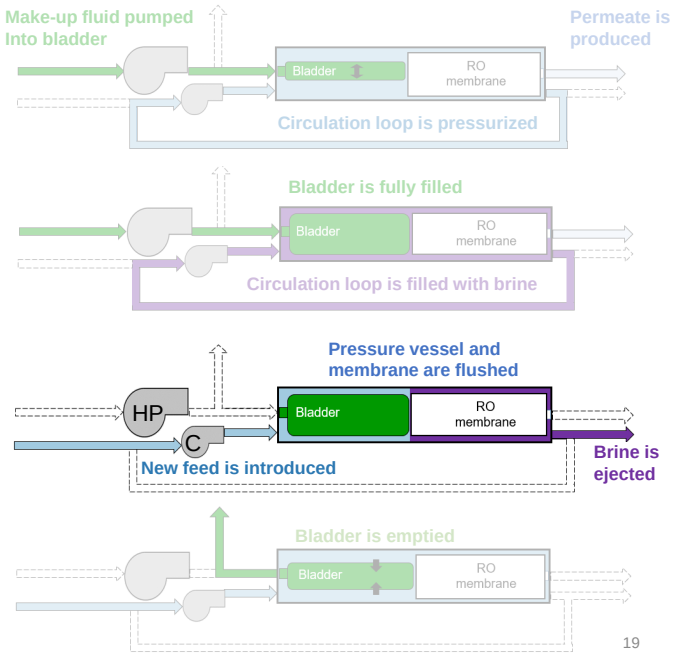

19

Batch RO system operates on a cycle

1 START OF PERMEATE PRODUCTION

2 END OF PERMEATE PRODUCTION

3 FLUSH

4 RECHARGE

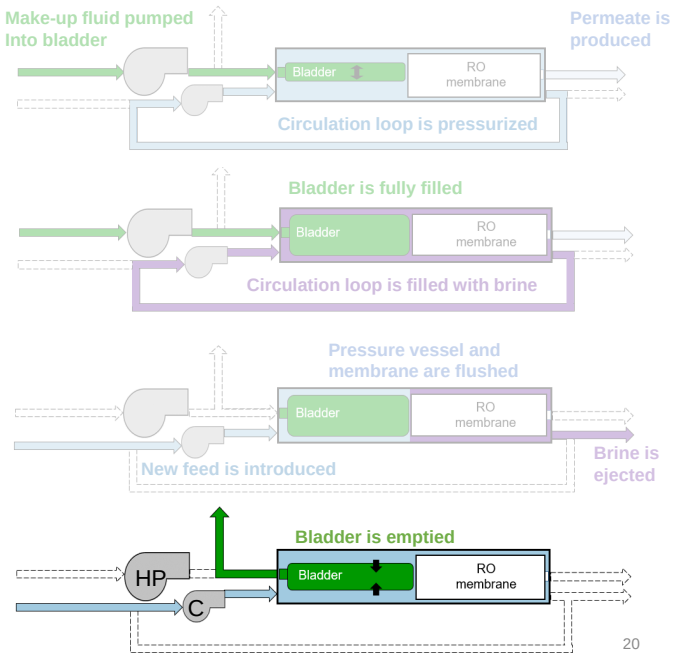

20

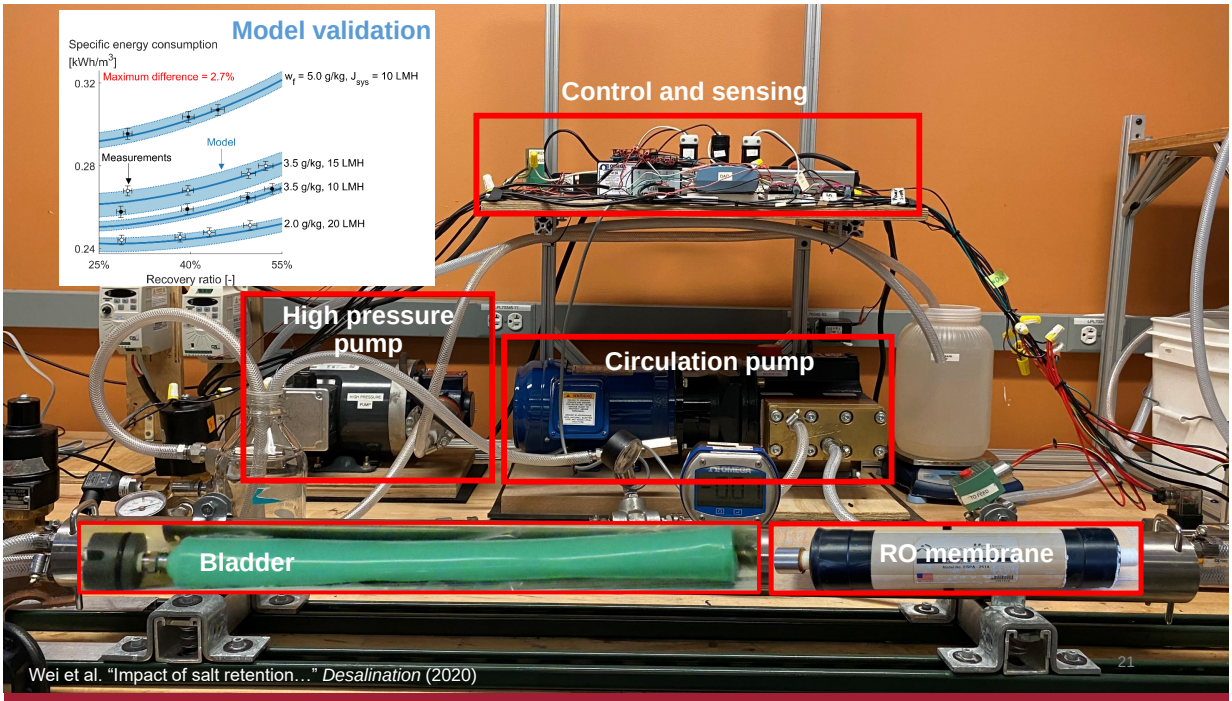

Wei et al. "Impact of salt retention…" *Desalination* (2020)

Looks good on paper…

Motivation

Practical Losses

- Cycle downtime
- Salt retention
- Water loss

Improved Design

Techno-economics

Conclusions

Cycle Downtime

Less water

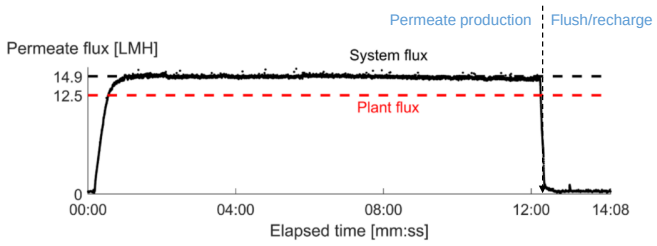

Permeate flux
or
"Water production"

$$J_v = \frac{\text{Permeate flow rate}}{\text{RO membrane area}} \qquad \frac{[L/h]}{[m^2]} \longleftrightarrow \text{LMH}$$

15 LMH → $\frac{\text{15 Liters per hour}}{\text{1 square meter}}$ → 1 square meter of membrane produces 15 Liters of water per hour

Wei et al. "Impact of salt retention…" *Desalination* (2020)

Salt Retention

Saltier water

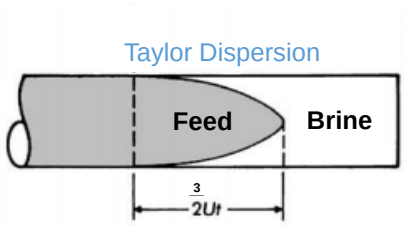

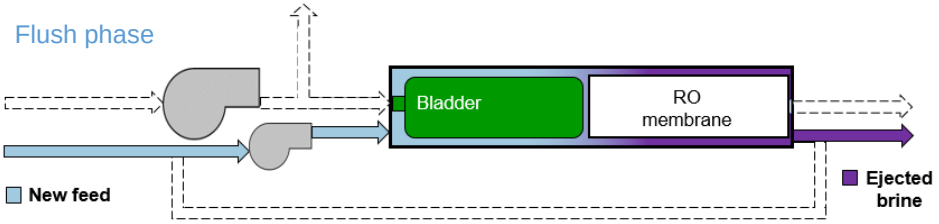

Feed salinity $w_f = 35$ g/kg → $\frac{\text{35 grams salt}}{\text{1 kilogram seawater}}$

$\pi_f = 28$ bar

$w_{br} = 70$ g/kg

$\pi_{br} = 56$ bar

Probstein, *Physochemical Hydrodynamics*

Water production

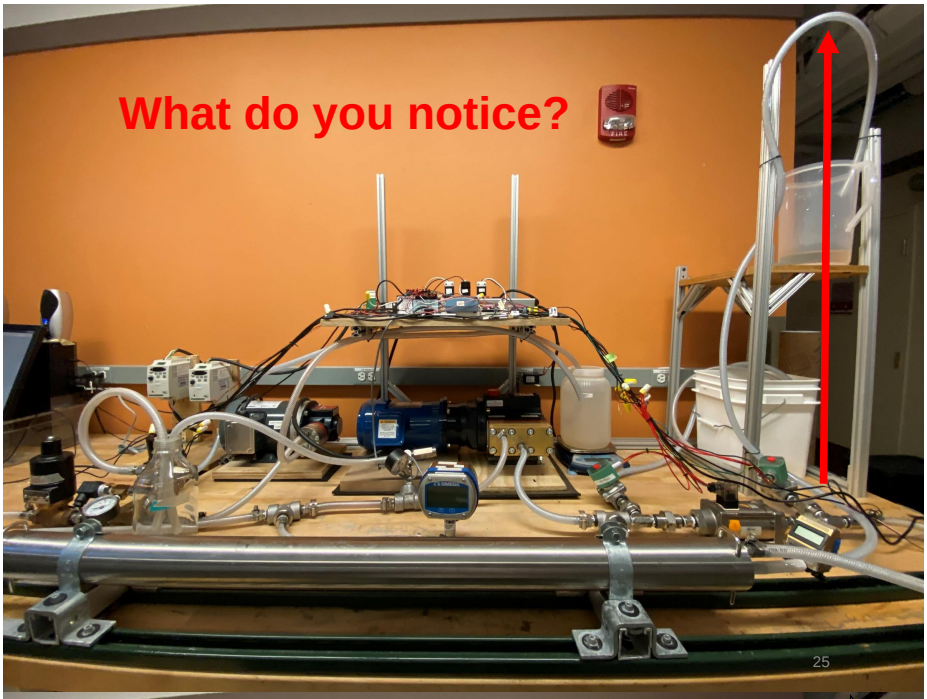

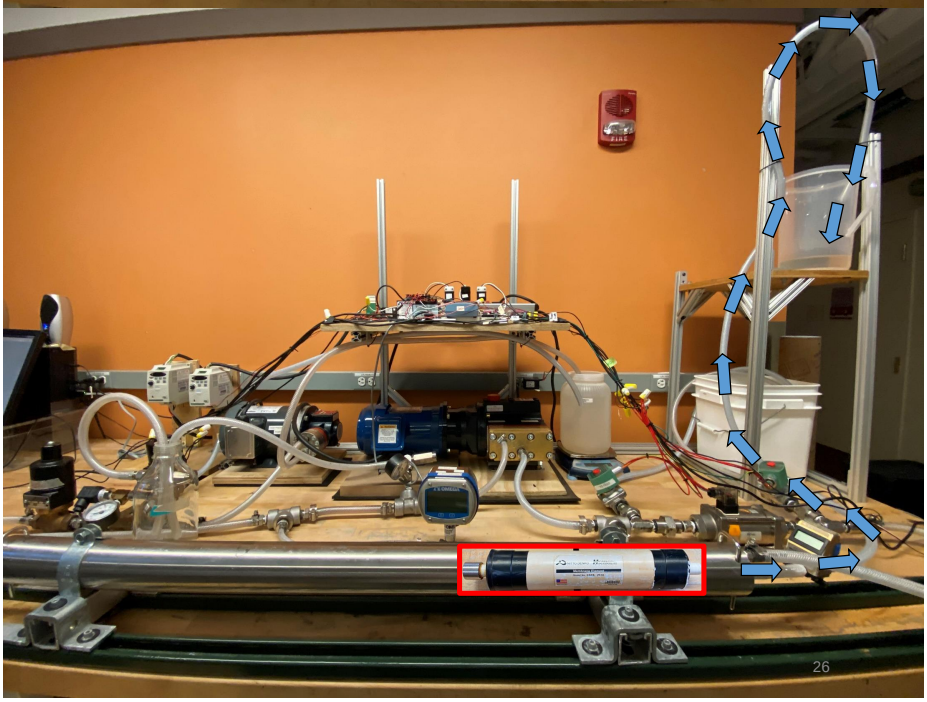

Water loss

once we start flushing

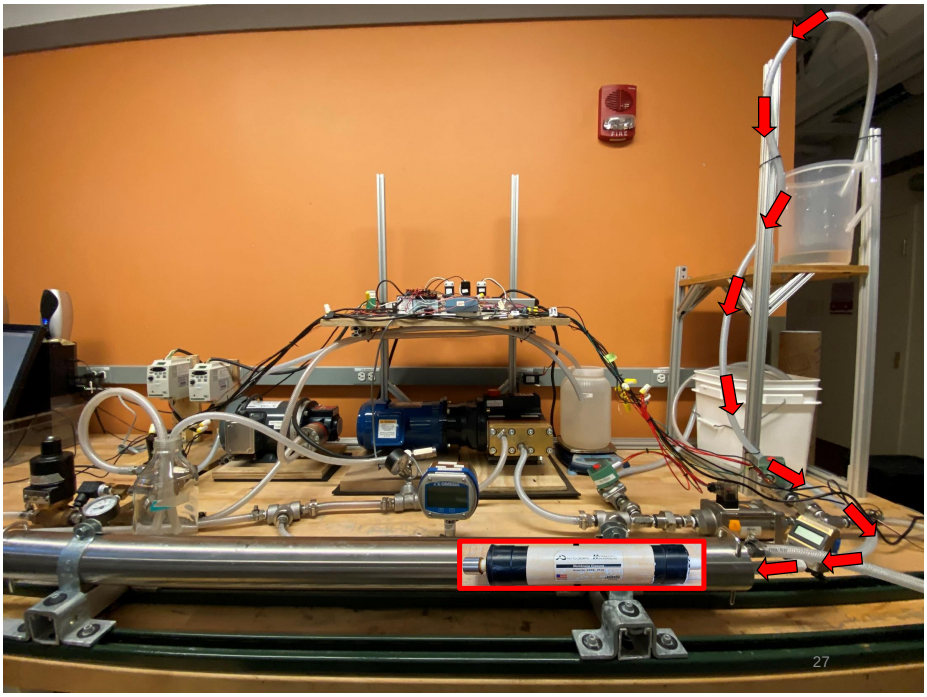

Water Loss ⟶ Less water

Recovery ratio: $RR = \frac{\text{Volume of permeate}}{\text{Volume of feed}}$

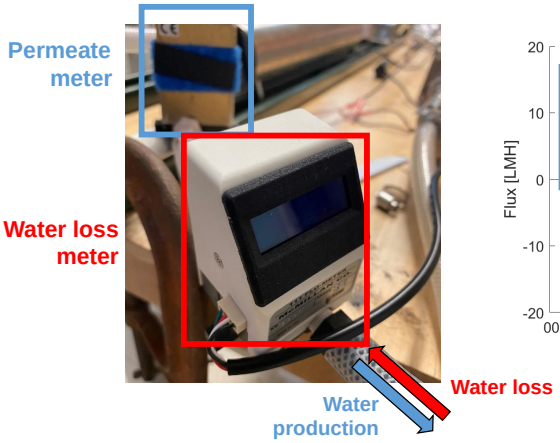

$RR_{eff} = RR - LR = 48\%$

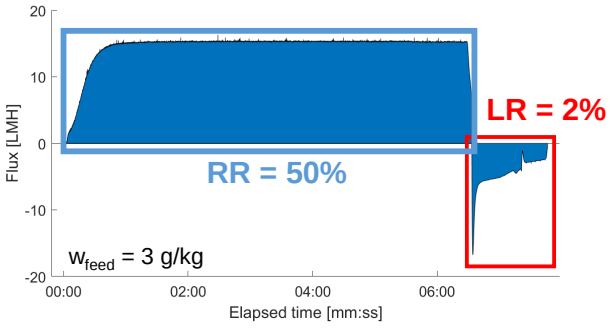

Water flux Driving force

$$J_v = A(P_f - \pi_f)$$

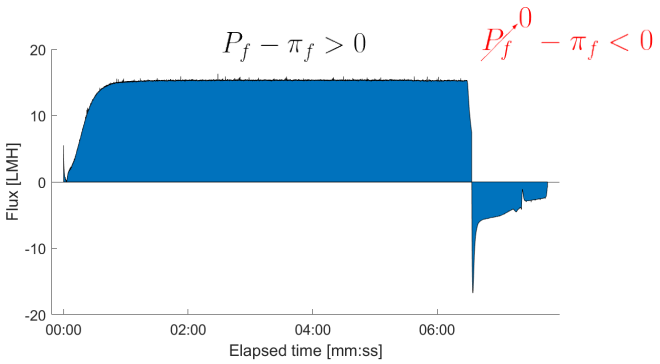

Apples to apples

Specific energy consumption

$$\text{SEC} = \frac{\text{Energy consumption}}{\text{Volume of permeate}}$$

Typical seawater RO conditions

SEC = 2.2 kWh/m^3 → 2.2 kWh of energy / 1 m^3 of permeate

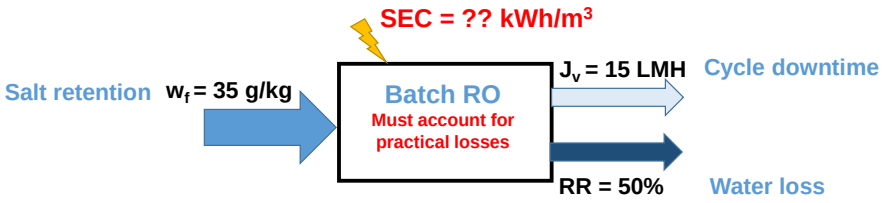

Cycle Downtime

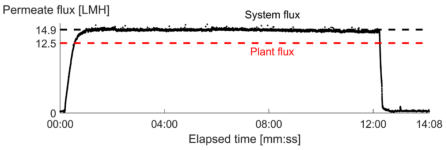

Salt Retention

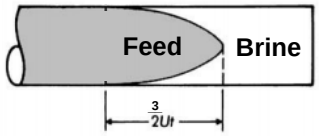

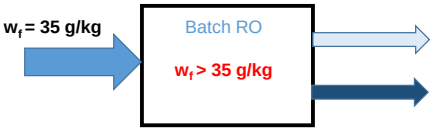

To reduce salinity elevation, flush longer

Elevated feed salinity / Original feed salinity / Original brine salinity / Original feed salinity

$$\Theta = \frac{w_{f,sys} - w_{f,pl}}{w_{b,pl} - w_{f,pl}} = \frac{\text{Feed salinity elevation}}{\text{Degree of mixing}}$$

Saltier feed

$$t^* = \frac{t_{fl}}{t_{fl,plug}}$$

Duration of flush phase / Duration of flush phase, plug flow

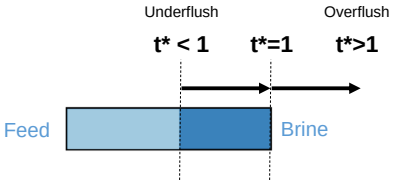

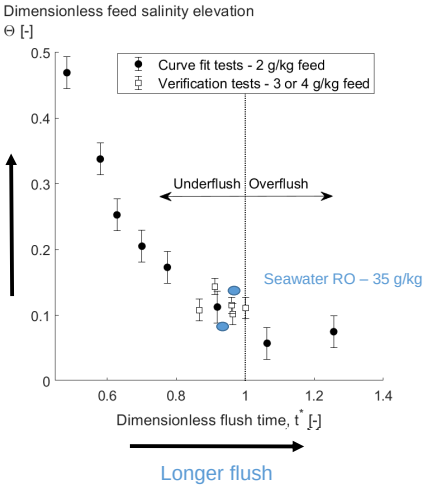

Measured salinity elevation matches theory

Ideal plug flow $\Theta = (1 - RR)\left(\frac{1}{t^*} - 1\right)$

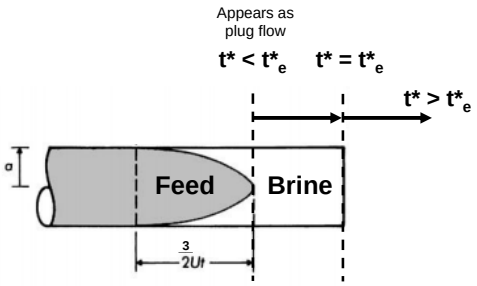

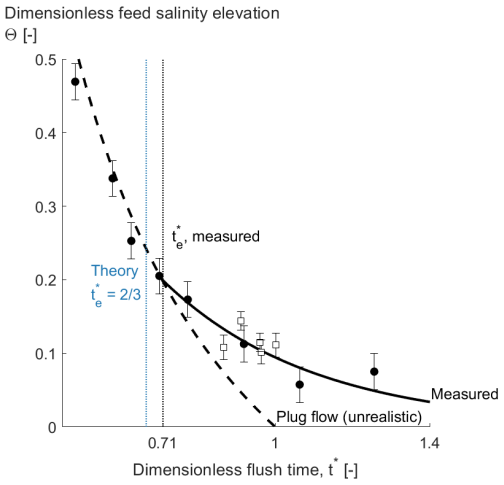

Probstein, *Physochemical Hydrodynamics*

Taylor dispersion accounts for majority of salinity elevation

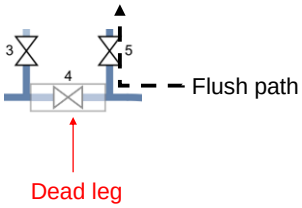

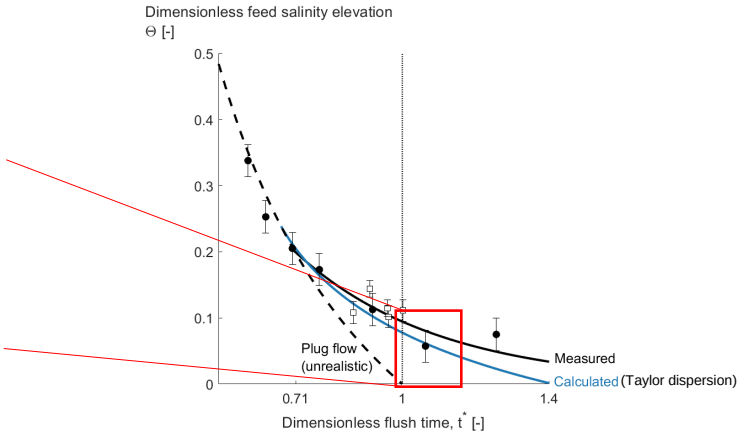

Wei et al. “Impact of salt retention…” *Desalination* (2020)

Minimum salt retention penalty

G. I. Taylor

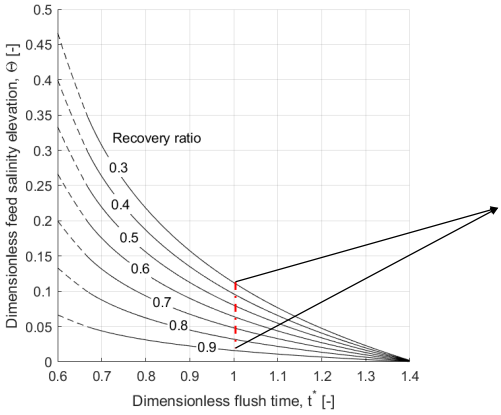

$\Theta_{TD} = -0.16RR + 0.16 \quad \text{for } t^* = 1$

Wei and Lienhard, "More water, cheaper…" *In prep*

Cycle Downtime

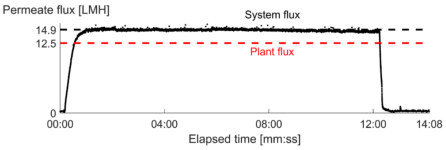

Salt Retention

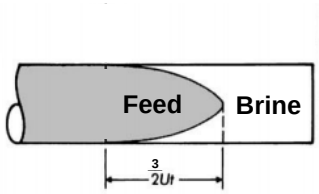

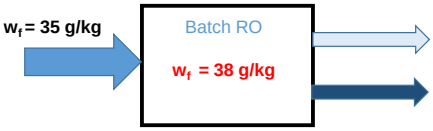

Water Loss

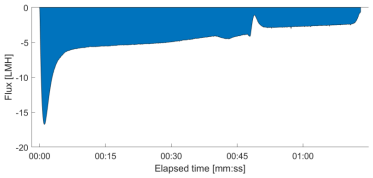

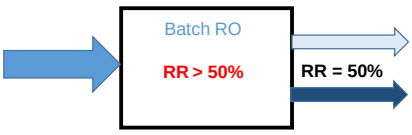

Water loss model requires 2D transient equations

Transient Convection Diffusion

$$\frac{\partial c}{\partial t} + u\frac{\partial c}{\partial x} + v\frac{\partial c}{\partial y} = D_m\left(\frac{\partial^2 c}{\partial x^2} + \frac{\partial^2 c}{\partial y^2}\right)$$

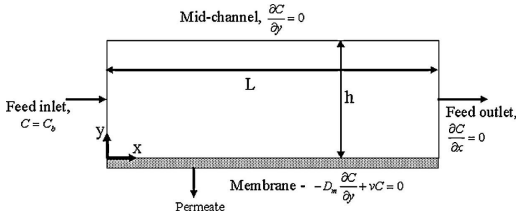

Vertical velocity component — Water flux — ICP

$$v = J_w = A[\pi_{F,m} - \pi_{p,b}e^{J_w K}]$$

New work:

Internal concentration polarization (ICP)
ICP development
Taylor dispersion
Permeate salinity model
Recharge phase → u = 0

Horizontal velocity component

Model adapted from:
Ramon et al., *Journal of Membrane Science,* (2010)

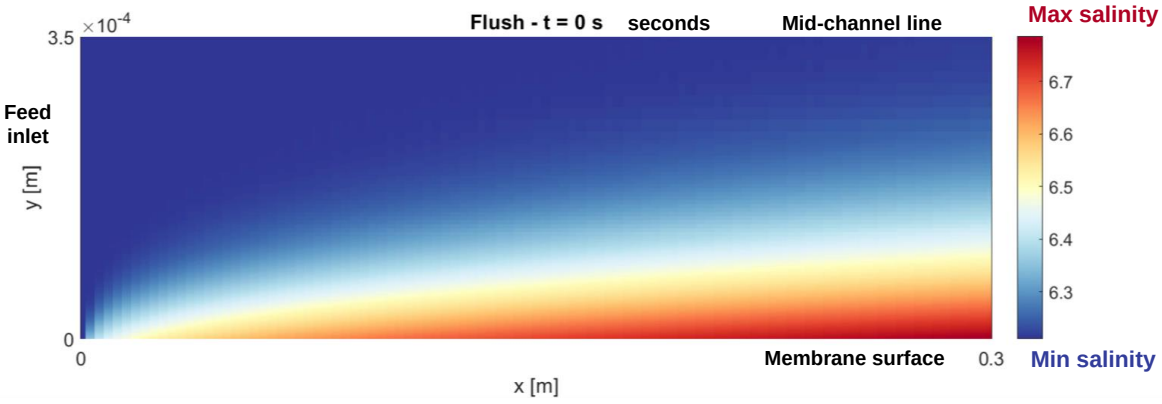

Model successfully predicts water loss

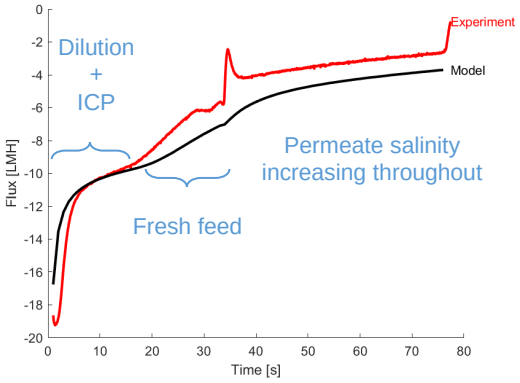

$$\text{Error} = \frac{\text{Model} - \text{Experiment}}{\text{Experiment}} \times 100$$

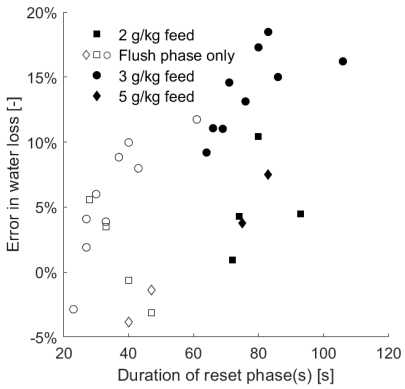

Wei et al., "Water loss in batch RO…" *In prep*

Cycle Downtime

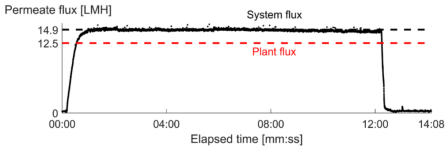

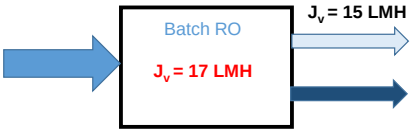

Salt Retention

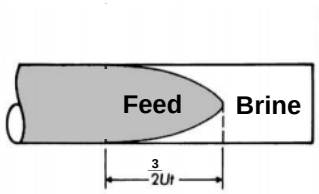

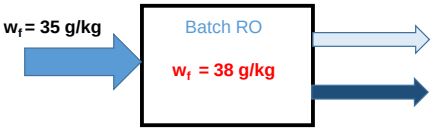

Water Loss

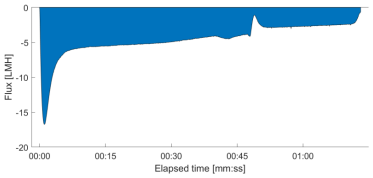

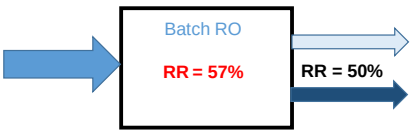

Salt retention + water loss reduce energy savings of batch RO

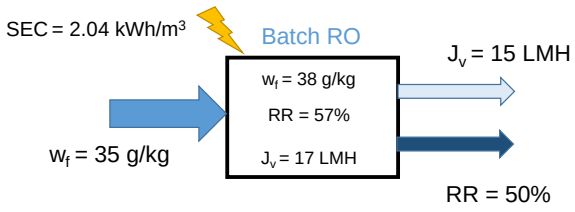

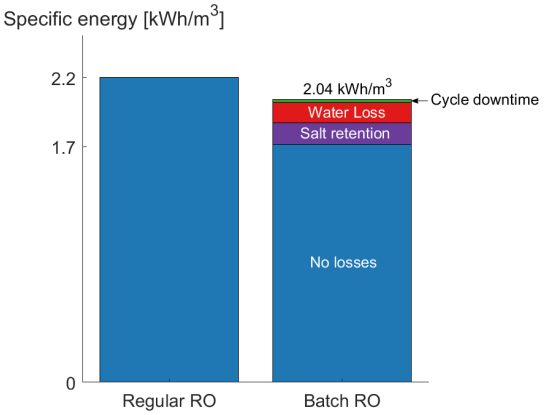

Energy savings
22% → 7%

Wei et al., "Water loss in batch RO…" *In prep*

Good things happen in the RK lab

Motivation
Practical Losses
Improved Design
- Bottleneck
- Branching out
- Performance

Techno-economics
Conclusions

More downtime → More water loss

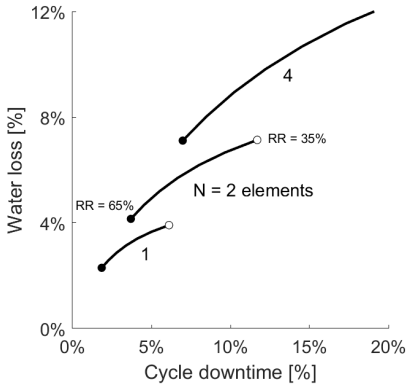

Wei et al., "Water loss in batch RO…" *In prep*

Membrane = bottleneck

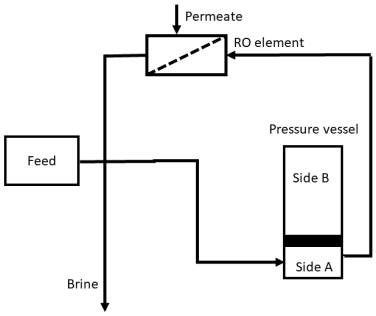

a) Double-acting system

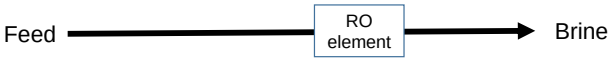

Max flow = **4.4 L/s**
Brine volume = 88 L
Flush time = 20 s

Cycle downtime = **10%**

Branch out!

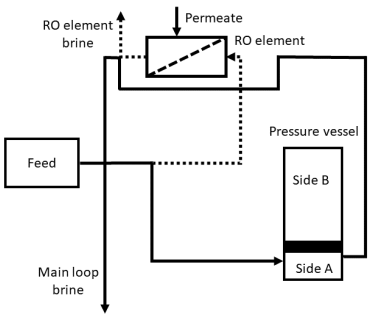

b) Double-acting system with rapid flush

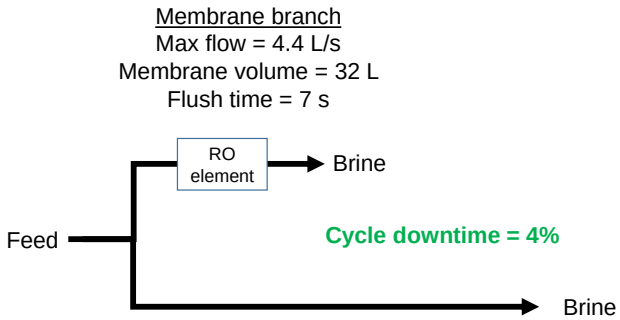

Systems and methods for rapid flushing of a membrane-based system, U.S. Provisional Pat. Ser. No. 63/182,761, April 30, 2021

Big reduction in water loss

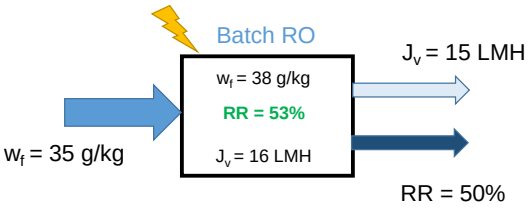

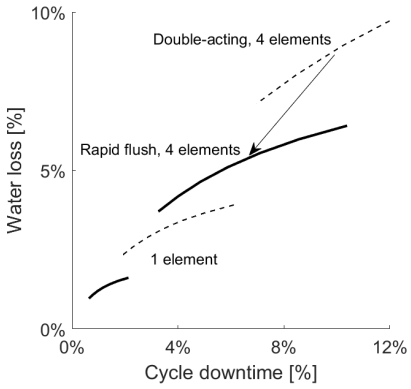

Wei et al., "Water loss in batch RO…" *In prep*

Rapid flushing nearly doubles batch RO energy savings

n = 4 elements

Lower energy possible, but might be impractical

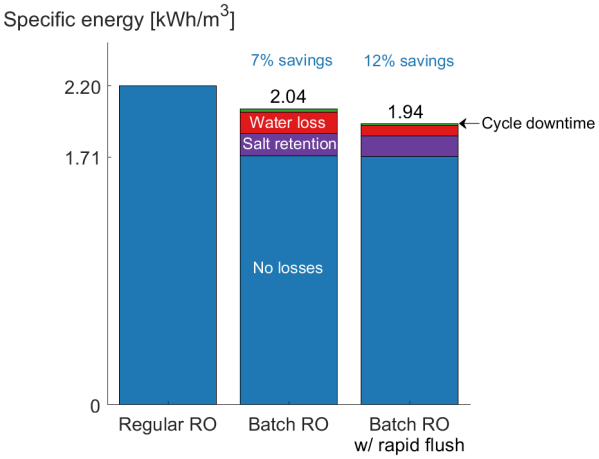

Wei et al., "Water loss in batch RO…" *In prep*

Impact matters

Motivation
Practical Losses
Improved Design
Techno-economics
- Less energy
- More water

Conclusions

Batch RO: Less energy!

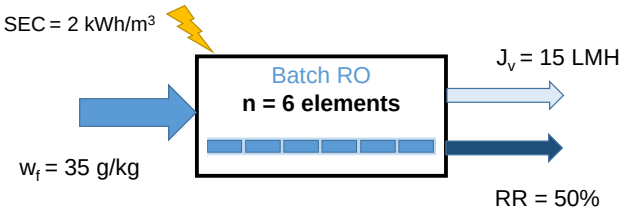

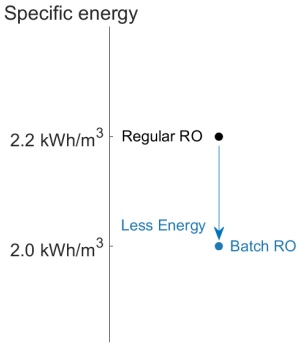

Energy savings | Plant capacity | 95% uptime | Electricity price

0.2 kWh/m^3 × **100,000** m^3/day × **347** day/yr × **$0.1**/kWh$_e$

$700,000

Annual energy savings

$120M	**$12M**
CAPEX – Regular RO 100,000 m^3/day	Additional CAPEX - batch RO 10% premium
Energy savings	**$0.7M**
Payback period	**17 years**
Electricity price	$0.10/$kWh_e$

	$120M	**$12M**	
	CAPEX – Regular RO 100,000 m^3/day	Additional CAPEX - batch RO 10% premium	
Energy savings	**$0.35M**	**$0.7M**	**$1.4M**
Payback period	**34 years**	**17 years**	**8.5 years**
Electricity price	$0.05/$kWh_e$	$0.10/$kWh_e$	$0.20/$kWh_e$

Batch RO: More water?

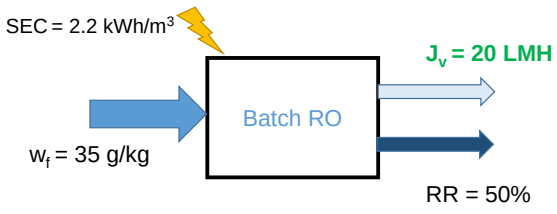

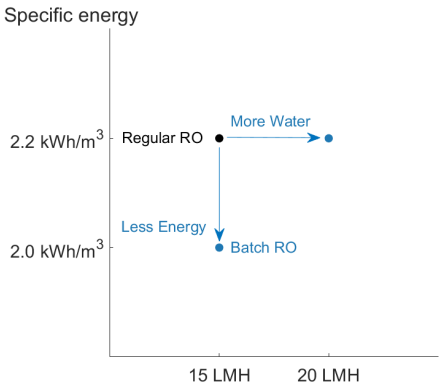

Batch RO can operate at higher fluxes without compromising membrane life

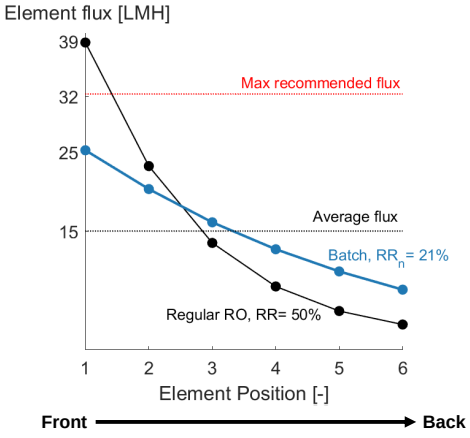

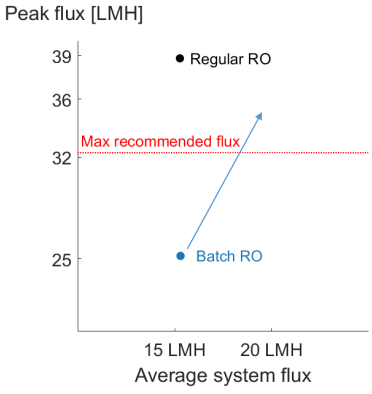

Wei and Lienhard, "More water, cheaper…" *In prep*

Increase productivity with batch RO

	Regular RO		**Batch RO**	
Membrane area	280,000		280,000	m^2
Flux	15		20	L/m^2-h
Capacity	**100,000**	+30% →	**130,000**	m^3/day

Additional capacity — Water price — 95% uptime

30,000 m^3/day × **\$0.80**/m^3 × **347** day/yr

Additional water revenue **\$8,300,000**/yr

Additional capacity — Specific energy — 95% uptime — Electricity price

30,000 m^3/day × **2.2** kWh/m^3 × **347** day/yr × **\$0.1**/kWh_e

Additional energy cost **\$2,300,000**/yr

Net benefit **\$6,000,000**/yr

$120M

CAPEX – Regular RO
100,00 m^3/day

$24M

Additional CAPEX –
batch RO + increased feed, brine
20% premium

$6M

Net benefit, annual

Independent of electricity price!

4 years

Payback period

Can batch RO make desalination more affordable?

$$\text{Levelized Cost of Water} = \frac{\text{Total costs}}{\text{Total water production}}$$

CAPEX
OPEX
Energy
Labor

$0.80/$m^3$

Regular RO

Less energy, but at what cost?

$0.80/m³ —+1%→ **$0.81/m³**

Regular RO — Batch RO – Less energy

Energy ↓ CAPEX ↑

$$\textbf{Cost of Water} = \frac{\textbf{Total costs}}{\textbf{Total water production}}$$

More water, cheaper

$0.80/m³ —-6%→ **$0.75/m³**

Regular RO — Batch RO – More water

↓ $$\textbf{Cost of Water} = \frac{\textbf{Total costs}\ \text{Energy ↑ CAPEX ↑}}{\textbf{Total water production}}$$ ↑↑

Only the beginning

Intro
Practical Losses
Improved Design
Techno-economics
Conclusions

First batch RO w/ a bladder

Validated energy models

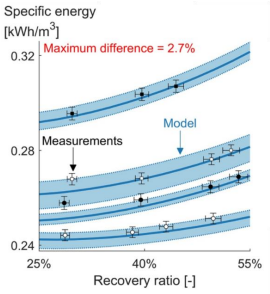

Minimum salt retention penalty

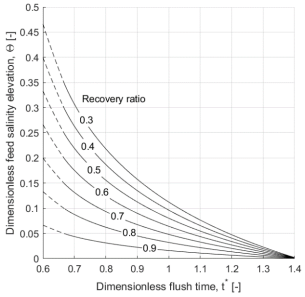

Full accounting of practical losses

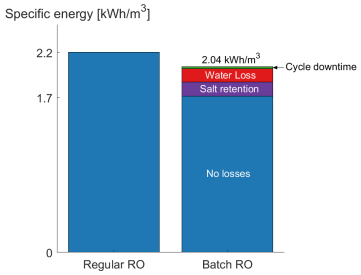

Branch out

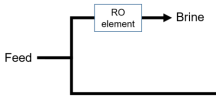

More water, cheaper

Cost of Water = Total costs / Total water production

Energy ↑ CAPEX ↑

Journal papers

Q. J. Wei and J. H. Lienhard, "**More water, cheaper with batch reverse osmosis: a techno-economic assessment**" *In Prep.*

Q. J. Wei, A. T. Bouma, C. I. Tucker, and J. H. Lienhard, "Reducing water loss in batch reverse osmosis with a rapid-flushing design" *In Prep.*

A. T. Bouma, Q. J. Wei, J. Parsons, J. H. Lienhard, and J. Buongiorno, "Co-locating a desalination plant with a nuclear power plant: feasibility study" *In Prep.*

E. Nagy, I. Hegedüs, D. Rehman, Q.J. Wei, Y.D. Ahdab, and J.H. Lienhard, "The need for accurate osmotic pressure and mass transfer resistances in modeling osmotically driven membrane processes," *Membranes*, **11**(2):128, 14 February 2021.

Q.J. Wei, C.I. Tucker, P.J. Wu, A. Trueworthy, E.W. Tow, and J.H. Lienhard, "Impact of salt retention on true batch reverse osmosis energy consumption: experiments and model validation," *Desalination*, online 3 February 2020, **479**:114177, 1 April 2020

D.N. Subramani, Q.J. Wei, and P.F.J. Lermusiaux, "Stochastic time-optimal path-planning in uncertain, strong, and dynamic flows." *Computer Methods in Applied Mechanics and Engineering* 333 (2018): 218-237

Q.J. Wei, R.K. McGovern, and J.H. Lienhard, "Saving energy with an optimized two-stage reverse osmosis system," *Environmental Science: Water Research & Technology*, online 05 June 2017, 3(4):659-670, July 2017.

Conference papers

Q.J. Wei, C. Tucker, P. Wu, E.W. Tow, and J. H. Lienhard, "True batch reverse osmosis prototype: model validation and energy savings," IDA World Congress on Desalination and Water Reuse, Dubai, UAE, 20–24 Oct. 2019. IDA Ref. No. IDAWC19-Wei.

Q.J. Wei, C.I. Tucker, P.J. Wu, A.M. Trueworthy, E.W. Tow, J.H. Lienhard, "Batch reverse osmosis: experimental results, model validation, and design implications," 2019 Membrane Technology Conference & Exposition, 25 – 28 Feb. 2019, New Orleans, Louisiana. **Best Student Paper Award**

Q.J. Wei, R.K. McGovern, and J.H. Lienhard, "Two-stage reverse osmosis: optimal element configuration and energy savings," IDA World Congress on Desalination and Water Reuse, São Paulo, Brazil, 15–20 Oct. 2017. IDA Ref. No. IDA17WC-57917-Wei

Q.J. Wei, R.K. McGovern, J.H. Lienhard, "Two-stage reverse osmosis: energy savings and economic viability," 2017 North East Graduate Student Water Symposium, 9 Sep. 2017, Amherst, Massachusetts.

Q.J. Wei, R.K. McGovern, J.H. Lienhard, "Energetic Benefits of Staged Reverse Osmosis," 2016 UCOWR/NIWR Conference, 21–23 June 2016, Pensacola, Florida. **Best Student Presentation Award**

Patents

Systems and methods for rapid flushing of a membrane-based system, Q.J. Wei, A.T. Bouma, and J.H. Lienhard, U.S. Provisional Pat. Ser. No. 63/182,761, 30 April 2021

Multi-Stage Reverse Osmosis Systems and Methods, Q.J. Wei, R.K. McGovern, and J.H. Lienhard, US Patent #10,603,635, 31 March 2020.

Reif, "A better way to deliver innovation to the world" (2015)


More sustainable?


I think so

It takes a village.

Intro
Practical Losses
Improved Design
Techno-economics
Conclusions

Afterword
- Why water?
- Thank you

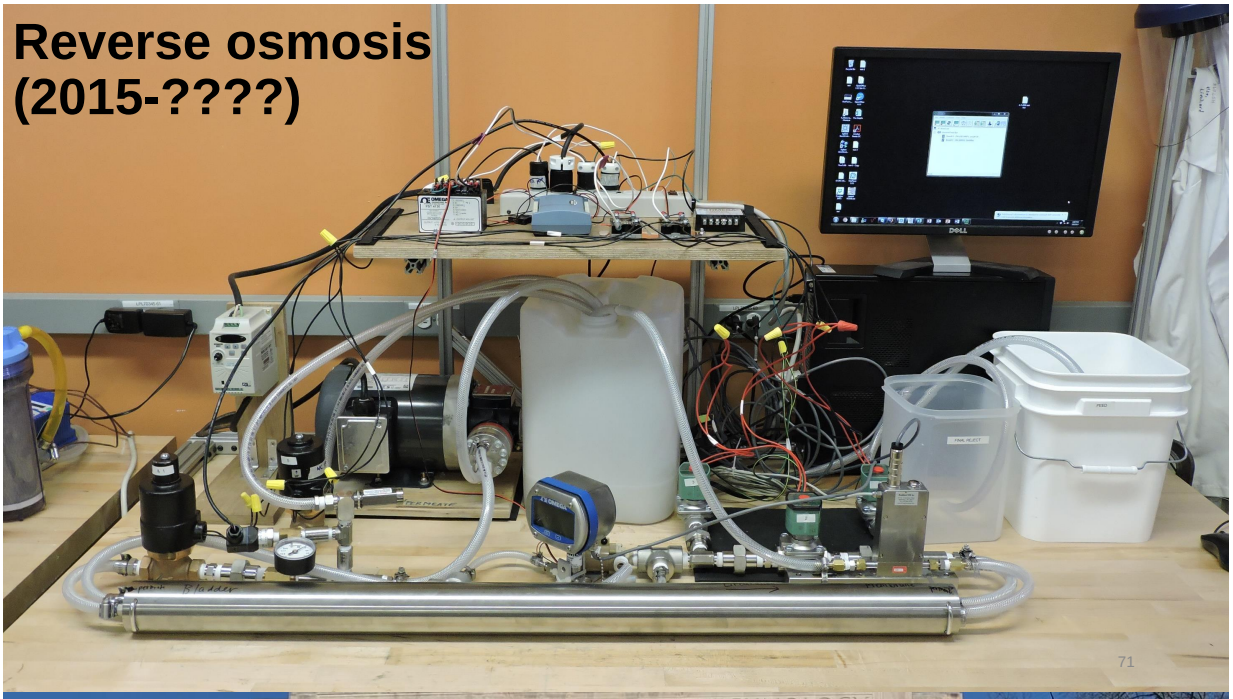
Reverse osmosis
(2015-????)


MASSACHVSETTS INSTITVTE OF TECHNOLOGY
WILLIAM BARTON ROGERS FOVNDER
MIT Student
(2011-2021)


MIT
MIT
NOVEMBER
PROJECT

MIT INTRAMURALS

ROHSENOW KENDALL HEAT TRANSFER LABORATORY

2 Course 2's
we build shit

CHI PHI

Quals Study Group

Water Diplomacy

2.05/2.005 teaching team

Batch RO UROPS

THE SCIENCE POLICY INITIATIVE

TEALS

GRADUATE ASSOCIATION OF MECHANICAL ENGINEERS

Harmony

PAGU

FEEDING FAMILIES PRU E. 2020 SAVING RESTAURANTS

mseas
multidisciplinary simulation, estimation, and assimilation systems

MITWATER

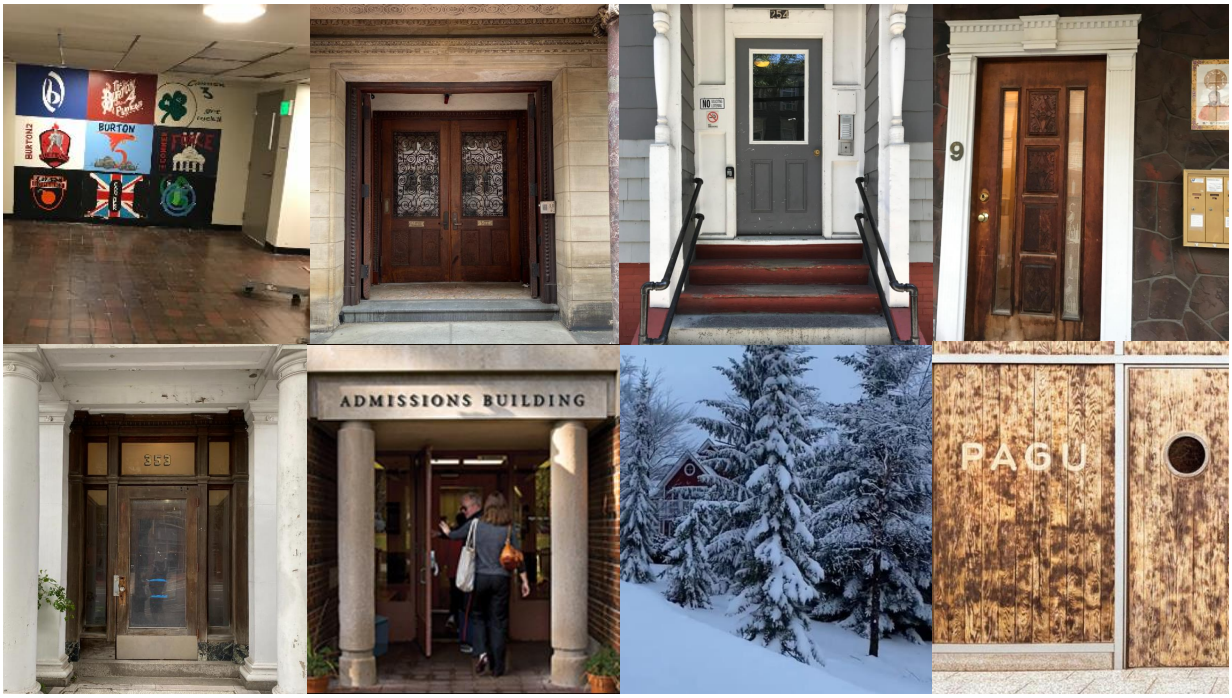


DUKE
x = A\b;


Quark
Quasar
Quantum
Mama
Baba

Appendix

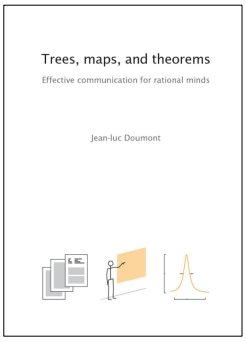
Trees, maps, and theorems
Effective communication for rational minds
Jean-luc Doumont

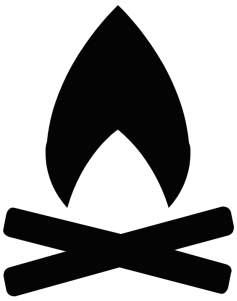

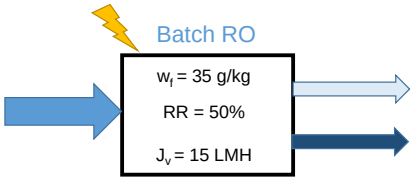
Batch RO
w_f = 35 g/kg
RR = 50%
J_v = 15 LMH

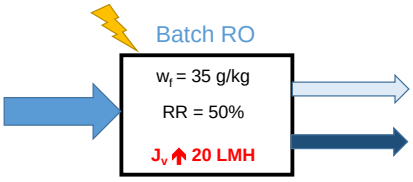
Batch RO
w_f = 35 g/kg
RR = 50%
J_v ↑ 20 LMH

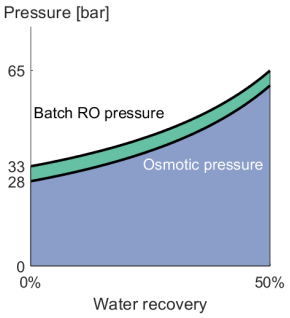
Pressure [bar]
65
Batch RO pressure
33
28
Osmotic pressure
0
0%
50%
Water recovery

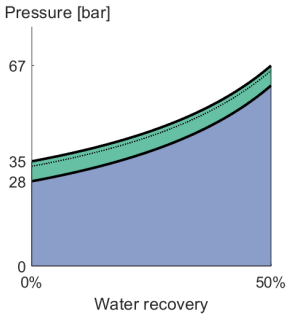
Pressure [bar]
67
35
28
0
0%
50%
Water recovery

83

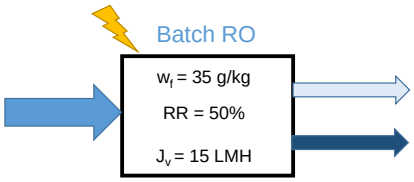
Batch RO
w_f = 35 g/kg
RR = 50%
J_v = 15 LMH

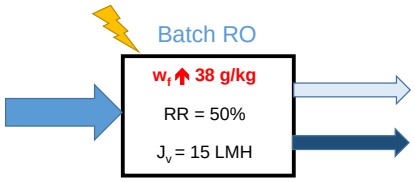
Batch RO
w_f ↑ 38 g/kg
RR = 50%
J_v = 15 LMH

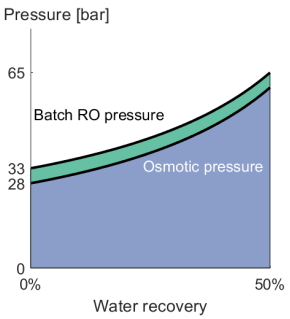
Pressure [bar]
65
Batch RO pressure
33
28
Osmotic pressure
0
0%
50%
Water recovery

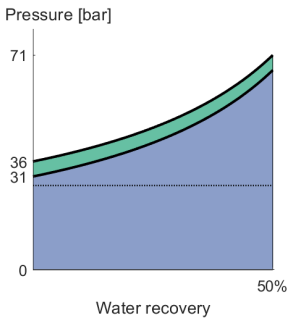
Pressure [bar]
71
36
31
0
50%
Water recovery

84

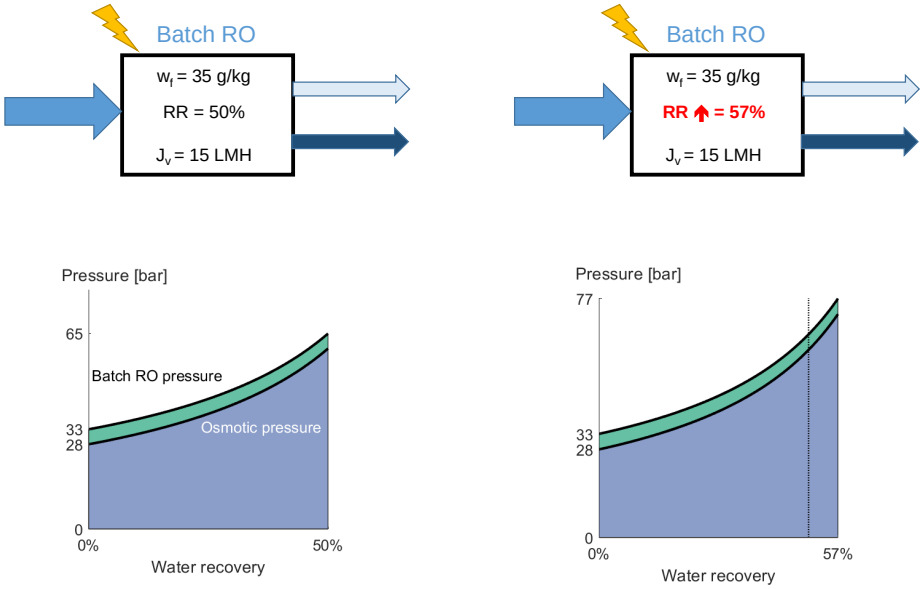

Beachhead markets

Less brine for BWRO
(10,000 m³/day plant)

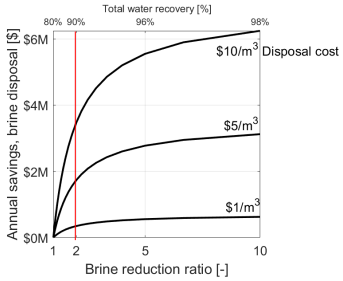

1,000 m³/day brine reducer: $2-3M

Less energy for old SWRO
(1,000 m³/day plant)

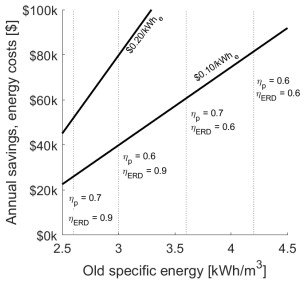

1,000 m³/day plant retrofit: $250-500k

Less batteries for off-grid RO

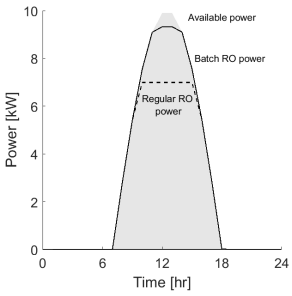

Net benefit independent of electricity price!

Net benefit = Water revenue – Energy cost

Water revenue = unit water price **x production**

Energy cost = unit energy cost **x production**

Unit energy cost **= Electricity price x Specific energy**

Net benefit = (unit water price **– unit energy cost) x production**

Unit water price **= CAPEX + OPEX +** unit energy cost **+ Labor**

Net benefit = (CAPEX + OPEX + Labor) x production

Internal concentration polarization desirable in batch RO

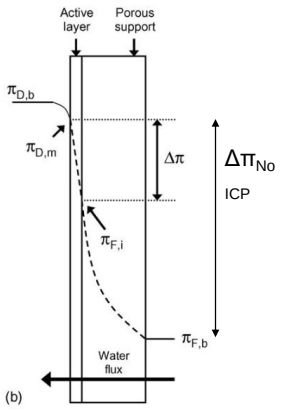

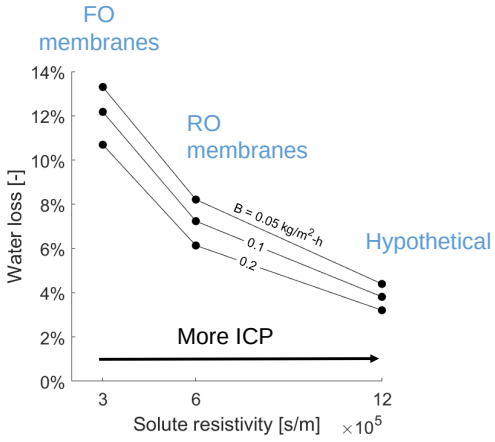

McCutcheon & Elimelech, *Journal of Membrane Science,* (2006)

Bibliography

[1] U. N. Water. "2018 UN World Water Development Report, Nature-based Solutions for Water". In: (2018).

[2] A. Boretti and L. Rosa. "Reassessing the projections of the World Water Development Report". In: *npj Clean Water* 2.1 (2019), p. 15. DOI: 10.1038/s41545-019-0039-9.

[3] P. H. Gleick. "Global freshwater resources: soft-path solutions for the 21st century". In: *Science* 302.5650 (2003), pp. 1524–1528.

[4] C. Fritzmann, J. Löwenberg, T. Wintgens, and T. Melin. "State-of-the-art of reverse osmosis desalination". In: *Desalination* 216.1-3 (2007), pp. 1–76. DOI: 10.1016/j.desal.2006.12.009.

[5] C. Liu, K. Rainwater, and L. Song. "Energy analysis and efficiency assessment of reverse osmosis desalination process". In: *Desalination* 276.1-3 (2011), pp. 352–358. DOI: 10.1016/j.desal.2011.03.074.

[6] T. Y. Qiu and P. A. Davies. "Longitudinal dispersion in spiral wound RO modules and its effect on the performance of batch mode RO operations". In: *Desalination* 288 (2012), pp. 1–7. DOI: https://doi.org/10.1016/j.desal.2011.11.054.

[7] S. Lin and M. Elimelech. "Staged reverse osmosis operation: Configurations, energy efficiency, and application potential". In: *Desalination* 366 (2015), pp. 9–14. DOI: 10.1016/j.desal.2015.02.043.

[8] G. P. Thiel, R. K. McGovern, S. M. Zubair, and J. H. Lienhard. "Thermodynamic equipartition for increased second law efficiency". In: *Applied Energy* 118 (2014), pp. 292–299. DOI: 10.1016/j.apenergy.2013.12.033.

[9] Q. J. Wei, R. K. McGovern, and J. H. Lienhard. "Saving energy with an optimized two-stage reverse osmosis system". In: *Environmental Science: Water Research and Technology* (2017). DOI: 10.1039/c7ew00069c.

[10] T. Y. Qiu and P. A. Davies. "Concentration polarization model of spiral-wound membrane modules with application to batch-mode RO desalination of brackish water". In: *Desalination* 368 (2015), pp. 36–47. DOI: 10.1016/j.desal.2014.12.048.

[11] D. Warsinger, E. Tow, K. Nayar, L. Maswadeh, and J. Lienhard. "Energy efficiency of batch and semi-batch (CCRO) reverse osmosis desalination". In: *Water Research* 106 (2016), pp. 272–282. DOI: 10.1016/j.watres.2016.09.029.

[12] J. R. Werber, A. Deshmukh, and M. Elimelech. "Can batch or semi-batch processes save energy in reverse-osmosis desalination?" In: *Desalination* 402 (2017), pp. 109–122. DOI: 10.1016/j.desal.2016.09.028.

[13] J. Swaminathan, E. W. Tow, R. L. Stover, and J. H. Lienhard. "Practical aspects of batch RO design for energy-efficient seawater desalination". In: *Desalination* 470 (2019), p. 114097. DOI: 10.1016/j.desal.2019.114097.

[14] P. A. Davies, J. Wayman, C. Alatta, K. Nguyen, and J. Orfi. "A desalination system with efficiency approaching the theoretical limits". In: *Desalination and Water Treatment* 57.48-49 (2016), pp. 23206–23216. DOI: 10.1080/19443994.2016.1180482.

[15] D. M. Warsinger, J. H. Lienhard, E. W. Tow, R. K. McGovern, and G. P. Thiel. *Batch Pressure-Driven Membrane Separation with Closed-flow Loop and Reservoir*. 2017.

[16] D. M. Warsinger, E. W. Tow, L. A. Maswadeh, G. B. Connors, J. Swaminathan, and J. H. Lienhard. "Inorganic fouling mitigation by salinity cycling in batch reverse osmosis". In: *Water Research* 137 (2018), pp. 384–394. DOI: 10.1016/j.watres.2018.01.060.

[17] J. Swaminathan, R. L. Stover, E. W. Tow, D. M. Warsinger, and J. H. Lienhard. "Effect of practical losses on optimal design of batch RO systems". In: *The International Desalination Association World Congress*. Sao Paulo, Brazil: International Desalination Association, 2017.

[18] D. M. Warsinger, J. Swaminathan, and J. H. Lienhard. "Ultrapermeable membranes for batch desalination: maximum desalination energy efficiency, and cost analysis". In: *The International Desalination Association World Congress*. Sao Paulo, Brazil: International Desalination Association, pp. 1–10.

[19] B. R. L. Stover and N. Efraty. "Low-Energy Consumption With Closed-Circuit Desalination". In: *IDA Journal of Desalination and Water Reuse* 4.3 (2012), pp. 12–19. DOI: 10.1179/ida.2012.4.3.12.

[20] T. Lee, J. Y. Choi, and Y. Cohen. "Gypsum scaling propensity in semi-batch RO (SBRO) and steady-state RO with partial recycle (SSRO-PR)". In: *Journal of Membrane Science* (2019). DOI: 10.1016/j.memsci.2019.05.030.

[21] P. A. Davies, A. Afifi, F. Khatoon, G. Kuldip, S. Javed, and S. J. Khan. "Double-acting batch-RO system for desalination of brackish water with high efficiency and high recovery". In: *Desalination for the Environment – Clean Energy and Water*. Rome, Italy, 2016.

[22] S. Cordoba, A. Das, J. Leon, J. M. Garcia, and D. M. Warsinger. "Double-acting batch reverse osmosis configuration for best-in-class efficiency and low downtime". In: *Desalination* (2021). DOI: 10.1016/j.desal.2021.114959.

[23] K. Park and P. A. Davies. "A compact hybrid batch/semi-batch reverse osmosis (HBSRO) system for high-recovery, low-energy desalination". In: *Desalination* (2021). DOI: 10.1016/j.desal.2021.114976.

[24] Y. Cohen, A. Rahardianto, and T. Lee. *Desalination and Water Purification Research and Development Program Report No. 179: Autonomous Low Energy Consumption Cyclic Desalination Systems*. Tech. rep. 179. Denver, Colorado: Bureau of Reclamation, Department of the Interior, 2017.

[25] Q. Wei, C. Tucker, P. Wu, A. Trueworthy, E. Tow, and J. Lienhard. "Impact of salt retention on true batch reverse osmosis energy consumption: Experiments and model validation". In: *Desalination* 479 (2020). DOI: 10.1016/j.desal.2019.114177.

[26] DuPont Water Solutions. *DuPont FILMTEC ™ Reverse Osmosis Membranes Technical Manual*. Tech. rep. 2. 2019, p. 205.

[27] T. Shedlovsky. "The electrolytic conductivity of some uni-univalent electrolytes in water at 25°". In: *Journal of the American Chemical Society* (1932). DOI: 10.1021/ja01343a020.

[28] R. B. McCleskey. "Electrical conductivity of electrolytes found in natural waters from (5 to 90) °c". In: *Journal of Chemical and Engineering Data* (2011). DOI: 10.1021/je101012n.

[29] R. J. Moffat. "Contributions to the Theory of Single-Sample Uncertainty Analysis". In: *Journal of Fluids Engineering* 104.2 (1982), p. 250. DOI: 10.1115/1.3241818.

[30] R. J. Moffat. "Describing the Uncertainties in Experimental Results". In: *Experimental Thermal and Fluid Science* (1988), pp. 3–17.

[31] K. S. Pitzer, J. C. Peiper, and R. H. Busey. "Thermodynamic Properties of Aqueous Sodium Chloride Solutions". In: *Journal of Physical and Chemical Reference Data* (1984). DOI: 10.1063/1.555709. arXiv: 0002114v1 [arXiv:cond-mat].

[32] G. P. Thiel, E. W. Tow, L. D. Banchik, H. W. Chung, and J. H. Lienhard. "Energy consumption in desalinating produced water from shale oil and gas extraction". In: *Desalination* 366 (2015), pp. 94–112. DOI: 10.1016/j.desal.2014.12.038.

[33] A. Zydney. "Stagnant film model for concentration polarization in membrane systems". In: *Journal of Membrane Science* 130.1-2 (1997), pp. 275–281. DOI: 10.1016/S0376-7388(97)00006-9.

[34] J. Schwinge, P. R. Neal, D. E. Wiley, D. F. Fletcher, and A. G. Fane. *Spiral wound modules and spacers: Review and analysis*. 2004. DOI: 10.1016/j.memsci.2003.09.031.

[35] G Schock. "Mass transfer and pressure loss in spiral wound modules". In: *Desalination Elsevier Science Publishers B.V* 64 (1987), pp. 339–352.

[36] C. P. Koutsou, S. G. Yiantsios, and A. J. Karabelas. "A numerical and experimental study of mass transfer in spacer-filled channels: Effects of spacer geometrical characteristics and Schmidt number". In: *Journal of Membrane Science* 326.1 (2009), pp. 234–251. DOI: 10.1016/j.memsci.2008.10.007.

[37] Q. Wei, C. Tucker, P. Wu, A. Trueworthy, E. W. Tow, and J. Lienhard. "Data for: Impact of salt retention on true batch reverse osmosis energy consumption: experiments and model validation". In: *Mendeley Data* (). DOI: 10.17632/3r7388bhz7.1.

[38] Q. J. Wei, A. T. Bouma, C. I. Tucker, and J. H. Lienhard. "Reducing water loss in batch reverse osmosis with a rapid-flushing design". In Prep.

[39] G. Taylor. "Dispersion of Soluble Matter in Solvent Flowing Slowly through a Tube". In: *Proceedings of the Royal Society A: Mathematical, Physical and Engineering Sciences* 219.1137 (1953), pp. 186–203. DOI: 10.1098/rspa.1953.0139. arXiv: 1402.1118.

[40] R. F. Probstein. *Physicochemical Hydrodynamics: An Introduction*. 1994. DOI: 10.1056/NEJMra0800885.

[41] K. Park, L. Burlace, N. Dhakal, A. Mudgal, N. A. Stewart, and P. A. Davies. "Design, modelling and optimisation of a batch reverse osmosis (RO) desalination system using a free piston for brackish water treatment". In: *Desalination* (2020). DOI: 10.1016/j.desal.2020.114625.

[42] G. Ramon, Y. Agnon, and C. Dosoretz. "Dynamics of an osmotic backwash cycle". In: *Journal of Membrane Science* 364.1-2 (2010), pp. 157–166. DOI: 10.1016/j.memsci.2010.08.008.

[43] A. A. Eftekhari. *FVTool: a finite volume toolbox for Matlab*. 2015. DOI: http://doi.org/10.5281/zenodo.32745.

[44] J. R. McCutcheon and M. Elimelech. "Influence of concentrative and dilutive internal concentration polarization on flux behavior in forward osmosis". In: *Journal of Membrane Science* 284.1-2 (2006), pp. 237–247. DOI: 10.1016/j.memsci.2006.07.049.

[45] J. Wayman. "Brackish Ground Water Desalination Using Solar Reverse Osmosis". In: June (2015). DOI: <http://dx.doi.org/10.13140/RG.2.1.1256.6881>.

[46] J. R. Werber, A. Deshmukh, and M. Elimelech. *The Critical Need for Increased Selectivity, Not Increased Water Permeability, for Desalination Membranes*. 2016. DOI: 10.1021/acs.estlett.6b00050.

[47] S. S. Manickam, J. Gelb, and J. R. McCutcheon. "Pore structure characterization of asymmetric membranes: Non-destructive characterization of porosity and tortuosity". In: *Journal of Membrane Science* 454 (2014), pp. 549–554. DOI: 10.1016/j.memsci.2013.11.044.

[48] Q. J. Wei, A. T. Bouma, and J. H. Lienhard. *Systems and methods for rapid flushing of a membrane-based system*. 2021.

[49] Q. J. Wei and J. H. Lienhard. "More water, cheaper with batch reverse osmosis: a techno-economic assessment". In Prep.

[50] T. Pankratz. "The looming membrane drought". In: *Water Desalination Report* (2019), Volume 55, Issue 20.

[51] A. T. Bouma, Q. J. Wei, J. Parsons, J. H. Lienhard, and J. Buongiorno. "Colocating a desalination plant with a nuclear power plant: feasibility study". In Prep.

[52] Dupont Water Solutions. *DuPont™ XUS180808 Reverse Osmosis Element*. Tech. rep. 2020.

[53] Protec Arisawa America. *BPV-8-1800-EP*. Tech. rep. 2021.

[54] N. Voutchkov. *Desalination Project Cost Estimating and Management*. 2018. DOI: 10.1201/9781351242738.

[55] A. Panagopoulos, K.-J. Haralambous, and M. Loizidou. "Desalination brine disposal methods and treatment technologies - A review". In: *Science of The Total Environment* 693 (2019), p. 133545. DOI: https://doi.org/10.1016/j.scitotenv.2019.07.351.

[56] J. Edgley. *Personal communication to Quantum Wei*. Tech. rep. 2020.

[57] W. He, A.-C. Le Henaff, S. Amrose, T. Buonassisi, I. M. Peters, and A. G. Winter. "Voltage- and flow-controlled electrodialysis batch operation: Flexible and optimized brackish water desalination". In: *Desalination* 500 (2021), p. 114837. DOI: https://doi.org/10.1016/j.desal.2020.114837.

[58] A.-C. Le Henaff, W. He, T. Buonassisi, A. G. Winter, and I. M. Peters. *Flexible operation of photovoltaic electrodialysis (PV-ED) low-cost community-scale desalination systems*. 2019. DOI: 10.1109/PVSC40753.2019.9198962.